

CHAPTER 5

STRATOSPHERIC OZONE CHANGES AND CLIMATE



*About the cover image:
The Hunga Tonga-Hunga Ha'apai volcanic eruption in January 2022 lofted water vapor and other emissions well into the stratosphere in the southern hemisphere. Downwind, sunsets changed color as seen from the Maïdo Observatory on Réunion Island.*

Photo credit: Elizabeth Asher, NOAA CSL / CIRES

CHAPTER 5

STRATOSPHERIC OZONE CHANGES AND CLIMATE

Lead Authors : Hella Garny
Harry Hendon

Coauthors : Marta Abalos
Gabriel Chiodo
Ariaan Purich
William J. Randel
Karen Smith
David Thompson

Contributing Authors : James A. Anstey
Blanca Ayarzagüena
Antara Banerjee
Ramiro Checa Garcia
Martyn P. Chipperfield
Martin Dameris
Rishav Goyal
Paul A. Newman
Felix Plöger
Lorenzo Polvani
Karen H. Rosenlof
Anja Schmidt
William Seviour
Keith Shine
Neil Swart
Paul J. Young

Review Editors : Amy H. Butler
Amanda Maycock

CONTENTS

CHAPTER 5: STRATOSPHERIC OZONE CHANGES AND CLIMATE

SCIENTIFIC SUMMARY	277	
5.1 INTRODUCTION	279	
5.1.1	Summary of Findings from the Previous Assessment	279
5.1.2	Scope of Chapter	279
5.2 OBSERVED AND SIMULATED CHANGES IN STRATOSPHERIC CLIMATE	280	
5.2.1	Overview of Relevant Anthropogenic and Natural Forcing Agents	280
Box 5-1	The Hunga Tonga-Hunga Ha’apai Volcanic Eruption of January 2022	280
5.2.2	Stratospheric Temperatures	281
5.2.2.1	<i>Observed Temperature Changes</i>	281
Box 5-2	Impact of GHG-Induced Stratospheric Cooling on Ozone Chemistry	282
5.2.2.2	<i>Simulation and Attribution of Past and Future Stratospheric Temperature Changes</i>	283
5.2.3	Stratospheric Water Vapor	284
5.2.3.1	<i>Processes Controlling Water Vapor Entry Across the Tropical Tropopause</i>	284
5.2.3.2	<i>Updates on Modeling and Understanding of Radiative Effects of Stratospheric Water Vapor</i>	285
5.2.4	Brewer-Dobson Circulation	285
5.2.5	Stratosphere-to-Troposphere Transport	288
5.2.6	Stratospheric Winds	289
5.2.6.1	<i>Polar Vortices</i>	289
5.2.6.2	<i>Quasi-Biennial Circulation</i>	291
5.3 EFFECTS OF CHANGES IN STRATOSPHERIC OZONE AND ODSs ON CLIMATE	292	
5.3.1	Radiative Impacts of Ozone and ODSs on Tropospheric Climate and Ozone-Climate Feedbacks	292
5.3.1.1	<i>Ozone Radiative Forcing</i>	292
Box 5-3	Radiative Forcing from Ozone and ODSs: Methods and Uncertainties	294
5.3.1.2	<i>ODSs Direct Effects on Climate</i>	295
5.3.1.3	<i>Role of Stratospheric Ozone for the Climate Response to CO₂ Forcing</i>	296
Box 5-4	Ozone-Climate Feedbacks and Ozone-Circulation Coupling	297
5.3.2	Ozone/Dynamical Coupling	298
5.3.2.1	<i>Ozone-Circulation Coupling on Seasonal to Interannual Timescales</i>	299
5.3.2.1.1	Antarctic	299
5.3.2.1.2	Arctic	301
5.3.2.1.3	Tropics	302
5.3.2.2	<i>Impact of Ozone Trends on the Tropospheric Circulation and Surface Climate</i>	303
5.3.2.2.1	Impact of Two-Way Ozone-Circulation Coupling on Antarctic/SH Trends	305
5.3.3	Impacts of Ozone Changes on the Oceans and the Cryosphere	306
5.3.3.1	<i>Ocean Impacts</i>	306

5.3.3.2	<i>Sea Ice Impacts</i>	308
5.3.3.3	<i>Ocean Carbon</i>	309
5.3.3.4	<i>Ice Sheet and Shelf Impacts</i>	309

5.4 CLIMATE IMPACTS OF THE MONTREAL PROTOCOL **309**

5.4.1	Realized Climate Impacts of the Montreal Protocol	309
5.4.2	Future Climate Impacts of the Montreal Protocol	310

REFERENCES **313**

SCIENTIFIC SUMMARY

Since the last Assessment, new research has continued to quantify, attribute and improve the understanding of long-term changes in stratospheric climate. New studies are assessed that quantify the effects of ozone-depleting substances and ozone changes on the climate system, including atmospheric temperatures and circulation, the ocean and the cryosphere. The new results support the main conclusions from the previous Assessment.

Changes in stratospheric climate

- **Stratospheric Temperature: The global middle and upper stratosphere continues to cool at a rate of ~ -0.6 K decade⁻¹ because of growing levels of well-mixed greenhouse gases (GHGs; primarily carbon dioxide [CO₂]) and evolving stratospheric ozone in response to changing ozone-depleting substances (ODSs).** Lower-stratospheric temperatures have been near constant since the late 1990s. The overall evolution is consistent with the well-understood effects of ozone, ODSs, GHGs, stratospheric aerosols, and solar variability. This is in agreement with previous Assessments.
- **Stratospheric Water Vapor: Since the last Assessment, the understanding of processes that influence water vapor entry into the stratosphere has strengthened.** Interannual variations in lower-stratospheric water vapor are quantitatively consistent with observed tropical tropopause temperatures, with small contributions from monsoon circulations and overshooting convection. Models predict small multi-decadal increases in tropopause temperature and lower-stratospheric water vapor as a response to GHG increases, but these changes are still not evident within the variability of the observational records.
- **Brewer-Dobson Circulation⁷ (BDC):**
 - **The BDC in the lower stratosphere has accelerated in recent decades and is predicted to continue to accelerate in the future given continued increases in GHG abundances.** This result is confirmed by models, observations, and reanalyses. New studies since the last Assessment confirm the attribution of the BDC acceleration by models to increases in GHGs and ODS-induced ozone depletion over the last decades of the 20th century. Model simulations indicate that the decline of ODSs and subsequent recovery of ozone should have acted to reduce the rate of BDC acceleration after the year 2000, but there is not yet sufficient analysis to determine whether this change has been detectable outside of the natural variability in the BDC.
 - **Estimates of past BDC trends in the middle and upper stratosphere based on observations**

continue to be opposite in sign from modeled trends. However, new observationally based estimates since the last Assessment bring observed trends closer to modeled trends.

- **Polar Vortex Trends and Variability: Recent extreme polar vortex events in both hemispheres caused strong variations of polar ozone. However, currently there is no evidence for a systematic trend toward more frequent polar vortex disruptions in either hemisphere.**
 - Two sudden stratospheric warming (SSW)⁸ events have been observed in the Southern Hemisphere (SH) since the start of comprehensive satellite records in 1979. New model studies show that this is consistent with model simulations, and no change in SSW frequency is necessary to explain this occurrence rate. The delay of the austral polar vortex breakup date, which in the past was driven by ozone depletion, is not expected to fully reverse by the end of the 21st century, due to the opposing effect of GHG increases under moderate and high emission scenarios.
 - In the Northern Hemisphere (NH), new studies confirm that changes in SSW frequency and in polar vortex strength are not robustly detected in the historical record, and future changes are not robust across models.
- **Quasi-Biennial Oscillation (QBO)⁹: Since the last Assessment, there is more confidence that the amplitude of the QBO will weaken in the future as a result of acceleration of the BDC,** but there is still large uncertainty about any change in its periodicity and the associated ozone variability.
 - New model studies infer that further disruptions of the QBO, such as occurred in 2016 and 2019, might become more likely as a result of increasing GHGs.

Ozone and ODS effects on climate

- **Ozone and ODS Radiative Forcing (RF): New estimates confirm previous Assessments in that the RF from ODSs, including the indirect effect on ozone abundances, has been positive over the second half of the 20th century, contributing to anthropogenic GHG forcing.** The newest best estimate of stratosphere-adjusted RF over the period 1850–2011 from stratospheric ozone changes is -0.02 W m⁻², with an uncertainty of ± 0.13 W m⁻². The range in this RF remains smaller than the RF from ODSs (0.337 W m⁻²). However, new studies reveal uncertainties in the estimation of radiative forcing, due to 1) rapid adjustments arising from tropospheric circulation changes and 2) uncertainties in modeled ozone

⁷ The global zonal mean circulation that transports mass, heat, and tracers in the stratosphere.

⁸ Based on an adapted SSW definition in the Southern Hemisphere; see Chapter 5, Section 5.2.6.1.

⁹ Quasi-periodic (period ~ 28 months) oscillation of stratospheric equatorial winds from easterly to westerly.

trends. Since the late 1990s, the RF from ODSs and changes in stratospheric ozone abundances has remained approximately constant as a consequence of the Montreal Protocol.

- **ODS Effects on Climate:** There is new evidence since the last Assessment that suggests that the direct radiative effects of ODSs on climate not only contributed to global warming but also enhanced Arctic amplification¹⁰ in the late 20th century.
- **Role of Stratospheric Ozone in the Climate Response to GHG Forcing:** Evidence suggests that GHG-induced ozone changes act to dampen the GHG-induced surface temperature warming. New estimates since the last Assessment confirm that this climate feedback by stratospheric ozone is negative but smaller than previously estimated. In addition, there is new evidence for an influence of stratospheric ozone on the tropospheric and stratospheric circulation response to GHGs via ozone-circulation coupling.
- **Relevance of Stratospheric Ozone-Circulation Coupling for Trends and Interannual Variability:**
 - Two-way ozone-circulation coupling modulates the effects of ozone depletion and recovery on SH stratospheric circulation trends, as well as stratospheric interannual variability in the tropics and extratropics in both hemispheres.
 - There have been no detectable effects of long-term ODS-driven ozone trends in the Arctic on tropospheric and surface climate. Yet, new evidence shows that for individual years low springtime Arctic ozone can amplify existing stratospheric circulation anomalies and their subsequent influence on tropospheric circulation and surface climate.
- **Signature of Ozone Recovery in the Southern Hemisphere Circulation:**
 - **Antarctic ozone depletion led to pronounced changes in the SH atmospheric circulation, as summarized in the previous Assessments.** New evidence suggests that the recovery of Antarctic ozone is now evident as changes in SH atmospheric circulation trends between the ozone depletion and recovery eras (the eras before and after roughly the year 2000, respectively). The observed changes in circulation trends are significant at stratospheric altitudes but on the fringe of significance in the troposphere; model simulations support the hypothesis that the changes in atmospheric circulation trends are driven by the onset of ozone recovery.
 - Climate simulations suggest that in the future the effects of ozone recovery will compete with the effects of GHG increases on SH tropospheric circulation changes, resulting in a poleward shift of the mid-latitude jet in all seasons

under high GHG emissions scenarios but little change or even an equatorward shift of the jet in austral summer under low GHG emissions scenarios.

- **Ozone-Induced Impacts on the SH Ocean and Cryosphere:**

- **Ocean and Sea Ice:** Observed upper Southern Ocean warming and freshening since the 1950s is driven primarily by increasing GHGs. Stratospheric ozone depletion plays a secondary role in the warming. In agreement with previous Assessments, ozone trends are unlikely to have driven the observed high-latitude sea surface temperature cooling and weak sea ice changes since 1979. Ocean eddies continue to remain a source of uncertainty in the ocean's response to wind changes.
- **Carbon Uptake:** The Southern Ocean carbon uptake exhibits strong decadal variations. Ozone changes are unlikely to have substantially contributed to the observed net change in Southern Ocean carbon uptake, consistent with the conclusion from the previous Assessment.
- **Antarctic Ice Sheet:** New modeling evidence suggests that stratospheric ozone depletion could potentially have influenced the surface mass balance of the Antarctic ice sheet by enhancing precipitation over the continent in the latter part of the 20th century. However, the underlying processes whereby stratospheric ozone depletion influences continentwide precipitation are poorly constrained; further, observed Antarctic surface mass balance shows large variability.

Climate impacts of the Montreal Protocol

- New evidence since the last Assessment shows that the decline in ODS emissions due to the implementation of the Montreal Protocol has already had an influence on SH circulation trends due to the stabilization and slow recovery of the Antarctic ozone hole, leading to a change in trends in the austral summer tropospheric circulation.
- Recent modeling studies estimate that the Montreal Protocol has already resulted in the avoidance of 0.17 ± 0.06 K global surface warming and 0.45 ± 0.23 K of Arctic surface warming in 2020, and will likely avoid about 0.5–1 K (0.79 ± 0.24 K) of global surface warming by the mid-21st century compared to a scenario with uncontrolled ODS emissions.
- New evidence since the last Assessment suggests that the Montreal Protocol has also potentially avoided an additional 0.5–1.0 K globally averaged surface warming by the end of the 21st century by protecting the terrestrial carbon sink from ultraviolet (UV) radiation damage, which would cause additional CO₂ to remain in the atmosphere.

¹⁰ Arctic amplification refers to the ratio of Arctic warming (60–90°N) to global warming over a given time period.

5.1 INTRODUCTION

A dedicated chapter on ozone-climate interactions has been part of the Ozone Assessment reports since 2006. While the main focus was initially on how anthropogenic climate change affects stratospheric ozone, since 2010 the focus has broadened on two-way interactions between stratospheric ozone and climate. The chapter is similar in scope to Chapter 5 of the 2018 Assessment (Karpechko, Maycock et al., 2018), assessing past and projected future changes in stratospheric climate and the role of stratospheric ozone and ozone-depleting substances (ODSs) for the climate system. The chapter builds on the chapters of previous Assessments with similar scope, as summarized below.

5.1.1 Summary from the Previous Assessment

Chapter 5 of the previous Assessment (Karpechko, Maycock et al., 2018) provided a detailed assessment of our knowledge of stratospheric temperature evolution. It was concluded that global average temperature in the lower stratosphere (13–22 km) cooled by about 1 K between 1979 and the late 1990s but has not changed significantly since then. In the lower stratosphere, ozone trends were the major cause of the observed cooling between the late 1970s and the mid-1990s. In the middle and upper stratosphere, long-lived greenhouse gases (GHGs) played a larger role in the cooling trends over this period. For the upper stratosphere (40–50 km), one-third of the observed cooling over the period 1979–2005 was due to ODSs and associated ozone changes, while two-thirds was due to well-mixed GHGs. Chemistry-climate model projections showed that the magnitude of future stratospheric temperature trends is dependent on the assumed future GHG concentrations, with higher GHG scenarios showing more cooling in the middle and upper stratosphere over the 21st century. The projected increase in global stratospheric ozone during this period (due to both decreasing ODSs and increasing GHGs) would offset part of the stratospheric cooling due to increasing GHGs.

The last Assessment concluded that there are indications for the acceleration of the stratospheric overturning circulation, the Brewer-Dobson circulation (BDC), in the lower stratosphere. In particular, observed changes in temperature and constituents indicate that tropical upwelling in the lower stratosphere has strengthened over the last ~30 years, in qualitative agreement with model simulations and reanalysis datasets. It is well understood that enhanced abundances of well-mixed GHGs lead to increased tropical upwelling in the lower stratosphere via changes in atmospheric wave dissipation. Moreover, changes in ODSs (and associated changes in ozone) were concluded to be a main driver of past and future changes of the BDC. In particular, increases in ODS concentrations between about 1980 and 2000 induced a notable increase in downwelling over the Antarctic, with an associated increase of tropical upwelling. The reduction of ODS concentrations after 2000 were simulated to reduce the GHG-induced acceleration of the BDC in the future. However, observational evidence for externally forced long-term changes in the BDC remain uncertain. The last Assessment concluded that as a consequence of a strengthening of the stratospheric overturning circulation and stratospheric ozone recovery, a future increase in stratosphere-troposphere exchange of ozone is projected to occur, increasing the future global tropospheric ozone burden.

Antarctic ozone depletion was concluded to be the

dominant driver of the changes in Southern Hemisphere tropospheric circulation in austral summer during the late 20th century, with associated weather impacts including a trend toward the positive polarity of the Southern Annular Mode (SAM) index and a wider Hadley cell. The trend toward the positive phase of the SAM index is associated with a southward shift of the mid-latitude westerly jet and storm track, resulting in drier conditions at higher latitudes of New Zealand and, as a result of the associated expansion of the Hadley cell, wetter conditions over subtropical latitudes of eastern Australia. Surface cooling occurs over Antarctica and warming on the peninsula. During other seasons, the contribution from increasing well-mixed GHGs played a more dominant role. In contrast, no robust links between stratospheric ozone depletion and long-term changes in Northern Hemisphere surface climate were established.

The changes in tropospheric weather patterns driven by ozone depletion were concluded to have played a role in the observed recent temperature, salinity, and circulation trends in the Southern Ocean, but the impact on Antarctic sea ice remained unclear. Modeling studies indicated that ozone depletion should have contributed to a decrease in Antarctic sea ice extent; hence, it cannot explain the observed sea ice increase between 1979 and 2015. The unprecedented rapid decline of Antarctic sea ice in 2016 was linked with the strong negative SAM (i.e., an equatorward shift of the extratropical surface westerlies) and extratropical sea surface temperature (SST) anomalies forced by the tropics. It was concluded that the inability of climate models to reproduce the observed Antarctic sea ice trends since 1979 limits confidence in the modeled sea ice response to ozone depletion. No robust evidence was found for a hypothesized causal link between the strength of the Southern Ocean carbon sink and ozone depletion. A remarkable reinvigoration of the Southern Ocean carbon sink was reported to have occurred since the early 2000s, following the previously reported slowdown of the carbon sink between the 1980s and early 2000s. Those results indicate that atmospheric circulation changes (whether driven by ozone depletion or not) have not had a considerable impact on the net strength of the Southern Ocean carbon sink.

The last Assessment concluded that as a result of the Montreal Protocol, global sea level rise of at least several centimeters has been avoided. This sea level rise would have occurred due to thermal expansion of the oceans stemming from the additional global warming from unregulated ODS emissions.

5.1.2 Scope of Chapter

The overall scope of this chapter is similar to that of Chapter 5 of the 2018 Assessment (Karpechko, Maycock et al., 2018) and Chapter 4 of the 2014 Assessment (Arblaster, Gillett et al., 2014). It provides an update to our knowledge of changes in stratospheric climate and assesses the role of stratospheric ozone changes for the climate system. Changes in stratospheric climate including temperature, circulation, and water vapor are assessed in *Section 5.2*; the changes are attributed to natural and anthropogenic forcing agents. The evolution of most relevant forcing agents is discussed elsewhere in the Assessment (*Chapters 1 and 2*) and therefore is only briefly summarized here (in *Section 5.2.1*). *Section 5.3* discusses the effects of stratospheric ozone changes on the whole climate system, from the stratosphere to the ocean, including the effect of ODS changes on surface climate through their direct radiative effects, for which new evidence has

been found since the last Assessment. Since the last Assessment, the role of two-way coupling between ozone and circulation received much attention, motivating a section on ozone-dynamical coupling. The last section of this chapter (*Section 5.4*) updates our knowledge of the climate impacts of the Montreal Protocol. Since we are by now well into the period of declining ODS concentrations, we can report on already-realized climate impacts of the Montreal Protocol in this section.

5.2 OBSERVED AND SIMULATED CHANGES IN STRATOSPHERIC CLIMATE

5.2.1 Overview of Relevant Anthropogenic and Natural Forcing Agents

Stratospheric climate change is influenced by a number of anthropogenic and natural external forcings. The evolution of most of those forcing agents is described elsewhere in the Assessment, so we provide only a brief summary below.

The evolution of ODS concentrations to date is described in detail in *Chapter 1* and hydrofluorocarbons (HFCs) in *Chapter 2*. Overall, ODS concentrations and the related total chlorine and bromine loading of the atmosphere have continued to decline since the last Assessment. ODSs impact the climate system through their important role in stratospheric ozone chemistry and because they are potent GHGs (see *Section 5.3.1*).

Anthropogenic GHGs, defined here as the three most important well-mixed GHGs (carbon dioxide [CO₂], methane [CH₄], and nitrous oxide [N₂O]), affect stratospheric temperatures directly, leading to cooling (see *Box 5-1* in Karpechko, Maycock et al., 2018). Further, GHG-induced tropospheric warming plays an

important role in stratospheric climate through its effect on large-scale circulation. An update on the evolution of global abundances and growth rates of CH₄ and N₂O is given in *Section 1.5.1* and the development of CO₂ abundances are covered in great detail in the recent Intergovernmental Panel on Climate Change (IPCC) report (IPCC, 2021). Briefly, the atmospheric abundance of all three GHGs continued to increase at rates similar to or higher than in previous years, and CO₂ reached a global average annual mean mixing ratio of 412.45 ppm in 2020. The CH₄ annual mean mixing ratio reached about 1874 ppt in 2020, and N₂O reached about 333 ppt in 2020 (see *Section 1.5.1*). The effects of the COVID-19 pandemic on the world economy resulted in a notable reduction of CO₂ emissions of about 7% compared to 2019 (Le Quéré et al., 2021; Szopa et al., 2021). But since atmospheric CO₂ concentrations are the result of the balance of a number of source and sink processes, the effect of those reduced emissions was not detected in global abundances or in the atmospheric concentration growth rate (Szopa et al., 2021).

The evolution of the global stratospheric ozone layer is determined by atmospheric chemistry and dynamics (described in detail in *Chapter 3*), but stratospheric ozone also acts as a forcing agent on the atmosphere and the climate system. The global ozone layer is beginning to recover from the effects of ODSs, with the near-global mean (60°S–60°N) total ozone column increasing by about 0.3% decade⁻¹ since the late 1990s. Therefore, the impacts of stratospheric ozone changes on the climate system (*Section 5.3*) are generally expected to reverse with ozone recovery, which started to appear in the late 1990s to early 2000s. However, ozone changes over the past two decades are regionally dependent, and they are strongly influenced by interannual variability (see *Chapters 3* and *4*), complicating the detection of reversals of ozone-induced trends in stratospheric temperature

Box 5-1. The Hunga Tonga-Hunga Ha'apai Volcanic Eruption of January 2022

Some past major volcanic eruptions have impacted the ozone layer, the stratospheric circulation, and surface climate (see *Sections 5.2* and *6.6*, and the *Chapter 6 Appendix*). The observed stratospheric changes from these events are particularly valuable for understanding the Earth's response to volcanic eruptions, but also for testing, and improving the representation of stratospheric aerosol microphysics, chemistry and dynamics in Earth system models. A very recent major eruption that injected a large amount of material into the stratosphere was the Hunga Tonga-Hunga Ha'apai (20.5°S, 175.4°W; hereafter referred to as HTHH) eruption in January 2022. HTHH produced two major phreatomagmatic (magma and seawater) eruptions on 13 and 15 January 2022. The second eruption initially injected material to altitudes greater than 55 km, which is higher than the stratopause and into the lower mesosphere (Carr et al., 2022). Satellite observations showed westward transport and diffusion of the HTHH plume in the stratosphere throughout the SH low latitudes and into the tropics in the months following the eruption.

The HTHH eruption led to significant perturbations in the stratosphere. Observations from satellite remote-sensing and balloon-borne instruments show the eruption injected SO₂ and HCl into the stratosphere, along with large amounts of H₂O. The H₂O injection was far beyond anything previously observed (Millán et al., 2022), while SO₂ and HCl amounts were within the emissions range from past observed eruptions. The total SO₂ amount emitted into the stratosphere (eventually converted into sulfate aerosol particles) was estimated to be 0.4–0.5 Tg. In comparison, the SO₂ amount injected into the stratosphere by the 1991 Mt. Pinatubo eruption was 15–20 Tg. Measurements from the Microwave Limb Sounder on the Aura satellite and balloon profiles show perturbations of stratospheric water that are unprecedented in the observational record in terms of both magnitude and altitude range. Initial estimates indicate that HTHH added about 10% to the total stratospheric water vapor burden.

Over the next few years, the eruption impact on ozone will be determined from observations and analyzed using model simulations. The injected H₂O and sulfate aerosol are expected to continue to perturb the stratosphere globally and, in particular, in the polar regions over the next years. A more complete understanding of this major and unique event will be available in the 2026 ozone assessment.

and circulation. In the future, stratospheric ozone is projected to recover from the effects of ODSs and to be influenced by increasing GHG concentrations, leading to considerable dependency of the future evolution of stratospheric ozone on the GHG scenario (see *Chapter 3*).

Perturbations to stratospheric aerosol concentrations can have a substantial impact on stratospheric temperatures (see *Section 5.2.2* and *Chapter 6*). Sources of stratospheric aerosols are primarily volcanic eruptions, but pyrocumulonimbus events associated with wildfires can also inject substantial amounts of aerosols into the stratosphere. In particular, the recent devastating bushfires that occurred in austral spring to summer 2019/20 in Australia (often referred to as Australian New Year fires) injected an unprecedented amount of aerosols from wildfire sources into the stratosphere, estimated to be comparable to a smaller-magnitude volcanic eruption (see *Section 6A.4*). While there has been no major volcanic eruption since Mt Pinatubo in 1991, smaller eruptions led to enhanced aerosol levels between 2005 and 2014, approximately doubling stratospheric aerosol optical depth compared to volcanic quiescent periods (see *Section 6.6*). The explosive eruption of Hunga Tonga-Hunga Ha'apai in January 2022 is expected to impact stratospheric ozone, circulation, and potentially surface climate (see **Box 5-1**). The origins and impacts of stratospheric aerosol injection are further detailed in *Chapter 6*.

Another external natural forcing on stratospheric climate is variability in the amount of total solar irradiance reaching the top of Earth's atmosphere. Particularly relevant for the understanding of stratospheric climate trends over recent decades is the 11-year solar cycle. While the total solar irradiance varies by less than 0.1% (or about 1 W m^{-2} ; Haigh, 2007) across the 11-year solar cycle, it has a notable influence on stratospheric ozone and temperature, as detailed in *Chapter 3*.

5.2.2 Stratospheric Temperatures

Stratospheric temperature variability and trends are key aspects of the climate system related to stratospheric ozone. Ozone and temperature changes are coupled in the stratosphere, where ozone influences temperature via radiative effects and temperatures impact both ozone-photochemical reaction rates and, in the polar regions, the frequency of occurrence of polar stratospheric clouds (PSCs) and associated impacts on heterogeneous chemical reaction rates (*Section 4.2.2.2*, see also **Box 5-2**). Quantifying and modeling past temperature changes are key goals for attribution and a requisite for confidently projecting future changes.

The 2018 Assessment highlighted improved estimates of observed stratospheric temperature trends from reprocessed datasets and attributed past and future temperature variability based on chemistry-climate model simulations (see *Section 5.1.1*). The major updates since 2018 involve lengthening and further analyses of the observational record, including use of radio occultation measurements beginning in 2002 and further modeling studies of past and future temperature evolution.

5.2.2.1 Observed Temperature Changes

Observations of stratospheric temperature come from operational and research satellite measurements, radiosondes, and long-term lidar measurements at a limited number of stations. Radiosonde observations extend from the surface to the lower stratosphere ($\sim 25 \text{ km}$) and span the longest period (since the late

1950s) but are influenced by discontinuities due to instrumentation changes and limited global sampling. Homogenized radiosonde datasets, such as RAOBCORE and RICH (Haimberger et al., 2012), have been constructed to address the instrumentation changes and derived trend results show reasonable agreement with temperature trends across broad layers in the lower stratosphere from satellite data (e.g., Steiner et al., 2020).

Global satellite measurements of tropospheric and stratospheric temperatures are available from the series of operational MSU and SSU instruments from late 1978 to 2005. These data represent broad-layer $\sim 10 \text{ km}$ and $\sim 20 \text{ km}$ averages atmospheric temperatures for the MSU and SSU measurements, respectively. The MSU time series have been updated using measurements from the series of AMSU instruments, which began in 1998. Merged time series of MSU/AMSU have been produced by several teams, including at the University of Alabama in Huntsville (UAH; Spencer et al., 2017), Remote Sensing Systems (RSS; Mears et al., 2011), and the NOAA Center for Satellite Applications and Research (STAR; Zou and Wang, 2011), with all three taking into account instrument calibration, satellite orbit changes, and other influences. These different merged datasets produce reasonably consistent time series and trend results, especially for the lower stratosphere (Steiner et al., 2020). The SSU time series from 1978 to 2005 were separately merged by Zou et al. (2014) and Nash and Saunders (2015), producing similar results within data uncertainties (Seidel et al., 2016; Maycock et al., 2018); the Zou et al. (2014) data exhibited more consistent vertical structure among the different SSU channels (Seidel et al., 2016). Zou and Qian (2016) extended the Zou et al. (2014) SSU data record beyond 2005 using AMSU measurements, and time series were independently updated by Randel et al. (2016) using research satellite data from Aura MLS (Livesey et al., 2022) and SABER (Remsberg et al., 2008). The updated SSU/AMSU and SSU/MLS time series show excellent agreement through 2018 (Steiner et al., 2020).

Time series of global average temperatures in the troposphere and stratosphere continue to develop as expected (see **Figure 5-1**, providing an update of the data in Steiner et al., 2020), with a warming troposphere and a cooling stratosphere. The stratospheric cooling increases with height, with a net cooling over the period 1979–2020 of approximately 0.8, 2.2, 2.6, and 3.1 K for the lower to upper stratosphere, respectively. As noted in the 2018 Assessment and in the recent IPCC report (Gulev et al., 2021), the rate of decadal-scale stratospheric cooling is larger prior to the late 1990s, with very small long-term changes in the lower stratosphere (TLS) after this time. The long-term trends are modulated by the well-known transient warming events in the lower to middle stratosphere following the El Chichón (1982) and Pinatubo (1991) volcanic eruptions, and the upper stratosphere is further modulated by the 11-year solar cycle. The lower stratospheric temperature (TLS) shows a short-term (~ 4 months) transient warming in early 2020 following enhanced stratospheric aerosols from the Australian New Year fires (Yu et al., 2021; Rieger et al., 2021).

Recent stratospheric temperature trend analyses include results from high-quality radio occultation measurements, covering an altitude range of ~ 10 – 30 km with a vertical resolution of $\sim 1 \text{ km}$, with global observations after 2002 (Shangguan et al., 2019; Steiner et al., 2020). While the data record is still relatively short for climate variability and trends, these measurements will become increasingly important as the data record lengthens in time.

In addition to satellite and radiosonde stratospheric temperature measurements, there are several meteorological reanalysis datasets covering the stratosphere provided by meteorological services. Reanalysis products are widely used in the research community for process studies, but developers have cautioned

against their use for long-term trend studies because of discontinuities introduced by the integration of different satellite data records (see also [Box 3-2](#)). There continue to be refinements in reanalysis systems that improve representation of trends in the relatively data-rich lower stratosphere (e.g., for ERA5.1; Simmons et

Box 5-2. Impact of GHG-Induced Stratospheric Cooling on Ozone Chemistry

The observed cooling of the stratosphere is driven by changes in ozone, ODSs, GHGs, stratospheric aerosols, and solar variability. Increasing concentrations of CO₂ are a major contributor to this cooling (see [Box 5-1](#) in Karpechko and Maycock et al., 2018 and [Section 5.2.2](#)). Other GHGs modestly enhance this cooling in the middle and upper stratosphere, while in the lower stratosphere, some GHGs (in particular halocarbons) oppose it to some extent (Ramaswamy et al., 2001). This radiatively driven decrease in stratospheric temperatures can be modified by dynamical processes. Climatologically, the stratospheric global overturning circulation leads to adiabatic cooling of the tropics, and adiabatic warming in the extratropics; the projected strengthening of the overturning circulation in response to GHG increases (see [Section 5.2.4](#)) can increase this dynamical cooling/heating. However, any forced modifications of the circulation at polar latitudes (i.e., changes in the polar vortex and associated polar descending motion) have been obscured by strong interannual variability in the past, and are largely model dependent for future projections, in particular in the Arctic ([Section 5.2.6.1](#)). This masks any clear trend in winter/spring Arctic lower stratospheric temperatures ([Chapter 4](#)).

The GHG-induced changes in stratospheric temperatures alter ozone chemistry. The abundance of ozone at a particular location in the stratosphere is governed by three processes: photochemical production, destruction by catalytic cycles, and transport processes. The catalytic destruction cycles occur through homogeneous gas-phase chemistry. In the polar lower stratosphere, heterogeneous chemical processes are also essential for creating the conditions that allow gas-phase ozone loss to occur. The efficiencies of both homogeneous as well as heterogeneous chemical processes depend on temperature, but in different ways. Therefore, stratospheric cooling from GHGs can have contrasting impacts on chemical ozone changes in different regions of the atmosphere, as detailed in the following.

Homogeneous Chemistry

In the stratosphere, ozone is produced by the photolysis of molecular oxygen in a process that is independent of temperature and maximizes in the tropical upper stratosphere. Globally this production is balanced by ozone loss through catalytic cycles involving homogeneous (gas-phase) chemical reactions. The stratospheric circulation transports ozone from regions of net production to regions of net loss. Globally, the most important ozone loss cycles involve reactive nitrogen and hydrogen, although chlorine and bromine play important roles in certain regions such as the polar lower stratosphere ([Chapter 4](#)) and upper stratosphere ([Chapter 3](#)). The reaction rates of these loss cycles are temperature dependent, and generally slow down with lower temperatures, causing a net increase in ozone. This inverse relationship between ozone and temperature changes was discovered for the upper stratosphere in the 1970s (Barnett et al., 1975) and the mechanisms have been explored in model simulations since the early 1980s (Haigh and Pyle, 1982). Overall, the slowdown in gas-phase ozone destruction leads to an increase in ozone due to GHG-induced cooling, particularly evident in the middle and upper stratosphere (see [Chapter 3](#)).

Heterogeneous Chemistry in the Polar Stratosphere

In the polar lower stratosphere, heterogeneous reactions that occur on the surface of polar stratospheric clouds (PSCs; frozen particles and supercooled liquid aerosols) become important. These reactions are responsible for converting chlorine (and to a lesser extent bromine) species into active, ozone-destroying forms. This leads to rapid gas-phase ozone loss once sunlit after the end of the polar night. PSCs form at temperatures below about 195 K. The Antarctic stratosphere reaches temperatures low enough for PSC formation for several weeks in winter and spring every year, but PSC occurrence is much less common and extensive in the Arctic except during very cold winters and springs. Under these specific conditions, significant springtime Arctic ozone destruction is observed ([Chapter 4](#)). While GHG-induced cooling is generally weak in the lower stratosphere (see [Section 5.2.2](#)), it could potentially lead to favorable conditions for PSC formation in the Arctic lower stratosphere, and therefore increase ozone depletion. Therefore, if GHG-induced cooling dominates Arctic lower stratosphere temperature changes in the future, we could expect enhanced springtime ozone depletion ([Chapter 4](#) and [Section 4.5.3.3](#)), especially while chlorine and bromine levels remain elevated.

In summary, it is well understood that global ozone, especially in the middle and upper stratosphere, increases with decreasing temperatures as the key gas-phase ozone destruction reactions slow down. The GHG-induced cooling has contributed to the observed increase in upper stratospheric ozone over the past two decades (since about year 2000), and will continue to do so in future projections that include rising GHG abundances (see [Chapter 3](#)). At polar latitudes, there is potential for enhanced ozone depletion due to an increased occurrence of PSCs with lower temperatures. However, it is still under debate whether GHG-forced changes in Arctic lower stratospheric temperatures have already affected PSC formation. Since the Arctic stratosphere is highly dynamically variable, it is also difficult to assess whether future GHG increases will lead to more favorable conditions for PSC formation (see discussion in [Chapter 4](#)).

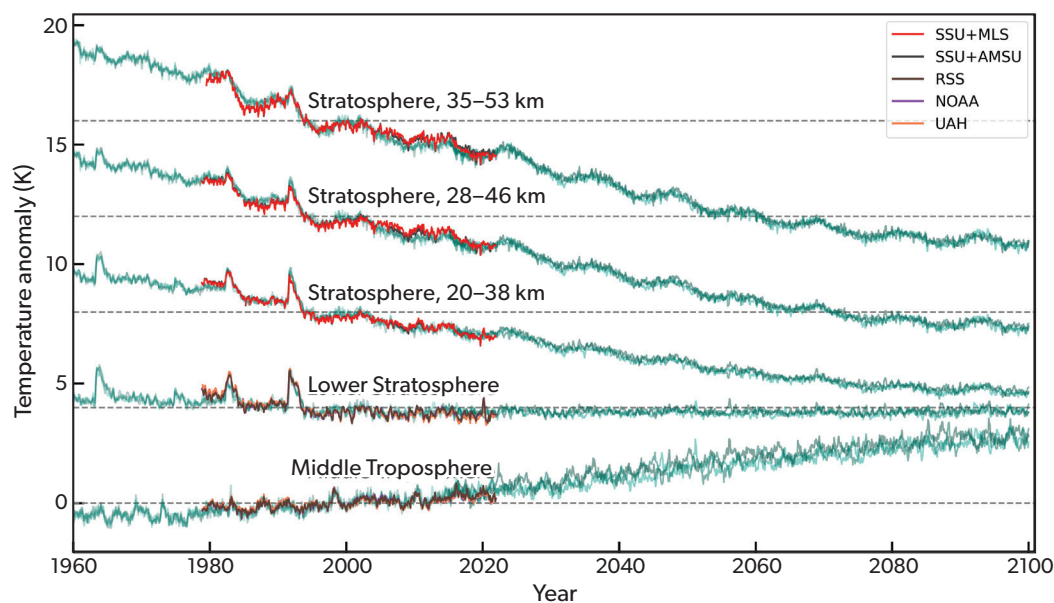


Figure 5-1. Time series of global average temperature anomalies for broad-layer averages from the middle troposphere to the upper stratosphere (bottom to top). Satellite observations are shown for 1979–2020 (see legend), updated from data described in Steiner et al (2020). Note that results from the different observational data sets often overlap, highlighting broad-scale agreement. Temperature anomalies are also shown for WACCM model simulations (green colors) for the recent past (1960–2018), from the so-called Ref-D1 CCMI-2022 simulations incorporating known historical forcings, and including 4 separate realizations. Simulations for 2015–2100 follow the Ref-D2 CCMI-2022 specifications, using SSP2-4.5 forcing and WMO2018 A1 halogens; the runs include an interactive ocean, and 3 realizations are shown. Anomalies from the two sets of model runs are merged for the overlap period 2015–2018.

al., 2020; Santer et al., 2021). However, significant differences in temperature variability and trends are evident among the current generation of reanalyses in the middle and upper stratosphere, where they rely primarily on satellite data (e.g., Long et al., 2017; SPARC, 2022).

5.2.2.2 Simulation and Attribution of Past and Future Stratospheric Temperature Changes

The 2018 Assessment included a review of chemistry-climate model simulations compared to observations, concluding that the model-simulated temperatures were in agreement with observations from the lower to the upper stratosphere for the period 1979–2016. GHG increases are the dominant mechanism for cooling in the middle and upper stratosphere, modulated by ozone changes linked with evolving ODSs and temperature-dependent photochemistry (Aquila et al., 2016; Maycock et al., 2018). Ozone changes that occurred between the start of the observational record in 1979 and the mid-1990s are the dominant influence on temperature in the global lower stratosphere. Stability of lower stratospheric ozone after the late 1990s accounts for the relatively constant TLS temperatures after that time, extending to 2020. **Figure 5-1** includes an updated comparison of observations with simulations of the recent past from one model, showing quantitative agreement for a model forced by observed SSTs, GHGs, and ODSs, along with volcanic and solar cycle effects. Comparisons of lower stratosphere temperature trends across the suite of CMIP6 models using historical forcings highlights

significant variability among models but consistent agreement (within uncertainties) with homogenized radiosonde data and ERA5.1 (Mitchell et al., 2020).

Model projections of future atmospheric temperature changes over the 21st century show continued cooling in the middle and upper stratosphere (**Figure 5-1**). Updated evaluations of past and future temperature changes quantify the relative roles of GHGs and ODSs in these trends (Garcia et al., 2019). Ozone decreases lead to relatively strong contributions to middle-to-upper stratosphere cooling during the period of strongest ozone losses (1975–1995); smaller stratospheric temperature trends have occurred prior to and after this period. Modeled future middle-atmosphere temperature trends are dominated by GHG changes, with simulated cooling directly related to the GHG scenario, e.g., stronger cooling for RCP8.5 versus RCP6.0 (**Figure 5-2**) and reduced cooling trends after about 2060 for SSP2-4.5 (**Figure 5-1**). Stratospheric cooling is modulated by corresponding ozone changes, with weaker cooling over the first half of the 21st century, driven by increases in ozone in the upper stratosphere due to decreasing ODSs under the Montreal Protocol.

Overall, our assessment is in agreement with the IPCC (Gulev et al., 2021; Eyring et al., 2021; Lee et al., 2021) in all aspects regarding the evolution of stratospheric temperature. In summary, observational records show continued cooling of the global middle and upper stratosphere (at a rate of about -0.6 K decade⁻¹), while lower-stratospheric temperatures have shown no significant trends since the late 1990s. Model projections of future

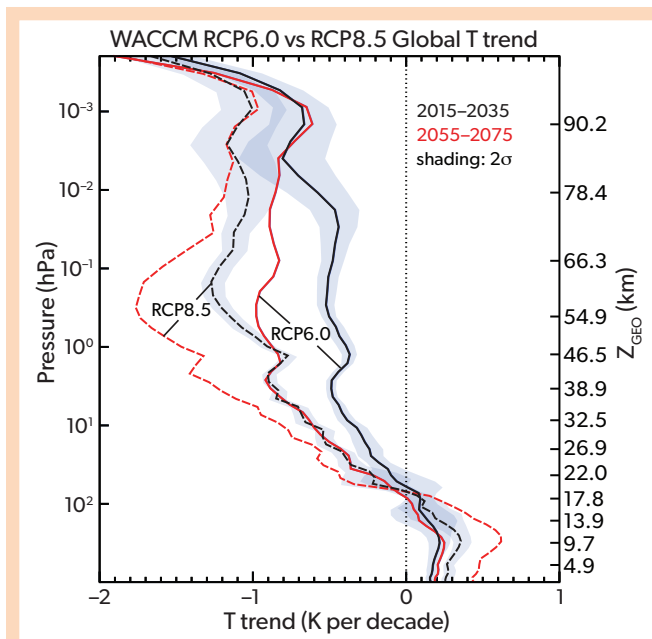


Figure 5-2. Projected global mean temperature trend profiles for periods in the early (2015–2035) and late (2055–2075) 21st century calculated from the WACCM chemistry-climate model for the RCP6.0 (solid) and RCP8.5 (dashed) emissions scenarios. The uncertainty ranges (2 standard deviations) are shown for 2015–2035 trends in both scenarios and are also representative of the uncertainties for the 2055–2075 profile. [From Garcia et al., 2019.]

atmospheric temperature changes over the 21st century show continued cooling in the middle and upper stratosphere, with the magnitude depending on the GHG emissions scenario. This evolution is consistent with the expected effects of changes in ozone, ODSs, and GHGs, as well as variability induced by stratospheric aerosols and solar variability.

5.2.3 Stratospheric Water Vapor

Stratospheric water vapor directly influences the climate system through longwave radiative processes, wherein increased water vapor cools the lower stratosphere and warms the troposphere (Forster and Shine, 1999; Solomon et al., 2010; Li and Newman, 2020). Stratospheric water vapor also influences ozone abundances through its role as a source of reactive hydrogen (HO_x) and via the formation of PSCs. The 2018 Assessment highlighted continuing measurements of water vapor from satellites and balloons and their general agreement in terms of variability and changes. The observational satellite data record of stratospheric water vapor, which is based on merged datasets from the early 1990s to the present, is characterized by large decadal-scale variability, including well-known decreases around the year 2000 (e.g., Solomon et al., 2010) and increases thereafter (Yue et al., 2019). However, there are no significant long-term trends in the observations over the period 1993–2020 (Yu et al., 2022). Recent work has strengthened the observational understanding of processes influencing water vapor entry across the tropical tropopause, along with improving the evaluation of updated model

simulations and improving theoretical knowledge on water vapor radiative effects, as discussed below.

5.2.3.1 Processes Controlling Water Vapor Entry Across the Tropical Tropopause

Stratospheric water vapor is primarily controlled by the freeze-drying of air passing through the cold tropical tropopause, under the influence of the mean upward tropical Brewer-Dobson circulation (BDC). Transport through monsoon circulations and overshooting deep convection can also contribute, but these are likely small effects (Nuetzel et al., 2019; Jensen et al., 2020; O’Neill et al., 2021). Water vapor increases with height in the stratosphere due to the slow oxidation of methane (CH_4), and this contribution becomes relatively important in the tropics above ~25 km, or at higher latitudes where stratospheric air is relatively “aged” (Waugh and Hall, 2002). Observed increases in tropospheric CH_4 (see Section 5.2.1) are estimated to contribute ~0.1 ppmv decade⁻¹ to the water vapor trend above the middle stratosphere, accounting for a substantial fraction of the 2002–2018 observed trends in this region from the SABER satellite (Yue et al., 2019). High-quality satellite measurements of stratospheric water vapor since the early 1990s (from the HALOE, SABER, and Aura MLS satellites) provide improved understanding of processes influencing variability and trends. Comparisons of satellite data with stratospheric balloon measurements at several locations (Hurst et al., 2016) suggested a possible drift in MLS v4.2 water vapor retrievals after 2010, which has been partially corrected in updated MLS v5.1 retrievals (Livesey et al., 2021).

Satellite observations demonstrate strong control of tropical tropopause temperatures on interannual water vapor changes throughout the near-global (60°S–60°N) stratosphere (Randel and Park, 2019). Tropical lower stratosphere water vapor variations are strongly correlated with the cold point tropopause (Figure 5-3, left panel). The associated near-equatorial water vapor anomalies subsequently propagate vertically in the tropics and poleward in the lower stratosphere, following the BDC. Reconstruction based on lagged regressions with tropopause temperatures capture a majority of water vapor variability in these regions (Figure 5-3, right panel). Water vapor variations in the extratropical lowermost stratosphere (below the 380 K isentrope), which are key for radiative effects, are less strongly coupled to the tropical tropopause. The close relationship of tropical stratospheric water vapor and tropopause temperature also occurs for zonal asymmetries (Suneeth and Das, 2020). Boreal summer monsoon circulations contribute to water vapor transport into the deep tropics (Nuetzel et al., 2019), contributing up to 14% to the moist phase of the annual cycle (i.e., the tropical tape recorder). This results in somewhat weaker coupling of water vapor with tropical tropopause temperatures in this season (Randel and Park, 2019). While convective ice lofting associated with extreme convection has been discussed as a possible contribution to the stratospheric water vapor budget, enhancements above background concentrations occur infrequently in the deep tropics and have a limited impact (Jensen et al., 2020; Plaza et al., 2020; Feng and Huang, 2021). Observations suggest direct hydration is more important over North America during boreal summer, with the influence of direct water injection reaching up to approximately 1 km above the local cold point tropopause (Yu et al., 2019; Wang et al., 2019a; Jensen et al., 2020). Over the coming years, we expect to see perturbations in stratospheric water vapor from

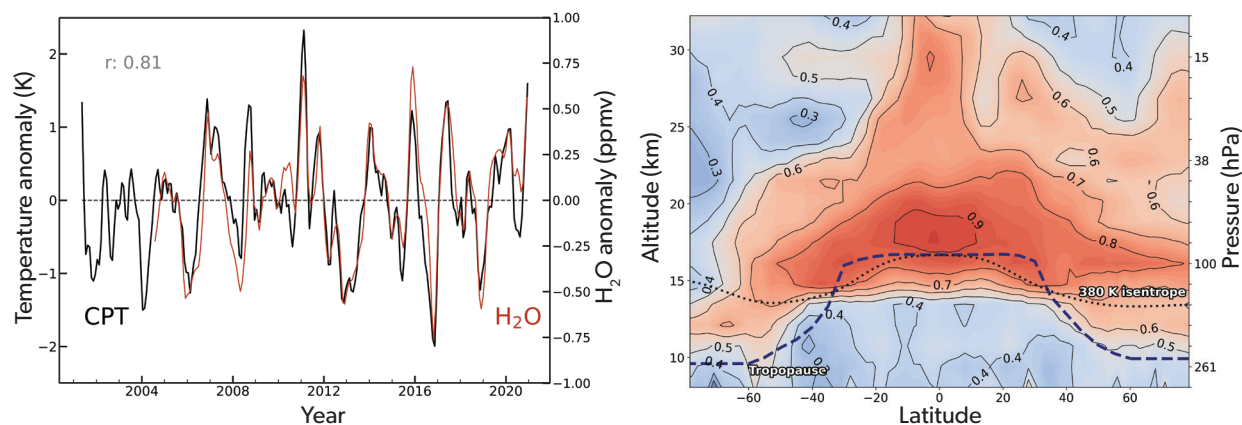


Figure 5-3. Temperature control of water vapor entry at the tropical tropopause. (left) Time series of deseasonalized anomalies in tropical cold point tropopause (CPT) temperature from GPS radio occultation (10°S–10°N) and equatorial (5°N–5°S) 83 hPa water vapor from Aura MLS. (right) Correlation of deseasonalized anomalies in Aura MLS water vapor over 2004–2020 versus water vapor reconstructed from lagged regressions onto the tropical CPT. [Updated from Randel and Park (2019) using MLS v5.1 H₂O retrievals (Lambert et al., 2020).]

the unprecedented eruption of the Hunga Tonga-Hunga Ha’apai volcano (see **Box 5-1**).

5.2.3.2 Updates on Modeling and Understanding of Radiative Effects of Stratospheric Water Vapor

Stratospheric water vapor has been analyzed in CCM1 and CMIP6 models, showing overall consistent behavior compared to observations and close coupling to tropical tropopause temperatures within each model. However, there is a large diversity among models in cold point temperatures and water vapor amounts (Keeble et al., 2021; Garfinkel et al., 2021). Climate change projections consistently show decadal-scale increases in tropopause temperatures and stratospheric water vapor. Detailed calculations demonstrate that water vapor exhibits a similar response to diverse climate forcing agents (including CO₂, CH₄, solar variability, and sulfate aerosol) through slow feedbacks involving equilibration of SSTs. For forcings that directly warm the tropical tropopause region, such as black carbon aerosols, water vapor changes mostly represent a fast (non-SST-mediated) rather than a slow response (Wang and Dessler, 2020).

There is improved understanding of the climate feedback through stratospheric water vapor changes from analyses of large perturbations in idealized CO₂ quadrupling experiments within the multi-model CMIP5 effort (Banerjee et al., 2019) and analyses from experiments in individual model studies (Li and Newman, 2020; Huang et al., 2020). Stratospheric water vapor increases produce a positive net climate feedback, contributing up to ~10% of the global mean surface warming under CO₂ quadrupling. However, there is considerable intermodel variability in these results, possibly due to both intermodel differences (e.g., in radiative transfer codes) and differences in calculation of the feedback (e.g., offline radiative feedback calculations versus fixed water vapor experiments). Results from one model suggest that associated feedbacks from upper-tropospheric temperatures and

clouds can reduce the surface warming feedback to a few percent (Huang et al., 2020). These differences call for improved understanding of the complex feedback mechanisms, and for quantifying the differences in methodologies used to calculate the feedbacks. Calculations highlight the important role of water vapor in the extratropical lowermost stratosphere for radiative feedback. Water vapor also impacts stratospheric temperatures and circulation, including contributing ~30% of the simulated acceleration of the BDC in one model (Li and Newman, 2020).

In summary, new studies since the last Assessment led to improved process understanding of water vapor entry to the stratosphere by showing that interannual changes in lower-stratospheric water vapor are quantitatively consistent with observed tropical tropopause temperatures. Monsoon circulations and overshooting convection have relatively small contributions. Models predict small decadal-scale increases in tropopause temperature and lower-stratospheric water vapor as a response to GHG increases, but these changes are not evident within the year-to-year variability of the observational records. Lastly, radiative effects of stratospheric water vapor under climate change are sizable but exhibit considerable model uncertainty.

5.2.4 Brewer-Dobson Circulation

Chapter 5 of the previous Assessment (Karpechko, Maycock et al., 2018) showed that the discrepancy in trends in the strength of the BDC between observations and models, first pointed out in the 2000s (Engel et al., 2009; Waugh et al., 2009), can be reconciled in the lower stratosphere but persists in the mid-to-upper stratosphere. Specifically, models project a robust strengthening of the BDC throughout the stratosphere in response to increasing GHGs. The 2018 Assessment shows that while there is observational evidence to support the strengthening of the BDC in the lower stratosphere, observations from tracer measurements show weakening trends (albeit not significant) at upper levels (above ~24 km).

Since the 2018 Assessment, a number of studies have advanced knowledge on this open question by providing new estimates of the uncertainty in stratospheric mean age of air (AoA) derived from tracer observations. Mean AoA is a measure of the average transport time from a reference surface (e.g., the tropopause or ground) to a certain point in the stratosphere and thus quantifies the integrated strength of the BDC. A negative trend in AoA would therefore be consistent with a strengthened BDC. AoA can be estimated from long-lived tracers and compared to models (see Box 5-2 in Karpechko, Maycock et al., 2018). However, deriving AoA values from observations that are comparable with models is not trivial, and understanding how different factors influence the trends is key, given the small trend values relative to the large internal variability. Uncertainties are due to the nonlinearity of tracer time series (Garcia et al., 2011; Fritsch et al., 2020), as well as to chemical sinks, in particular of SF₆ (sulfur hexafluoride; Kouznetsov et al., 2020; Kovacs et al., 2017; Leedham-Elvige et al., 2018; Adcock et al., 2021; Loeffel et al., 2022).

Similar to the 2018 Assessment, the best estimates of the observed and modeled trends are of opposite sign in the northern middle stratosphere. This is illustrated in Figure 5-4, which shows the most recent estimates of mean AoA trends at northern mid-latitudes in the middle stratosphere in observations and models. The model output has been subsampled to mimic the limited sampling of the observations (following Abalos et al., 2021). A new result is that the large observational uncertainties in the latest estimates result in a partial overlap with the model trends (over 50% of the simulation error bars have some overlap with the lower bound in the latest observational estimate). This modest step toward convergence of the modeled and observed ranges partly results from the larger uncertainties in the model trends when accounting for the limited spatial and temporal sampling in the observations (as pointed out in Garcia et al., 2011)

and partly from updated parameters in the derivation of AoA from observed tracer abundances (Fritsch et al., 2020). Additional uncertainty that is not fully taken into account arises from the model results being based on idealized AoA tracers and therefore not exactly comparable with the observational estimates, which are based on real tracers. While acknowledging these uncertainties is a key advance since the 2018 Assessment, there remains a clear disagreement in the sign of BDC trends between models and observations in the middle and upper stratosphere.

New evaluation of the BDC in reanalyses since the last Assessment provides evidence that the spread in the climatology and the trends is too large among different reanalysis products to help constrain their values (Chabrillat et al., 2018; Ploeger et al., 2019; Diallo et al., 2021; Chapter 5 of SPARC, 2022). Most reanalyses feature an acceleration of the BDC (i.e., a negative AoA trend) over the last ~30 years, consistent with models but inconsistent with observations, as shown in Figure 5-5. However, this figure also reveals the important differences in the magnitude and spatial structure of the trends across different reanalysis datasets. ERA-Interim is the only reanalysis showing positive AoA trends in the NH mid-to-upper stratosphere over the period considered. These positive trends are consistent with observations but inconsistent with other reanalyses, including the new-generation ECMWF reanalysis, ERA5 (Figure 5-5; for further details, see Chapter 5 of SPARC, 2022).

Decadal changes in AoA over the most recent period (since approximately 2002) obtained from satellite tracer measurements reveal an inter-hemispheric asymmetry, with BDC strengthening (AoA decrease) in the Southern Hemisphere and weakening (AoA increase) in the Northern (Stiller et al., 2012; Mahieu et al., 2014; Stiller et al., 2017; Strahan et al., 2020; Han et al., 2019). Such asymmetry in recent decadal AoA changes is captured by all modern reanalyses (Ploeger et al., 2019; 2021; Ploeger and

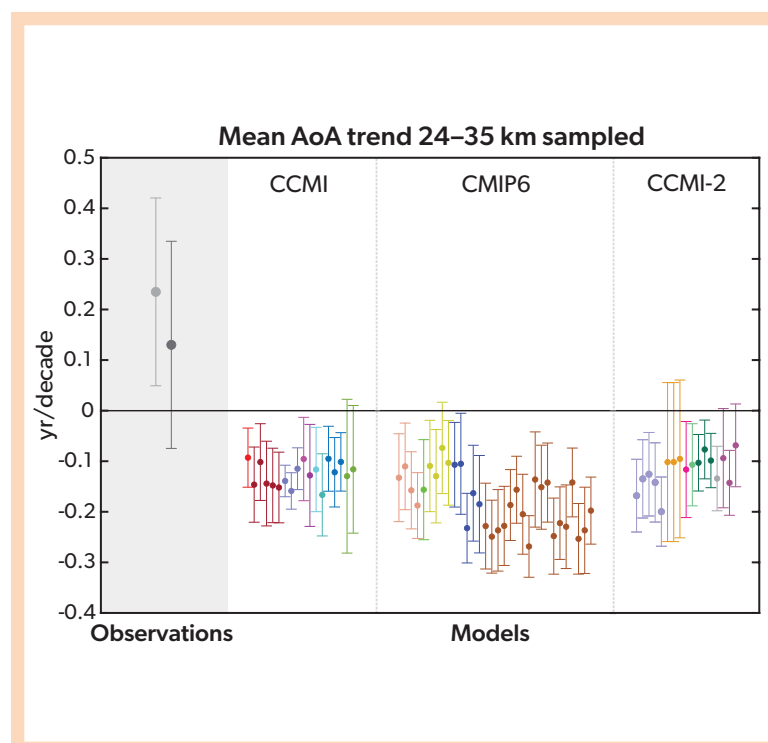


Figure 5-4. Mean AoA trends for the period 1975–2005 from observations and model simulations, with model data sampled at times and locations corresponding to the observations (Engel et al., 2009; Fritsch et al., 2020). Specifically, AoA is averaged over 24–35 km log-pressure altitudes and sampled at the same latitudes and months as the observations. Three families of model simulations are shown: CCM1 REF-C1, CMIP6 historical, and CCM12 REF-D1. Each model is represented in a different color, and multiple ensemble simulations are included for some models, to account for the influence of internal variability on the trends. The mean AoA trend derived from observations is shown on the left (inside the gray shaded area): the original value from Engel et al. (2009) (light gray), and that obtained from the same data but using an updated method to derive AoA from tracer concentrations, as described in Fritsch et al. (2020) (dark gray). Error bars represent least square regression slope uncertainty at the 95% confidence level for the models, while for the observations they include additional measurement error estimates. [Adapted from Abalos et al., 2021.]

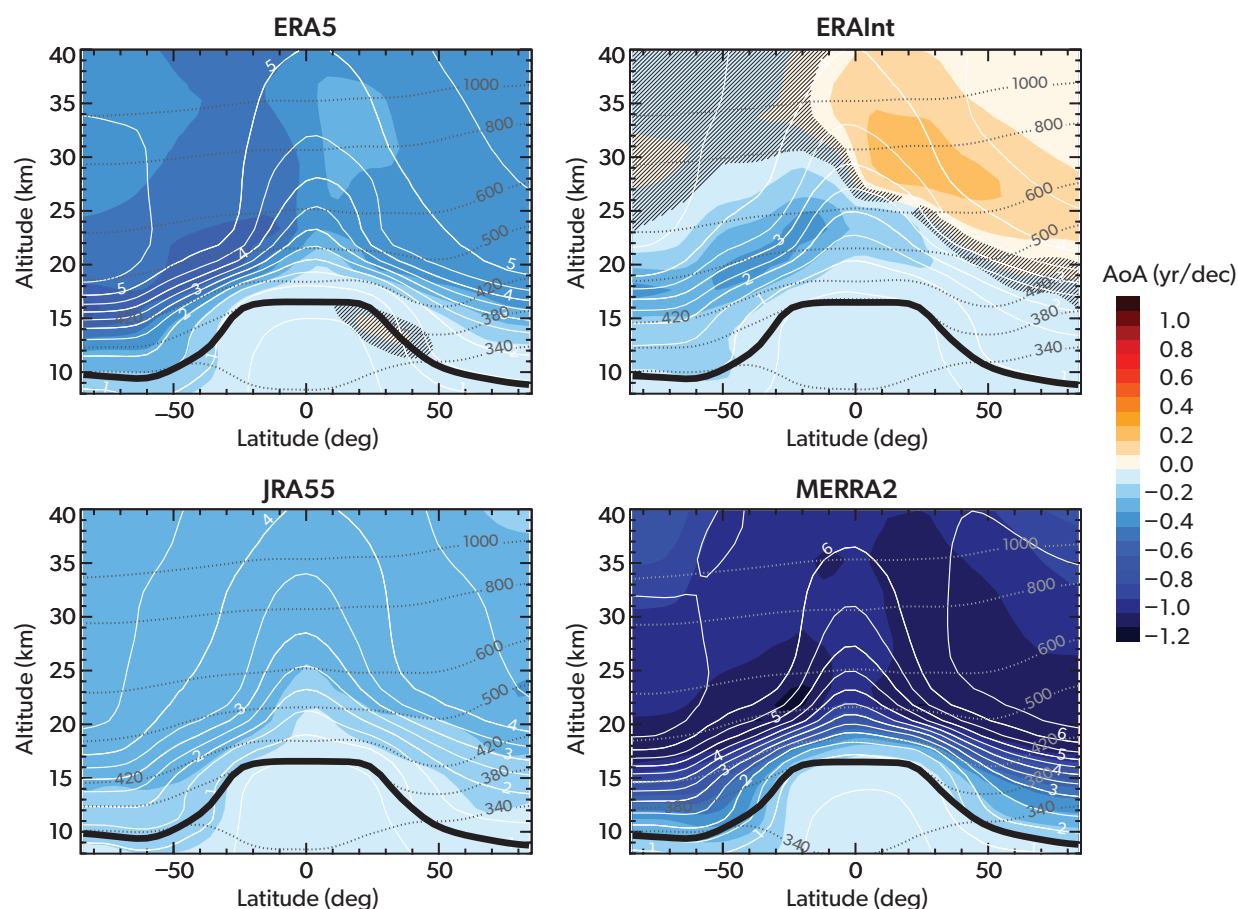


Figure 5-5. Trends in mean AoA in four modern reanalyses over the period 1989–2015 (shading), computed using the Lagrangian transport model CLaMS. Thin solid contours show the mean AoA climatology, with contour spacing of six months. The solid thick contour shows the lapse-rate WMO tropopause. Thin dashed contours show selected isentropes with labeled values in K. Note that the updated ERA5.1 is used for the 2000–2006 period in the ERA5 panel, as in Ploeger et al. (2021). [Adapted from Ploeger et al., 2019, 2021.]

Garny, 2022). The mechanism proposed to explain these changes consists of a southward displacement of the region of tropical upwelling and associated changes in mixing, which in turn has been linked to decadal variability associated with the Quasi-Biennial Oscillation (QBO; Strahan et al., 2020). Differences in changes in the deep and shallow residual circulation branches have also been proposed to affect the inter-hemispheric asymmetry (Han et al., 2019, Ploeger and Garny, 2022). These recent studies highlight the crucial role of internal climate variability in limiting the detection of externally forced long-term trends over the observational period. In particular, it is important to account for this decadal internal variability in transport in order to interpret recent trends in lower-stratospheric ozone (see Chapter 3).

In model simulations, two main external forcings dominate the long-term BDC trends: trends in GHGs and trends in ODSs. The proposed mechanism for the former is that as well-mixed GHGs warm the troposphere, the associated changes in thermal wind balance in the subtropical lower stratosphere modify wave propagation and dissipation conditions, which in turn accelerate the residual circulation (Shepherd and McLandress,

2011). A robust strengthening of the BDC with GHG increases has been projected by models for decades, and new multi-model studies provide updated confirmation of this result (Eichinger et al., 2019; Polvani et al., 2019; Abalos et al., 2021). The global stratospheric mean AoA is projected to decrease about -0.05 years decade⁻¹ over the 21st century under the RCP6.0 scenario (Eichinger et al., 2019). In general, trends emerge faster in the integrated measure of mean AoA compared to the residual circulation strength and emerge faster in the lower stratosphere (shallow branch) than in the middle stratosphere (deep branch) (Abalos et al., 2021). While ODSs are also well-mixed GHGs, their main impact on the BDC occurs through the dynamical coupling with Antarctic ozone depletion (Abalos et al., 2019). Specifically, the polar lower-stratospheric cooling due to ozone depletion delays the polar vortex breakdown (see Section 5.2.6.1) and leads to enhanced wave propagation in austral summer. The key role of ODSs on the BDC trends highlighted in the previous Assessment has been confirmed by further studies over the last few years. Specifically, ozone depletion was the main driver of the acceleration in austral summer polar downwelling over the

last decades of the 20th century. Moreover, its effect extends to the annual mean global circulation, such that more than half of the modeled mean BDC acceleration over the last few decades of the 20th century was driven by ozone depletion (Oman et al., 2009; Polvani et al., 2018; Li et al., 2018; Abalos et al., 2019; Polvani et al., 2019). Simulations using RCP6.0 and A1 WMO scenarios for well-mixed GHGs and ODSs, respectively, consistently predict a future (2000–2080) global mean AoA trend that is about 50% weaker than the simulated trends for the past (1980–2000) due to ozone recovery (Polvani et al., 2019). A weakening of the tropical upwelling trends after the year 2000 derived from satellite temperature observations (Fu et al., 2019) is consistent with the timing of ozone stabilization and recovery. However, the observationally derived trends of tropical upwelling in Fu et al. (2019) do not feature the expected seasonality of ozone depletion and recovery effects on the BDC, which maximizes in the December–January–February period for SH downwelling in models.

As reviewed in Chapter 5 of the last Assessment (Karpechko, Mayock et al., 2018), the mean transport time along the BDC, quantified by AoA, is the space- and time-integrated effect of two main processes: the residual circulation and two-way mixing (Plumb, 2002). Since the last Assessment, a number of studies highlighted the importance of those processes for the simulation of stratospheric transport and its trends. AoA trends are driven by a combination of an enhanced residual circulation and mixing changes, and intermodel differences in the trend magnitude relate to differences in mixing changes (Eichinger et al., 2019). Moreover, recent studies have shown that differences in mixing (independent of the residual circulation) are the main cause of the large intermodel differences in the AoA climatology (Dietmüller et al., 2018). These results highlight the importance of both resolved and sub-grid-scale mixing for constraining stratospheric transport in global models. Another important result from new studies is that nudging the model’s meteorology to reanalysis fields does not help constrain the BDC. On the contrary, it increases the intermodel spread (Chrysanthou et al., 2019; Orbe et al., 2020; Davis et al., 2020; Davis et al., 2022). This result cautions against the use of nudged simulations for studies of the BDC and underlines the need to improve nudging techniques, as nudged simulations are often used to compare with observations.

In summary, new studies on BDC changes confirm the long-known robust result that models simulate a BDC strengthening,

caused by both GHG increases and by ozone depletion that was driven by ODS increases over the last four decades of the 20th century. Future strengthening of the BDC due to increasing GHG concentrations outweighs the effects of ozone recovery in the RCP6.0 scenario; as a result, an acceleration (though weaker by about 50%) is expected in the future. The longstanding discrepancy between models and observational evidence of past BDC trends in the mid-stratosphere is not yet resolved. Nevertheless, updated calculations of observational AoA estimates marginally overlap with the simulated strengthening of the BDC. Overall, recent studies highlight the crucial role of observational uncertainties and internal decadal variability in limiting the detection of externally forced BDC trends.

5.2.5 Stratosphere-to-Troposphere Transport

Variations in stratosphere-troposphere exchange are important contributors to the variability of ozone concentrations, particularly in the troposphere, where the background concentrations are small compared to those of the stratosphere. The last Assessment stated that both greenhouse gas increase and stratospheric ozone recovery will tend to increase the future stratosphere-to-troposphere transport (STT) of ozone. This result has recently been shown to be robust across CCM1 models. This is due to the stronger STT associated with the strengthening of the BDC in response to increasing greenhouse gas abundances (see Section 5.2.4), as well as to an increased ozone reservoir in the lowermost stratosphere with ozone recovery (Abalos et al., 2020). Consistent with the latter mechanism, stratospheric ozone depletion has had a large impact on tropospheric ozone trends over the period 1979–1994 in some regions (Griffiths et al., 2020). The strong coupling between ozone STT and the acceleration of the residual circulation in models is illustrated in Figure 5-6; models with a stronger acceleration of the BDC feature larger increases of stratospheric-origin ozone concentrations in the troposphere. The stratospheric ozone tracer is the same as ozone in the stratosphere and has chemical and depositional loss (but no production) in the troposphere. In addition to this large-scale mechanism, an increase in tropopause fold frequency with climate change could contribute to local enhancements of ozone STT in the future (Akritidis et al., 2019).

In addition to the importance of ozone STT, the evolution of the global tropospheric ozone burden depends to a large extent

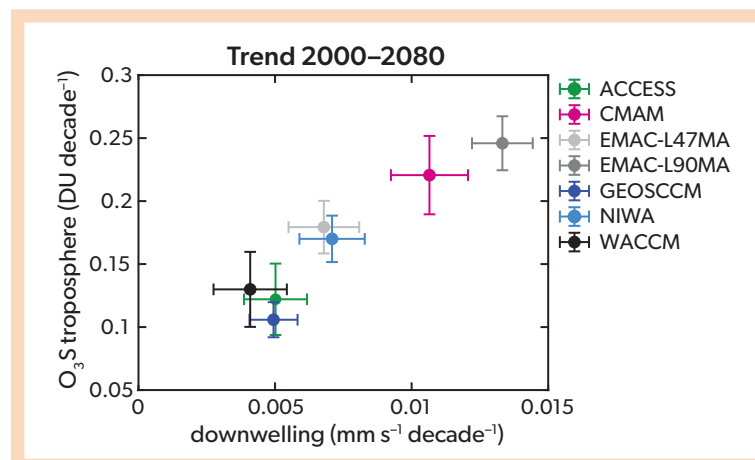


Figure 5-6. Relationship between downwelling changes and stratosphere-to-troposphere ozone transport, shown as a scatter plot of trends in a stratospheric ozone tracer integrated over the troposphere versus extratropical downwelling acceleration in the lower stratosphere (averaged 30°N/30°S and the poles at 70 hPa) for seven models, based on CCM1-1 REF-C2 simulations. The stratospheric ozone tracer is the ozone that originated in the stratosphere and has chemical and depositional loss (but no production) in the troposphere. [Adapted from Abalos et al., 2020.]

on the evolution of tropospheric ozone precursor emissions. This is reflected in the different evolution of tropospheric ozone in the various SSP scenarios, with methane emissions playing a particularly important role (Morgenstern et al., 2018; Abalos et al., 2020). More details on the future evolution of tropospheric ozone and the different factors affecting it can be found in *Section 3.4.5* and **Box 3-4**.

In order to best understand and model the externally forced long-term trends in ozone STT, it is important to quantify the internal interannual variability. New studies since the last Assessment find a significant increase in ozone STT during the positive El Niño-Southern Oscillation (ENSO) phase near the Pacific subtropical jet, in agreement with previous results, while the QBO effects on STT remain more uncertain (Olsen et al., 2019). The influence of stratospheric ozone on interannual variability in tropospheric concentrations is particularly strong in North America (Liu et al., 2020), due to enhanced STT mainly in spring (Breedon et al., 2021). Nevertheless, the effects of ENSO and the QBO on the globally integrated ozone STT are small (Olsen et al., 2019).

In summary, consistent with the previous Assessment, increased ozone transport from the stratosphere to the troposphere is expected in a future climate, due to both strengthened BDC and stratospheric ozone recovery.

5.2.6 Stratospheric Winds

5.2.6.1 Polar Vortices

The state of the stratospheric polar vortex in both the Southern and Northern Hemispheres is a crucial factor in determining the possibility for heterogeneous ozone depletion (see *Chapter 4*, including the definition of polar vortex in **Box 4-1**). Conversely, the strength of the polar vortex can be modified by strong polar ozone depletion through an increase of the meridional temperature gradient. The following section assesses dynamical variability of the polar vortex and its long-term changes, while *Chapter 4* discusses its role for polar ozone.

In previous Assessments, it was reported that the strong SH polar ozone depletion had led to an increase in vortex strength in austral spring and summer, resulting in a delay of the SH polar vortex breakdown. This trend attenuated over more recent years, consistent with the lack of trend in polar ozone (see *Chapter 4*). Ozone recovery is expected to lead to earlier vortex breakup dates. Models project that increasing GHG concentrations will delay recovery of the SH vortex breakup date, although the mechanism for this delay is not entirely understood (Ceppi and Shepherd, 2019; Mindlin et al., 2020). As a result of the two opposing effects of ozone recovery and GHG increase on the SH vortex, the delay caused by ozone depletion is projected to not be fully reversed by the end of the 21st century (Wilcox and Charlton-Perez, 2013; Rao and Garfinkel, 2021a). The vortex breakup date will rather remain constant or become delayed even further (Mindlin et al., 2021) in both moderate- and high-emissions scenarios (Rao and Garfinkel, 2021a). As further detailed in *Section 5.3.2*, recent studies indicate that two-way coupling between ozone and polar vortex dynamics enhanced past ozone-induced trends in the polar vortex.

As stated in the last Assessment and in the IPCC Sixth Assessment Report (IPCC AR6; see *Section 2.3.1.4.5* of Gulev et al., 2021), large interannual and decadal variability hinders

the detection of long-term changes in the NH polar vortex, and it was assessed that the vortex weakening over the last decades is likely a result of internal variability. There are no indications for a past influence of NH polar ozone depletion on long-term polar vortex trends, due both to the far weaker ozone depletion in the Northern compared to the Southern Hemisphere and to the strong interannual variability in the NH polar vortex.

Future changes in the NH polar vortex strength are uncertain, and the mechanisms for changes in the polar vortex, as well as reasons for the large intermodel spread, are still under discussion (Wu et al., 2019; Ayarzagüena et al., 2018, 2020; Rao and Garfinkel, 2021b). The nonlinearity of the response of the polar vortex strength to surface warming reported by Manzini et al. (2018) has been further supported by analysis of a multi-model dataset (Kretschmer et al., 2020). Arctic sea ice loss trends continue to be explored as potential drivers for a future decrease of the NH polar vortex strength (Kretschmer et al., 2020; Kim and Kim, 2020), although some studies question this connection (e.g., Seviour, 2017). Another suggested driver of the future trends in the NH polar vortex are changes in vertical planetary wave propagation conditions, driven by the warming trend in the tropical troposphere (Karpechko and Manzini, 2017). In addition to changes in its mean strength, studies report a possible future shift of the position of the vortex (Matsumara et al., 2021). Under high-emissions scenarios, it was projected that the occurrence of low temperatures within the polar vortex will increase in the future (von der Gathen, 2021), with potentially important impacts for polar ozone (see *Chapter 4* and **Box 5-2**). However, the robustness and mechanism for such increases in the occurrence of low temperatures, and how they are linked to dynamical changes of the polar vortex or to radiative effects, remain to be understood.

Recent winters have exhibited strong anomalies in both the Arctic and Antarctic polar vortices, resulting in strong ozone anomalies (see *Chapter 4*). In early 2020, the NH polar vortex was anomalously strong, leading to a record-low ozone (Lawrence et al., 2020; *Section 4.2.4.2*). In other years (e.g., 2018 and 2019), the Arctic polar vortex experienced sudden breakdowns, so-called sudden stratospheric warmings (SSWs; Baldwin et al., 2021; *Section 4.2.2.1*). Although there is not a unique definition, a frequently used criterion is that SSWs are classified as major if the zonal wind at 10 hPa and around 60° latitude reverses to easterlies (Charlton and Polvani, 2007; Baldwin et al., 2021; Butler et al., 2015 and references therein). SSWs occur about every other year in the Northern Hemisphere (with an average of about 6 major SSWs every 10 years). Polar ozone abundances are strongly modulated by SSWs, both due to transport anomalies associated with SSWs (de la Cámara et al., 2018; Hong and Reichler, 2021) and to the prevention of necessary conditions for polar ozone depletion (see *Chapter 4*). Strong natural, internal variability, including low-frequency decadal variability (Dimdore-Miles et al., 2021), prevents the detection of potential small-amplitude changes in SSW frequency, so that no consistent long-term change in SSW frequency has been detected in the Northern Hemisphere over the past decades. No robust future changes in the NH SSW frequency are projected in long model integrations from state-of-the-art multi-model studies (see **Figure 5-7**), irrespective of the climate change forcing scenario (Ayarzagüena et al., 2018; Rao and Garfinkel, 2021b). Moreover, in most recent model simulations with extreme CO₂ concentrations imposed, several individual models show statistically significant changes in the SSW

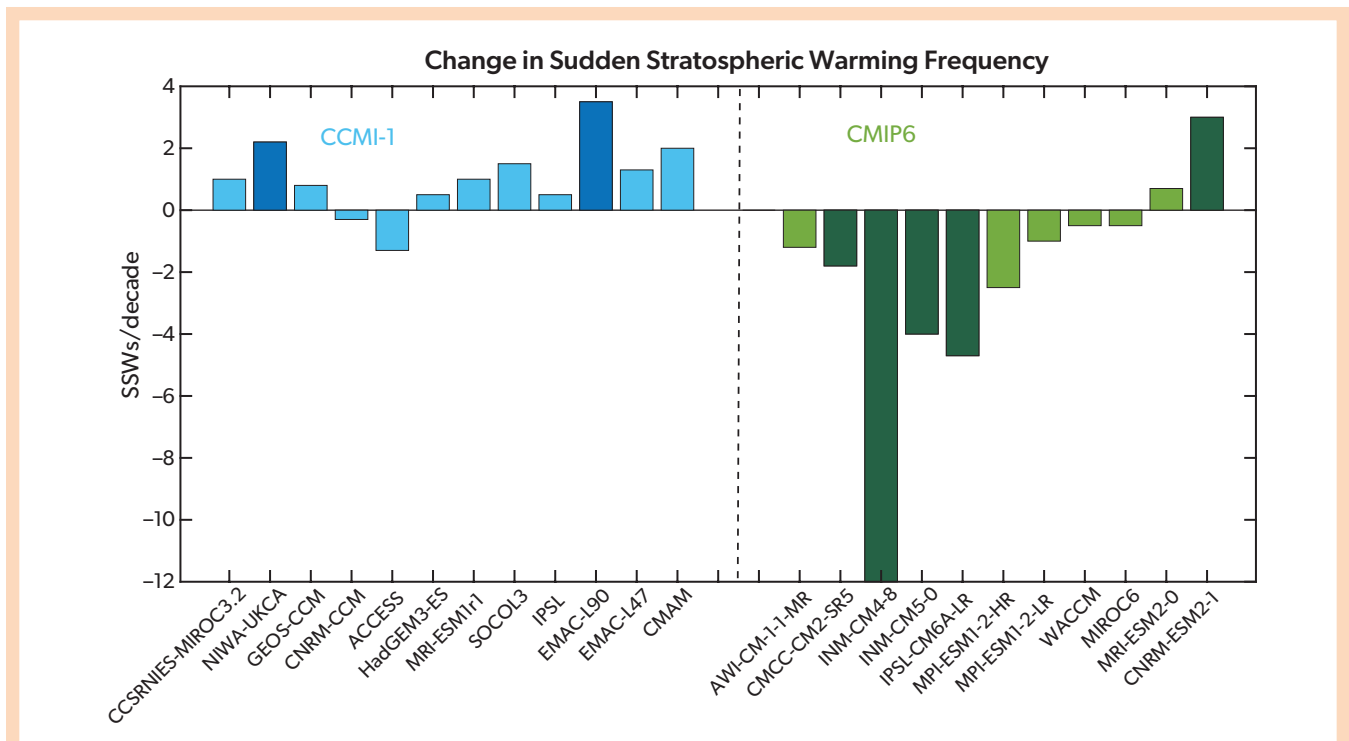


Figure 5-7. Simulated change in the frequency of NH Sudden Stratospheric Warming (SSW) events in the future (2061–2100) relative to the 1960–1999 average in CCMI-1 model simulations (REF-C2; blue bars) and in CMIP6 model simulations under scenario SSP3-7.0 (green bars). The SSW definition is based on the reversal of the zonal-mean zonal wind at 60°N and 10 hPa to easterlies (see Charlton and Polvani, 2007, for the exact definition). Darker colored bars in both indicate statistically significant future-minus-past differences at the 95% confidence level. [Updated from Ayarzagüena et al., 2018.]

frequency, but there is no consensus on the sign of this change (Ayarzagüena et al., 2020). Overall, in agreement with IPCC AR6 (Eyring et al., 2021), we assess that there is no evidence for forced changes in NH SSW frequency. On the other hand, recent studies have highlighted the importance of non-SSW influences of the polar vortex on both ozone and surface climate. In particular, shifts or stretching of the vortex may influence climate and weather differently (Kretschmer et al., 2018; Lee et al., 2019; Butler and Domeisen, 2021; Cohen et al., 2021).

In the Southern Hemisphere, only one major SSW has been observed so far (in 2002). In September 2019, the Antarctic polar vortex experienced its second-strongest disruption ever observed (Section 4.2.3.2; Lim et al., 2021). While the 2019 disruption did not meet the criterion of a major SSW, it is widely considered a SSW in terms of its dynamical characteristics. Therefore, it was suggested that the definition of SSW be adapted for the Southern Hemisphere based on the anomalies of the zonal wind at 60°S and 10 hPa passing below -40 m s^{-1} (Jucker et al., 2021), which is met by the two events in 2002 and 2019. In contrast to the strong disruption in 2019, the two following Antarctic spring seasons (2020 and 2021) both featured a strong and long-lasting polar vortex that led to a large and exceptionally persistent ozone hole (Section 4.2.3.3). This prompts the question of whether we can expect a future change in polar vortex variability. Given that SSWs are very rare events in the Southern Hemisphere, their frequency can be estimated only from long model integrations. Two recent studies were the first to attempt this task, and while

based on different models, they both report a similar SSW frequency of about one event in 25 years (Wang et al., 2020; Jucker et al., 2021). The observed rate of major SSWs is one event (i.e., the 2002 event) since the start of the comprehensive satellite record in 1979 and thus lies below the rate estimated from models. When using the adapted definition for the Southern Hemisphere, which includes the observed 2019 event, the observed rate of two events in 42 years is well within the range expected from the model studies. Therefore, current evidence suggests that the rate of occurrence over the past decades is within expectations, and there is no evidence for changes in SH SSW frequency.

Future changes in the SH SSW rate are addressed in a single study, which projects a strong decrease in the yearly occurrence probability of SSWs in the Southern Hemisphere (from 4.6% in the present day to 0.3% in a future $4\times\text{CO}_2$ climate based on the adapted SSW definition), linked to a general increase in polar vortex strength under increased GHG abundances (Jucker et al., 2021). This result by a single model is backed up by analysis of CMIP6 models in the same study (Jucker et al., 2021), but these results are very uncertain due to the limited simulation length (Ayarzagüena et al., 2020) and model biases in the SH polar vortex strength.

In summary, current evidence suggests that, in both moderate- and high-emissions climate scenarios, a delay in the vortex breakup date of the SH polar vortex that was driven by ozone depletion in the past will not reverse in the future due to the opposing effect of increasing GHGs. Trends in the strength of the

NH polar vortex remain insignificant in the observational period, and future trends are uncertain in sign. While recent years exhibited strong polar vortex variability in both hemispheres, there is currently no evidence for changes in the frequency of SSWs in either hemisphere up to the present day. For the future, climate models project inconsistent changes in NH SSW frequency, and one recent study suggests a possible decrease in the occurrence rate of SH SSWs in response to strong CO₂ forcing.

5.2.6.2 Quasi-Biennial Oscillation

The Quasi-Biennial Oscillation (QBO) refers to the alternating westerly and easterly zonal winds that descend in the tropical stratosphere with a period of about 28 months. The QBO affects stratospheric ozone (see also *Section 3.2.1.1*) both in the tropics and extratropics by modulating vertical and meridional transport and by modulating temperature that affects ozone chemistry (primarily in the mid-to-upper equatorial stratosphere). The descending easterly phase of the QBO is associated with enhanced tropical upwelling and so results in reduced ozone in the lower tropical stratosphere that lags the QBO-temperature anomaly by a quarter cycle. The compensating downwelling in the extratropics, primarily in the NH winter, results in enhanced extratropical stratospheric ozone. The opposite occurs during the descent of the westerly phase of the QBO. In the upper stratosphere, the induced ozone variation is controlled by temperature-dependent photochemistry and is out of phase with the QBO-temperature anomaly. Due to the decadal variation of the QBO (both intensity and period; Shibata and Naoe, 2022), the QBO-induced ozone variability has obscured detection of secular changes in ozone, such as those expected as a result of ozone recovery (Ball et al., 2019), and therefore effects of the QBO need to be carefully accounted for in assessing future secular changes in ozone. Nonetheless, the overall impact of the QBO on hemispheric or global mean ozone is small (Olsen et al., 2019). However, the disruption of the descending easterly phase of the QBO in 2016, which was unprecedented in the observational record at that time, resulted in a sustained increase of tropical ozone and decrease in extratropical ozone (Diallo et al., 2018). Another disruption of the QBO occurred in 2019 (Anstey et al., 2021), raising the possibility that the QBO and its impact on ozone may change in the future (Anstey et al., 2021; see also *Section 3.2.1.1*).

Since the last Assessment, there has been considerable progress in simulating the QBO in global climate models, with 15 out of the 30 models contributing to CMIP6 able to simulate a realistic QBO (Richter et al., 2020a). There is a consensus across the CMIP6 models that are able to depict the QBO, the QBOi models (Butchart et al., 2018), and other models (Naoe et al., 2017; DallaSanta et al., 2021) that the QBO will weaken in the mid-to-lower stratosphere in a warming climate. This occurs in the 2xCO₂ and 4xCO₂ time slice simulations with the QBOi models (Richter et al., 2020b) and for the CMIP6 simulations using the Shared Socioeconomic Pathways (SSP) SSP3-7.0 and SSP5-8.5 scenarios (Richter et al., 2020a). This is usually attributed to enhanced equatorial upwelling associated with an acceleration of the BDC in response to increasing GHGs (Kawatani and Hamilton, 2013), which acts to oppose the descent of the QBO wind variations.

Progress in simulating and projecting the changes in the QBO has been achieved by widespread adoption of non-orographic gravity-wave parameterizations that are able to drive the alternating equatorial descending easterly and westerly QBO

winds. A drawback of relying on non-orographic gravity-wave parameterizations is that the projected changes in the QBO as a result of climate change (and possibly ozone recovery) exhibit dependencies on these parameterizations (Anstey et al., 2022). Although the periodicity and latitudinal extent of the QBO in circulation and temperature are well simulated in these models, there remains a persistent underestimation of the amplitude of the QBO that extends from the lower stratosphere down to the tropopause (Bushell et al., 2020; Richter et al., 2019; Richter et al., 2020a; Anstey et al., 2022). This lower stratospheric bias in QBO amplitude means that processes that are strongly modulated by the QBO, such as troposphere-stratosphere exchange, are unlikely to be well captured, and therefore adds uncertainty in projections of how these processes might change in the future. The models also commonly underestimate the remote impact of the QBO on the NH winter vortex (Rao et al., 2020; Anstey et al., 2022), which partly results from a misrepresentation of the seasonal phase locking of the QBO (i.e., the tendency for phase transition at 50 hPa to occur during April–June and for the downward phase propagation to be slowest during the winter). For both the 2xCO₂ and 4xCO₂ time slice runs with the QBOi models (Richter et al., 2020b) and the various SSP projections with the CMIP6 models for the end of the century (Anstey et al., 2021), the subtropical westerlies in the lower-to-mid- stratosphere increase, acting to shift the critical line for wave dissipation closer to the equator. This equatorward shift of the critical line will result in an increase in equatorward penetration of extratropical wave driving that acts to decelerate the stratospheric zonal flow. Together with a weakening of the QBO as a result of a strengthened BDC (see *Section 5.2.4*), this enhanced equatorward penetration of extratropical wave driving in a warming climate implies that future disruptions of the QBO, such as occurred during 2016 and 2019, could become more common in the future (Anstey et al., 2021). No evidence of an increased frequency of disruptions was found in one model with interactive ozone (DallaSanta et al., 2021), but it is difficult to draw conclusions from any single model because the details of the projected changes in the QBO vary widely across the models (e.g., Richter et al., 2020b).

The QBO-induced ozone variations in the lower equatorial stratosphere are primarily governed by transport variations, while temperature-dependent photochemical ozone variations are dominant higher in the stratosphere (Zhang et al., 2021). This indicates that inclusion of interactive ozone chemistry is required in order to infer future changes in QBO-induced ozone variations, but the vast majority of the models examined in CMIP6 and the QBOi did not use interactive ozone. Furthermore, there is growing evidence that the observed QBO-induced ozone variations are of sufficient magnitude to potentially provide feedback onto the QBO (Kataoka et al., 2020; Pohlmann et al., 2019; Shibata, 2021). This possible feedback was inferred to be positive in two different chemistry-climate models (Naoe et al., 2017; DallaSanta et al., 2021), with the amplitude of the QBO-induced ozone variation also increasing. On the other hand, Shibata (2021) artificially increased the magnitude of the ozone variation passed to the radiation code in a CCM and found little impact on the amplitude of the QBO but a lengthening of the QBO period. However, because there has so far been little focus on the simulation of the QBO with interactive ozone, there is still low confidence in the simulated impacts and especially in the positive feedback on amplitude.

Strengthening of the QBO-induced ozone variation despite a projected weakening of the QBO partly derives from the expected recovery of ozone (Naoy et al., 2017; DallaSanta et al., 2021). The simulated ozone-dynamical feedback can also act to offset the decline in amplitude of the QBO as a result of increasing greenhouse gases (DallaSanta et al., 2021), indicating that increasing confidence in projected changes of the QBO and its impacts on ozone variations will require the inclusion of explicit ozone-dynamical coupling (see also **Box 5-4** and *Section 5.3.2.1.3*).

In summary, since the last Assessment, there is more confidence that the QBO will weaken in the future as a result of acceleration of the BDC in a warming climate. However, there remains large uncertainty about any change in its periodicity and about the associated impact on ozone variability. New evidence infers that disruptions of the QBO may become more likely in a warming climate.

5.3 EFFECTS OF CHANGES IN STRATOSPHERIC OZONE AND ODSs ON CLIMATE

The climate impacts of stratospheric ozone changes on tropospheric and surface climate are well established and widely documented. Ozone depletion has been deemed the key driver of late-20th century austral summer atmospheric circulation changes in the Southern Hemisphere, as well as one of the drivers of changes in the SH cryosphere and ocean. Here, we focus on new findings since the last Assessment. This includes new quantifications of the radiative forcing from ODSs and ozone (*Section 5.3.1*). We also highlight an emerging body of evidence pointing at the direct climate impacts of ODSs, independent of ozone depletion, and the importance of stratospheric ozone-climate feedbacks and ozone-circulation coupling on a range of timescales. In particular, we highlight new evidence concerning the climate

effects of the Montreal Protocol and reveal that some of these effects may have already begun to be realized (*Sections 5.3.2* and *5.4*).

5.3.1 Radiative Impacts of Ozone and ODSs on Tropospheric Climate and Ozone-Climate Feedbacks

Changes in stratospheric ozone can affect climate in a number of ways. Aside from inducing stratospheric cooling (*Section 5.2.2*) and changes in the stratospheric (*Sections 5.2.4* and *5.2.5*) and tropospheric (*Section 5.3.2*) circulation, trends in stratospheric ozone and ODS abundances introduce a radiative forcing perturbation that is a substantial fraction of the total anthropogenic radiative forcing over the second half of the 20th century (Forster et al., 2021). This section focuses on what has been learned about radiative forcing since the last Ozone Assessment (*Section 5.3.1.1*). The climate effects of stratospheric ozone and ODSs are traditionally studied in conjunction, as they are closely coupled via heterogeneous and homogeneous chemistry. Here, we review new evidence on their effects in isolation, such as the direct effects of ODSs on climate (*Section 5.3.1.2*) and those of GHG-induced stratospheric ozone changes on climate (*Section 5.3.1.3*).

5.3.1.1 Ozone Radiative Forcing

Radiative forcing is one of the key metrics for quantifying the potential climate effects of historical ODS emissions and the resulting ozone changes. Traditionally, the standard definition adopted to quantify the radiative forcing of historical ozone and ODS changes is the stratosphere-adjusted radiative forcing. In the following, the term “radiative forcing” (RF) refers to this stratosphere-adjusted radiative forcing definition. Some studies have adopted the “effective radiative forcing” (ERF) definition that was mandated by IPCC AR5. However, as detailed below, given the

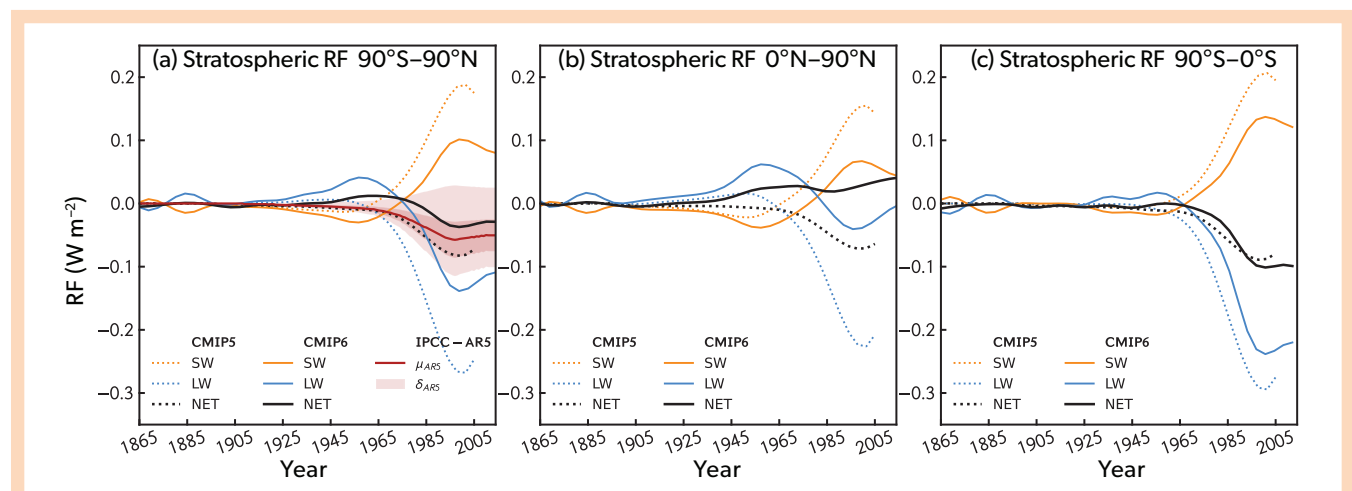


Figure 5-8. Radiative forcing from stratospheric ozone relative to 1850 and its evolution over the 20th century, from the ozone datasets compiled for CMIP6 (solid lines) and CMIP5 (Ciannoni et al., 2011; dotted lines), as well as the IPCC AR5 estimate (red line) and its uncertainty (shading), for the global mean (*left panel*), Northern Hemisphere (*center panel*), and Southern Hemisphere (*right panel*). The stratosphere-adjusted RF in this figure is evaluated at the tropopause. Yellow lines denote the SW forcing, while blue lines show the LW component in the CMIP5 and CMIP6 estimates. [Adapted from Checa-Garcia et al., 2018.]

larger uncertainty in the ERF quantification, the stratosphere-adjusted RF is the focus of our Assessment (see also **Box 5-3** on radiative forcing).

Since the last Assessment, updated RF values (relative to 1850) for whole-atmosphere ozone have been derived (Checa-Garcia et al., 2018; Skeie et al., 2020) and have recently been assessed in IPCC AR6 (Section 7.3.2.1 of Forster et al., 2021). These values are listed in **Table 5-1**, along with several previously reported values for reference. The 3-D ozone forcing dataset compiled for CMIP6 models without interactive chemistry (“CMIP6 ozone” in **Table 5-1**) produces a whole-atmosphere (stratospheric + tropospheric) ozone RF over the period 1850–2010 of 0.3 W m^{-2} , in agreement with the value reported in IPCC AR5 (0.35 W m^{-2}), and this RF is almost entirely due to tropospheric ozone (0.33 W m^{-2}). The whole-atmosphere ozone RF in the new CMIP6 dataset is double (0.30 versus 0.15 W m^{-2}) that in its predecessor, the CMIP5 ozone dataset (Cionni et al., 2011). Even larger values are obtained in Skeie et al. (2020) (0.41 W m^{-2}) and in IPCC AR6 (0.47 W m^{-2} ; Forster et al., 2021), which is likely due to the larger emissions of tropospheric ozone precursors used in CMIP6 models than in the two CCM1 models employed in the production of the CMIP6 ozone forcing dataset. In addition, the forcing in Forster et al., 2021 is relative to 1750 rather than 1850.

The RF arising from stratospheric ozone changes over the historical period has been estimated by a number of studies since the last Assessment, based on different reanalysis or model datasets (as summarized in **Table 5-1**). Consistent with previous

Assessments, the RF due to stratospheric ozone is much smaller than that due to tropospheric ozone, since it is the result of competing effects in the longwave (LW) and shortwave (SW) radiation (**Figure 5-8**; see also **Box 5-3**). The global mean RF is dominated by the Southern Hemisphere. Since stratospheric ozone trends are larger and more consistent across models in the Southern than in the Northern Hemisphere, the RF estimates there are more robust across the ozone datasets than in the Northern Hemisphere (**Figure 5-8**). New estimates of the net global mean stratospheric ozone RF in the historical period based on multiple CCMs generally range from a small ($<0.1 \text{ W m}^{-2}$) net positive to a small net negative RF (see **Table 5-1**), likely caused by the compensation of LW and SW effects, as seen in forcing datasets depicted in **Figure 5-8**. The reanalysis-based RF estimate over the period 1750–2010 is near zero ($+0.003 \pm 0.20 \text{ W m}^{-2}$) in the global mean (Bellouin et al., 2020; based on CAMS reanalysis data), which is well within the range of the model-based estimates.

Compared to previous model-based estimates of global mean stratospheric RF, newer estimates from CMIP6 are generally slightly smaller but also span a wider range (see **Table 5-1** and **Figure 5-8**). The ozone forcing dataset produced for CMIP6 results in a slightly smaller global mean stratospheric ozone RF over the period 1850–2010 compared to its CMIP5 predecessor ($-0.03 \pm 0.06 \text{ W m}^{-2}$ versus -0.08 W m^{-2} ; Checa-Garcia et al., 2018; Cionni et al., 2011; see also **Figure 5-8**). In Chapter 7 of the Working Group I contribution to IPCC AR6 (Forster et al., 2021), the 1850–2010 stratospheric ozone RF was suggested to be 0.02

Table 5-1. Radiative forcing from stratospheric, tropospheric, and total ozone from the studies assessed in this chapter, along with the definition of RF method (following the forcing definitions used by IPCC AR6), the time period of the forcing, and the input dataset for the calculations. The CMIP6 ozone dataset is constructed by averaging the output of two CCM1 models (WACCM and CMAM) driven with precursor and ODS emissions and all historical forcings over the period 1850–2014 (Checa-Garcia et al., 2018). In CMIP5, the ozone dataset is derived from simulated tropospheric ozone, while ozone in the stratosphere it is based on satellite observations since 1979 and statistical extrapolations before that date (Cionni et al., 2011). In studies using model simulations as the input dataset, the RF has been calculated from each individual CCM output. In Skeie et al. (2020), a different stratospheric ozone RF range of $-0.02 \pm 0.14 \text{ W m}^{-2}$ is obtained when excluding one outlier model (UKESM) but including all other models with comprehensive stratospheric chemistry. The uncertainty range represents the 5–95% range, unless otherwise noted. Some sensitivity of the RF to the tropopause definition arises when separating stratospheric and tropospheric ozone, but this effect is only marginal (Stevenson et al., 2013).

Study	RF definition	Time period	Input dataset	Stratospheric Ozone	Tropospheric Ozone	Total
Checa-Garcia et al., 2018	SARF	1850–2010	CMIP6 ozone	-0.03 ± 0.06 (a)	0.33 ± 0.16 (a)	0.30 ± 0.15 (a)
Skeie et al., 2020	SARF	1850–2010	CMIP6 models (b)	0.02 ± 0.07	0.39 ± 0.07	0.41 ± 0.12
Skeie et al., 2020*	SARF	1850–2010	CMIP6 models (c)	-0.02 ± 0.14		
Bellouin et al., 2020	SARF	1750–2010 (d)	Re-analysis (e)	0.00 ± 0.20 (f)	0.33 ± 0.27 (f)	0.32 ± 0.32 (f)
Thornhill et al., 2021	ERF	1850–2014	CMIP6 models			0.33 ± 0.11 (g)
Michou et al., 2020	ERF	1850–2010	Single CMIP6 model	-0.04		
IPCC-AR6	ERF (h)	1750–2019 (i)	assessed			0.47 ± 0.23
Cionni et al., 2011	SARF	1850–2011	CMIP5 ozone	-0.08	0.23	0.15
Stevenson et al., 2013	SARF	1750–2010 (i)	ACCIP models		0.41 ± 0.14	
IPCC-AR5	SARF	1750–2011 (i)	assessed	-0.05 ± 0.10 (a)	0.40 ± 0.20 (a)	0.35 ± 0.20 (a)

(*) differs from published range (see c)

(a) 5–95% interval using parametric formula (Myhre et al., 2013)

(b) excluding models without trop chem and model with excessive depletion (5 out of 11)

(c) including all models with strat chem, excluding model with excessive depletion (9 out of 11)

(d) end year is average 2003–2017

(e) reanalysis is based on modeling (CAMS)

(f) 5–95% interval calculated from combined structural uncertainties

(g) emission-based ERF (linear sum of individual GHGs)

(h) ERF is taken to be equal the SARF

(i) extrapolations to extended period made adding offsets

$\pm 0.07 \text{ W m}^{-2}$, based on CCMs participating in CMIP6 (Skeie et al., 2020), compared to a range of $-0.05 \pm 0.10 \text{ W m}^{-2}$ assessed by IPCC AR5. The CMIP6 range was obtained by excluding models without tropospheric chemistry (but which do simulate stratospheric chemistry) and one model with excessive ozone depletion (UKESM). Taking all CMIP6 models with interactive stratospheric chemistry except UKESM into account yields a range of $-0.02 \pm$

0.14 W m^{-2} , which is closer to previous estimates (see **Table 5-1**; Skeie et al., personal communication). In general, these different estimates agree on a flattening of the global stratospheric ozone RF since the late 1990s (Dhomse et al., 2018; **Figure 5-8**), consistent with the emergence of healing of the ozone layer (*Chapter 3*).

In the future, the stratospheric ozone RF is expected to remain

Box 5-3. Radiative Forcing from Ozone and ODSs: Methods and Uncertainties

The radiative forcing (RF) metric quantifies the radiative energy flux perturbation exerted by natural and anthropogenic forcings into the climate system. A positive forcing introduces a net radiative gain, ultimately leading to surface warming, until increased thermal emissions to space restore the balance; a negative forcing operates in the opposite way, causing cooling (Ramaswamy et al., 2019). Historically, RF has been defined by the change in the energy balance in the climate system when a forcing is introduced with respect to a preindustrial climate. However, this instantaneous evaluation of the energy imbalance (termed “instantaneous radiative forcing”) does not represent the actual climate impact of the forcing introduced, in particular regarding the surface warming, as rapid adjustments of the temperature in the stratosphere can mute the RF, making it substantially different from the instantaneous RF (Pincus et al., 2020). These adjustments in the stratospheric temperature are commonly estimated by the fixed dynamical heating (FDH) method (Forster and Shine, 1997). This method involves adjusting stratospheric temperatures until a new equilibrium is reached, assuming that the dynamical heating remains unchanged, and keeping tropospheric temperatures fixed. This is the standard method to estimate the RF of historical ozone changes and is commonly referred to as the stratosphere-adjusted radiative forcing (see IPCC AR5). An example of the implementation of this method in modern CCMs is given by Conley et al. (2013), and this method is used to calculate the ozone RF here in *Chapter 5*. Other Chapters (*Chapter 1, 2, 7*) infer the RF of individual source gases by using Tabulated Radiative Efficiency values (see the *Annex*), which include or neglect certain adjustments (e.g. lifetime, tropospheric adjustments), but these adjustments only have a small (<10%) effect on the total RF of major ODS species, making their RF sufficiently close to the SARF (e.g., Thornhill et al., 2021).

The stratosphere-adjusted RF definition reduces the sensitivity to the details of the tropopause definition. However, forcing agents such as ozone and ODSs can also produce rapid adjustments in the troposphere, such as adjustments in temperature and clouds, which can themselves be quantified as forcings; these are not captured by the stratosphere-adjusted RF. Incorporation of these responses in the forcing makes it more representative of the actual climate impacts of the forcing; this is achieved using the effective radiative forcing (ERF; Forster et al., 2016) definition. ODSs induce temperature changes in the upper troposphere / lower stratosphere (UTLS; Forster and Joshi, 2005; McLandress et al., 2014; Chiodo and Polvani, 2022), a large portion of which would be missed using the FDH; this raises the question whether the stratosphere-adjusted RF is an appropriate measure of the ERF for ODSs. However, given the considerable uncertainties associated with ERF estimates (see *Section 5.3.1.1*), most studies on ozone RF so far have focused only on the stratosphere-adjusted RF.

The RF originating from stratospheric ozone trends over the 20th century is primarily due to the modulation of ozone by ODSs. However, the division of ozone RF forcing into its components of stratospheric and tropospheric ozone does not directly attribute ozone RF forcing to ODSs. This is because tropospheric ozone can be influenced by ODS-driven stratospheric ozone decreases, a component deemed important in certain models (e.g., Shindell et al., 2013) but which strongly depends on stratosphere-troposphere exchange processes (Banerjee et al., 2018; see also *Section 5.2.5*). Existing estimates of ODS-attributed ozone RF are substantially stronger (more negative) than the stratospheric ozone RF arising from historical trends (see *Section 5.3.1.1*), but the net forcing by ODSs, including associated ozone changes, is still found to be positive in current estimates (Thornhill et al., 2021).

The radiative effects of ODSs and ozone are determined by their intrinsic properties. ODSs, among which CFCs contribute more than 85% of the RF, have a long lifetime and are relatively well mixed in the troposphere. ODSs have strong absorption bands in the LW part of the spectrum. As such, they reduce the outgoing LW flux, and an increase in ODS atmospheric abundance leads to a positive RF (see *Chapter 1*). Uncertainty in these properties has a small impact on their RF (Chiodo and Polvani, 2022). Their RF is partly balanced by the negative RF from the associated stratospheric ozone losses (Myhre et al., 2013; see *Section 5.3.1.1*). Ozone molecules have a more complex spectrum, with absorption bands in the solar shortwave (SW) and in the longwave (LW) (Goody and Yung, 1989). The radiative effect of ozone is strongly altitude dependent, with ozone changes near the tropopause being most effective at absorbing LW and thus contributing to climate change, due to the large temperature difference between this region (where the absorption takes place) and the Earth’s surface (the emissions source; Lacis et al., 1990). Ozone changes at upper-stratospheric levels have a much smaller or even slightly opposite effect on the net forcing. Further, the LW and SW effects of stratospheric ozone changes strongly compensate each other. Depletion of stratospheric ozone leads to reduced SW absorption and thus an increase in the incident SW flux at the tropopause (i.e., a positive forcing). Reduced SW absorption cools the stratosphere, which in turn reduces the LW flux at the tropopause, a negative forcing. The balance between the SW and LW terms crucially depends on the season, location, and magnitude of the ozone perturbation (Ramanathan and Dickinson, 1979). Taken together, the offsetting contributions of LW and SW explain the small net value of stratospheric ozone RF, leading to uncertainty even in its sign.

at a similar value as estimated for present-day or trend to slightly more negative values by the end of the 21st century, depending on the scenario (see **Table 5-2**, based on CMIP6 ozone forcing datasets and calculated consistent with the approach of Checa-Garcia et al., 2018). The small changes in future stratospheric ozone RF are due to the opposite effects of climate change in low and high latitudes. GHG increases lead to a decrease in ozone in the tropical lower stratosphere due to increasing tropical upwelling, driving a negative ozone RF in the tropics. In mid- and high latitudes, decreased stratospheric halogen loading and an enhanced BDC lead to an increase in ozone abundances, driving a positive ozone RF. Low and mid-range scenarios (SSP1-2.6 and SSP2-4.5) show small changes in stratospheric ozone RF values, likely because RF changes due to ODS-driven ozone recovery are compensated by RF changes due to GHG-driven tropical ozone decreases. For high-end scenarios (SSP5-8.5), future stratospheric ozone RF values decrease, likely because the RF effects of GHG-driven tropical ozone decreases dominate.

The RF by ODSs is assessed in *Chapters 1 and 2*, which report RFs in 2020 of 0.337 W m^{-2} for ODSs (defined as chlorofluorocarbons [CFCs] + hydrochlorofluorocarbons [HCFCs] + halons + solvents) and 0.04 W m^{-2} for HFCs. The combined effects of ODS and stratospheric ozone trends result in a net positive RF when taken as the sum of the two individual forcings and thus contribute to surface warming over the 20th century (see *Section 5.3.1.2*). A different approach to summing up the direct ODS RF and stratospheric ozone RF is to explicitly attribute (whole atmosphere) ozone changes to ODS emissions; this emissions-based RF of ODSs, including induced ozone changes, is likewise found to be positive by current model studies (Thornhill et al., 2021).

Studies that used the stratosphere-adjusted RF definition are discussed above. A few other studies have adopted ERF, the RF definition mandated by IPCC AR5 (Forster et al., 2016; see also **Box 5-3**). The ERF of ODSs inferred from observations, including the indirect effects via ozone and other rapid tropospheric adjustments, is estimated to lie between 0.03 and 0.14 W m^{-2} (Morgenstern et al., 2021, revising Morgenstern et al., 2020; see also *Chapter 7*). Taken at face value, the lower bound of this estimate would imply that ODS-driven changes in stratospheric ozone and rapid adjustments effectively cancel the direct RF of ODSs (0.337 W m^{-2} by 2020; see *Chapter 1*), resulting in a smaller warming influence of ODSs than considered likely in AR5 and most climate models (see *Section 5.3.1.2*). However, there is considerable uncertainty in those estimates arising from the methods (e.g., uncertainty in the linear regression), the limited number of models included in the assessment, and biases in the simulated

ozone trends. An important but highly uncertain component of the ERF due to ODSs are cloud changes arising from positive (ozone-induced) trends in the Southern Annular Mode (SAM) in the Southern Hemisphere (O'Connor et al., 2021); rapid adjustments of this type introduce uncertainty in ERF estimates. Other analyses of CMIP6 models suggest that in the global mean, rapid adjustments to ozone and ODSs are weak (Skeie et al., 2020; Hodnebrog et al., 2020). In line with this, the ERF of stratospheric ozone from one model study (Michou et al., 2020, reporting a value of -0.04 W m^{-2}) is well within the range of the stratospheric ozone stratosphere-adjusted RF from the aforementioned studies. We thus conclude, similar to IPCC AR6 (Forster et al., 2021), that confidence in rapid adjustments is still limited, and therefore our assessment is based on the stratosphere-adjusted RF.

Overall, we assess that the RF due to long-term stratospheric ozone trends over the historical period (1850–2010) is near zero due to the cancellation of LW and SW effects, with a large uncertainty range, at $-0.02 \pm 0.13 \text{ W m}^{-2}$, based on the uncertainties provided among all studies assessed here (see **Table 5-1**). The best estimate of -0.02 W m^{-2} is the average from three estimates—the CMIP6 ozone forcing (Checa-Garcia et al., 2018; -0.03 W m^{-2}), the reanalysis study of Bellouin et al. (2020; 0.003 W m^{-2}), and the average over all CMIP6 models with stratospheric chemistry (Skeie et al., 2020; -0.02 W m^{-2})—while the uncertainty range (0.13 W m^{-2}) encompasses all CMIP6 models with stratospheric chemistry (Skeie et al., personal communication), as well as methodological uncertainties (e.g., tropopause definition and the preindustrial ozone climatology). For the extended period 1850–2019, the stratospheric ozone RF is in the same range as for 1850–2010, as uncertainty outweighs any changes arising from ozone trends over 2010–2019. Hence, the net RF by ODSs ($+0.337 \text{ W m}^{-2}$; see *Chapter 1*), including its impacts on long-term stratospheric ozone trends, is positive and contributes to global warming, as assessed in *Section 5.3.1.2*. It has become clear since the last Assessment that rapid adjustments arising from tropospheric circulation changes might play a role in determining the climate response to ODSs at regional scales, but the magnitude of these adjustments is highly uncertain and model dependent, although it is unlikely to offset the global direct forcing by ODSs.

5.3.1.2 ODS Direct Effects on Climate

Several studies have highlighted the important role that ODSs alone have had on climate, in addition to their impact on climate through affecting stratospheric ozone abundances. As outlined in the previous section, *Chapter 1* of this Assessment, as well as in IPCC AR6 (see Figure 6.12a in Szopa et al., 2021, and

Table 5-2. Radiative forcing from future stratospheric ozone, calculated at the tropopause as in Checa-Garcia et al. (2018) using the future CMIP6 ozone datasets compiled for IPCC AR6 (Checa-Garcia 2022, personal communication).

Scenario	RF definition	Time period	Input dataset	Stratospheric ozone
SSP126	SARF	1850–2099	CMIP6 ozone	-0.03 ± 0.06
SSP245	SARF	1850–2099	CMIP6 ozone	-0.04 ± 0.08
SSP370	SARF	1850–2099	CMIP6 ozone	-0.02 ± 0.04
SSP460	SARF	1850–2099	CMIP6 ozone	-0.03 ± 0.06
SSP585	SARF	1850–2099	CMIP6 ozone	-0.09 ± 0.18

Uncertainty is taken using parametric formula (Myhre et al., 2013)

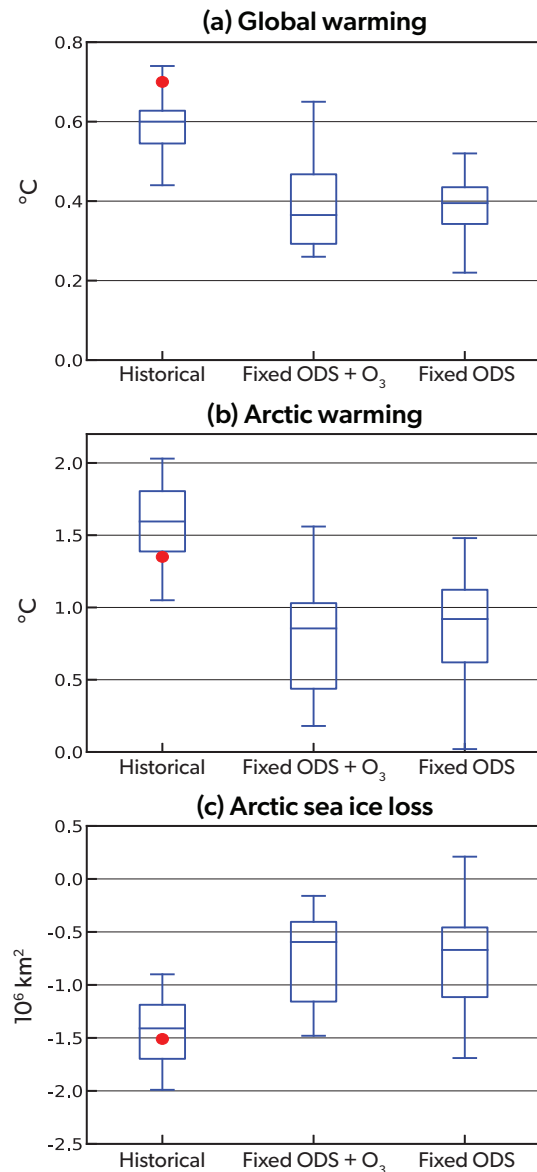


Figure 5-9. Climate impact of ODSs for the period 1955–2005. (a) Annual mean global surface-temperature change over the period 1955–2005 for each ten-member Community Earth System Model Version 1 (CESM-CAM5) ensemble, as labelled on the abscissa. The boxes extend from the lower to upper quartile of the data, with a line at the median and whiskers showing the entire range across each ensemble (b) As in (a) but for Arctic temperatures, averaged (60–90°N). (c) As in (a) but for September Arctic sea ice extent. Red circles denote the observed values obtained from GISTEMP27 v.3 for surface temperature and HadISST28v.2.2.0 for sea ice. The change over the period 1955–2005 is computed as the linear trend multiplied by the number of years (51). In each panel, the means of the Fixed ODS and ozone (Fixed ODS+O₃) (ODSs and stratospheric ozone fixed at year 1955 levels) and Fixed ODS (ODSs fixed at year 1955 levels) ensembles are significantly different from that of the Historical ensemble at the 99% confidence level by two-tailed t-test. [Adapted from Polvani et al., 2020.]

Section 7.3.2.4 and Table 7.5 of Forster et al., 2021), both the stratosphere-adjusted RF and the ERF (i.e., even when accounting for the RF via stratospheric ozone loss) of ODSs are likely to be positive. Over the second half of the 20th century (1955–2005), the RF by ODSs is second only to CO₂, making ODSs an important anthropogenic influence on climate in recent decades (Velders et al., 2007; Polvani et al., 2020). Since the last Assessment, new evidence from independent chemistry-climate and Earth-system model studies have shown the important role that ODSs have played in enhancing Arctic warming (Goyal et al., 2019; Polvani et al., 2020; Liang et al., 2022). **Figure 5-9** shows the large contribution of ODSs to global and Arctic warming and sea ice loss over the 1955–2005 period (Polvani et al., 2020). Excluding the trend in ODSs reduces annual mean historical global warming by approximately one-third (**Figure 5-9a**), and Arctic warming (and September sea ice loss) by approximately half. This indicates that ODSs appear to enhance Arctic amplification (**Figure 5-9b** and **c**); i.e. the Arctic warmed 2.7 times more than the global mean in the historical ensemble compared to only 2 times more in the ensemble with fixed ODS and ozone (comparing **Figure 5-9a** and **b**). This result is supported by another study (Liang et al., 2022), which reports that Arctic amplification caused by ODSs is 1.44 times stronger than that caused by CO₂ over the same time period. The impact of stratospheric ozone loss on global and Arctic temperature change appears negligible (comparing the Fixed ODS+O₃ and Fixed ODS ensembles in **Figure 5-9**). Although the specific mechanism responsible for enhanced Arctic amplification due to ODSs is not yet clear, radiative feedback analysis suggests a key contribution from local Arctic feedbacks (Polvani et al., 2020; Liang et al., 2022). However, the robustness of the effects of ODSs on Arctic warming is still questionable as these studies were all based on related models.

There is also evidence that ODSs have contributed to a weakening of the Walker circulation (a zonal overturning cell in the equatorial Pacific) over the 1955–2005 period due to a rapid warming of the Eastern Tropical Pacific SSTs (Polvani and Bellomo, 2019). However, there is no consensus as to whether the observed Walker circulation has indeed weakened since the middle of the last century, and questions have been raised about the fidelity of using climate models to simulate the response of Eastern Tropical Pacific SSTs to increasing greenhouse gases (Clement et al., 1996; Cane et al., 1997; Seager et al., 2019). Overall, evidence of the direct ODS effects on climate continue to emerge but are not yet robust.

5.3.1.3 Role of Stratospheric Ozone in the Climate Response to CO₂ Forcing

The effects of stratospheric ozone changes induced by ODS emissions on the climate system have been widely documented across many Ozone Assessments (WMO, 2010, 2014, 2018). Conversely, the role of stratospheric ozone in modifying the climate system's response to GHG increases has received less attention. The response of the stratospheric ozone layer to GHG forcing can impact the global mean surface temperature response to GHG forcing, thus acting as a true climate feedback (termed “ozone-climate feedback” in the following discussion). Furthermore, the stratospheric ozone response to GHG forcing can modify the stratospheric and tropospheric circulation response to GHGs via ozone-circulation coupling. The relevant processes involved in the ozone-climate feedback and ozone-circulation coupling are

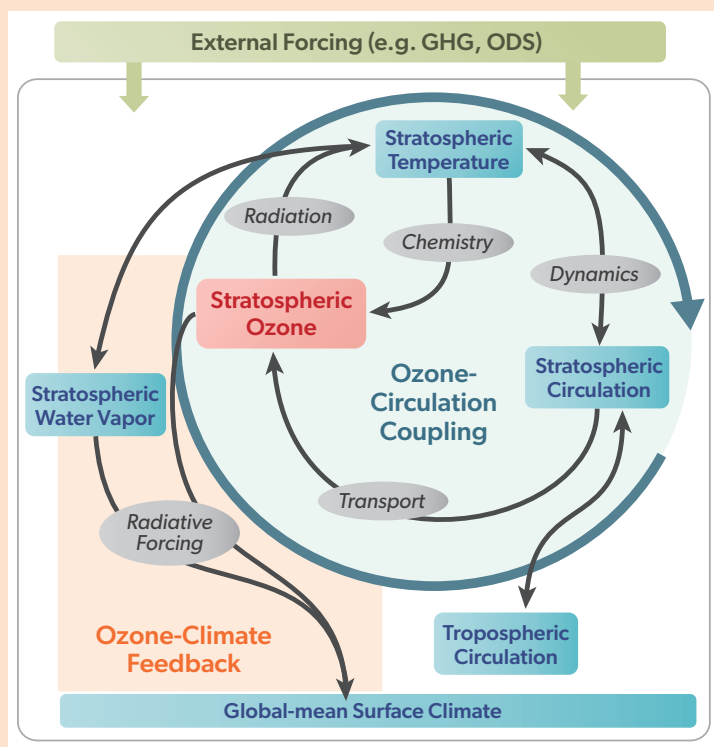
Box 5-4. Ozone-Climate Feedbacks and Ozone-Circulation Coupling

Stratospheric ozone plays an important role in the radiative budget of the atmosphere. It not only reduces the incidence of UV radiation at the surface but also plays a key role in determining the thermal structure of the stratosphere by heating the upper stratosphere by more than 20 K. Ozone heating also substantially influences the temperature near the tropical tropopause layer (TTL), thereby also influencing global stratospheric water vapor amounts (e.g., Ming et al., 2017). Ozone also acts as a greenhouse gas, due to its absorption band near 10 μm wavelength.

Previously, most research on the effects of stratospheric ozone on climate has focused on the impacts of chemical ozone depletion due to ODSs (WMO, 2010, 2014, 2018), considering ozone as a “forcing”. Recently, attention has focused on the quantification of the two-way coupling between stratospheric ozone and the climate system via radiation, dynamical, and chemical processes. This coupling is initiated by stratospheric ozone variations that are either externally forced (e.g., due to changes in CO_2) or internally produced by climate variability on a range of timescales from sub-seasonal to multi-decadal.

Stratospheric ozone is strongly coupled with temperature via radiation and chemistry; this coupling is at the core of the mechanism behind stratospheric ozone-circulation coupling, shown in **Box 5-4 Figure 1**. On sub-seasonal to interannual timescales, circulation and temperature anomalies, such as those associated with variations in the polar vortex strength, induce ozone anomalies. This is due not only to transport but also to temperature-dependent chemistry. Aside from homogeneous chemistry in the polar stratosphere, heterogeneous chemistry plays a key role when temperatures are low enough for PSC formation and sufficient abundances of ODSs are available (Calvo et al., 2015; Chapter 4). Ozone in turn affects temperature via radiation, feeding back on the initial temperature and circulation anomaly (see the light blue circle in **Box 5-4 Figure 1**). Thus, ozone modifies the initial stratospheric circulation anomalies, and this can further influence the tropospheric circulation via stratosphere-troposphere dynamical coupling. There is evidence that this coupling may influence the stratosphere-troposphere circulation in individual years and can influence sub-seasonal

prediction in both the Southern (Section 5.3.2.1.1) and Northern Hemispheres (Section 5.3.2.1.2).



Box 5-4 Figure 1. Schematic of stratospheric ozone-circulation coupling and ozone-climate feedbacks. The stratospheric ozone-climate feedback modifies the response of global surface climate to an external forcing such as increasing GHGs. Ozone-circulation coupling can be induced by changes due to external forcings (e.g., CO_2 -driven stratospheric temperature and circulation changes), and subsequent ozone changes modify the circulation response to the forcing. Ozone-circulation coupling is also induced by internal variability (e.g., an anomalous strong and cold polar vortex), and can modify the stratosphere-troposphere circulation in individual years.

The two-way coupling between ozone and the circulation also contributes to the response to forced changes to the climate system. For example, when atmospheric CO_2 concentrations increase, the stratosphere cools (as explained in Box 5-1 of Karpechko, Maycock et al., 2018) and the troposphere and surface warm. Globally, stratospheric cooling from CO_2 leads to an increase in ozone abundances due to the temperature dependence of ozone chemistry (see **Box 5-2**). Tropospheric warming leads to an acceleration of the BDC, driving an ozone decrease in the lower tropical stratosphere. These ozone changes radiatively warm the upper stratosphere and the polar regions and cool the TTL, leading to a decrease in stratospheric water vapor. These heating and cooling effects driven by ozone changes affects temperature gradients, inducing an ozone-circulation coupling that modulates the response of the stratospheric circulation to CO_2 forcing, as well as the tropospheric circulation response (see Section 5.3.1.3). These processes apply not only to increases in CO_2 but also to any external forcing, including ODSs (see Section 5.3.2.2.1), and also CH_4 or N_2O , although this is less well studied.

Furthermore, the CO_2 -driven stratospheric ozone changes, as well as subsequent stratospheric water vapor changes, induce an indirect RF, potentially impacting the global mean surface temperature response to CO_2 forcing. The relationship of the global mean surface temperature change to a change in the net energy budget at the top of the atmosphere (e.g., resulting from CO_2 forcing) is commonly defined as a climate feedback (see Box 7.1 in Forster et al., 2021). In the recent IPCC report (IPCC, 2021), climate feedbacks were grouped into physical feedbacks (for

example, those associated with water vapor and surface albedo), biogeophysical and biogeochemical feedbacks, and long-term feedbacks associated with ice sheets. Stratospheric ozone contributes to the group of biogeochemical climate feedbacks (Szopa et al., 2021). Recent studies on quantifying this stratospheric ozone climate feedback are assessed in *Section 5.3.1.3*.

Models without interactive stratospheric ozone chemistry do not simulate the coupling between ozone and the circulation and thus miss the modulation of temperature and circulation anomalies and trends, as well as the resulting climate feedback through stratospheric ozone. The quantification of the role of those processes is the subject of ongoing research, including their impact on the climate response to CO₂ (*Section 5.3.1.3*) and to ODSs (*Section 5.3.2.1*), as well as their role for stratospheric and tropospheric variability on interannual timescales (*Section 5.3.2.1*).

detailed in **Box 5-4**, and new research into the climate impacts of stratospheric ozone changes under GHG forcing (mainly CO₂) is assessed in the following.

In the last Assessment, it was stated that stratospheric ozone-climate feedbacks are more likely to reduce rather than increase the equilibrium climate sensitivity (ECS), quantified as the near-equilibrium global warming response to an abrupt quadrupling of atmospheric CO₂ concentrations. However, the uncertainty in the feedback across models is large (0–20% in the ECS, or –0.01 to –0.13 W m⁻² K⁻¹ in the climate feedback), contributing to a substantial fraction (~30%) of the uncertainty in the net non-CO₂ biogeochemical feedbacks under climate change (*Section 6.4.5* of Szopa et al., 2021). Since the last Assessment, new insights have been gained into possible reasons for the model uncertainty in the ozone-climate feedback. These include inconsistencies between the chemical and thermal tropopause when ozone abundances are prescribed (Nowack et al., 2018, 2015), leading to biases such as a too-warm cold point temperature and excessive moistening of the stratosphere (Hardiman et al., 2019; Nowack et al., 2018). It has been shown that this effect can lead to an overestimation of the ECS by about 10% (Hardiman et al., 2019) in one model that previously reported a very strong ozone feedback (20%) on ECS (e.g., Nowack et al., 2017, 2015), and this bias can generally be expected to be large in models with sufficiently high vertical resolution and high climate sensitivity.

Aside from specifications near the tropopause, the other possible source of uncertainty in the ozone-climate feedback is how ozone itself is affected by increasing GHGs, as it changes quite differently across climate models (Chiodo et al., 2018). In a simple 1-D radiative convective equilibrium model (Dacie et al., 2019), imposing a 4xCO₂ forcing while keeping ozone at preindustrial levels leads to cooling of the stratosphere and warming of the troposphere (**Figure 5-10**). Imposing ozone changes under 4xCO₂ (which are prescribed from CCMs) leads to 5–10 K less cooling in the upper stratosphere and enhanced cooling (of 2–3 K) of the lower stratosphere (compare solid blue and pink lines in right panel of **Figure 5-10**), consistent with the sign of the prescribed ozone change. Further, surface warming is slightly reduced (from 6.6 to 6.3 K), consistent with the negative feedback on ECS reported in other studies (Dietmüller et al., 2014; Muthers et al., 2014; Nowack et al., 2015). The reduction in ECS when imposing different ozone perturbations in this 1-D model ranges between 0 and 10%, whereas in a more complex CCM, imposing a range of ozone perturbations does not affect ECS at all (Chiodo and Polvani, 2019). This suggests that the magnitude of the stratospheric ozone feedback on ECS is likely to be model-dependent but unlikely to affect ECS by more than 10%, with most of the uncertainty originating in the interactions between ozone and

physical feedbacks, such as with clouds or the lapse rate. Ozone might also modulate the climate response to forcing agents other than CO₂, such as methane (Stecher et al., 2021), but this has not yet received much attention.

In addition, there is new evidence that stratospheric ozone-circulation coupling modifies the atmospheric circulation response to CO₂. Stratospheric ozone modulates the stratospheric cooling due to CO₂ (Chiodo and Polvani, 2019; Dietmüller et al., 2014; Nowack et al., 2018, 2015; Kuilman et al., 2020) and can subsequently affect dynamics through changes in the meridional temperature gradient. In the stratosphere, model simulations with interactive ozone show a dampening of GHG-induced tropical upwelling increases, reducing the QBO amplitude (DallaSanta et al., 2021). In the troposphere, interactive stratospheric ozone reduces the poleward shift of the eddy-driven jet in response to GHG increases (Chiodo and Polvani, 2017; Nowack et al., 2018; Chiodo and Polvani, 2019) and damps the ENSO response (Nowack et al., 2017). While these are individual model findings and have not yet been tested for consistency across multiple models, they consistently suggest that stratospheric ozone may affect several aspects of tropospheric and surface climate beyond the global mean surface temperature, inducing a negative feedback on a variety of circulation metrics and thereby counteracting the effects of GHGs.

Taken together, we assess that stratospheric ozone-climate feedbacks are still uncertain but more likely to reduce than increase ECS, consistent with the conclusions of the previous Assessment (WMO, 2018) and IPCC AR6 (Szopa et al., 2021). Based on new evidence since the last Assessment, we revise the range of ECS reduction due to the stratospheric ozone-climate feedback to 0–10%, with reductions beyond 10% deemed unlikely. While not yet quantified with high certainty, there is robust evidence that stratospheric ozone affects other aspects beyond ECS, such as the atmospheric circulation response to GHGs in both the stratosphere and troposphere.

5.3.2 Ozone/Dynamical Coupling

Stratospheric ozone is strongly coupled to the stratospheric circulation, as its abundances are largely determined by transport, especially in the lower stratosphere. In turn, stratospheric ozone itself affects the circulation via changes in radiative heating and temperature gradients (see **Box 5-4**). In previous Assessments, the effects of stratospheric ozone on circulation have been studied in the context of long-term depletion and recovery trends. Updates on the impact of ozone trends on circulation, with particular emphasis on the emerging signal from the Montreal Protocol since the early 2000s, are provided in *Section 5.3.2.2*.

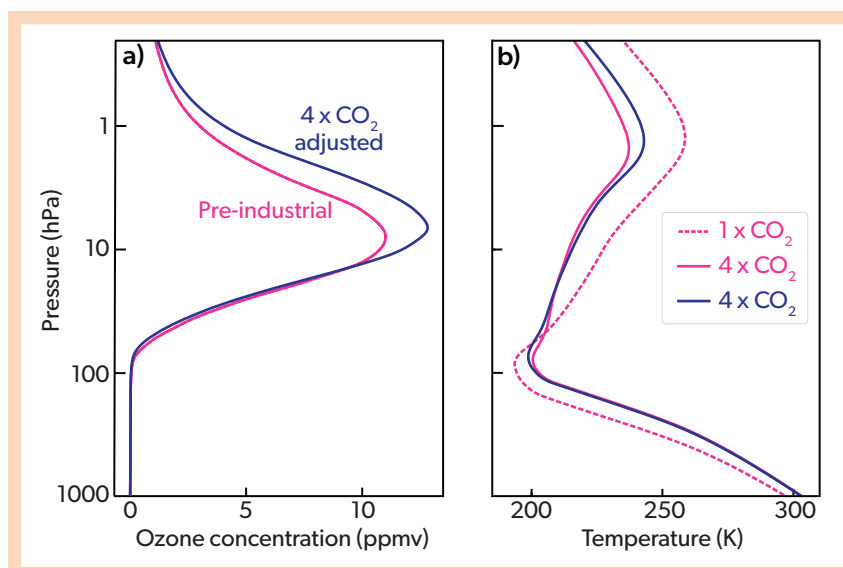


Figure 5-10. Stratospheric ozone feedback on temperature changes simulated by a simple 1-D radiative convective equilibrium model. Vertical profile of (left) tropical mean zonal mean ozone for preindustrial climate (pink) and for 4xCO₂ (blue), and (right) resulting temperature profiles from the model for preindustrial climate (pink dashed), and for 4xCO₂ forcing when prescribing the preindustrial ozone profile (pink) or the 4xCO₂ ozone profile (blue). [Adapted from Dacie et al., 2019.]

Since the last Assessment, new work has provided evidence that interannual variations in ozone may affect stratospheric circulation and its coupling to the troposphere, in much the same way as long-term trends. While interannual variations in ozone are largely driven by circulation variability, they are also affected by chemistry, in particular for polar ozone when ODS abundances are high (see *Chapter 4*). This radiative-dynamical-chemical coupling between ozone and circulation (see *Box 5-4*) can lead to ozone-induced surface impacts on sub-seasonal to interannual timescales, as assessed in *Section 5.3.2.1*. When integrated over longer timescales, the two-way ozone-circulation coupling also alters the circulation and climate response to long-term ozone trends, as discussed in *Section 5.3.2.2.1*.

5.3.2.1 Ozone-Circulation Coupling on Seasonal to Interannual Timescales

Stratospheric ozone has large variations on sub-seasonal to interannual timescales, particularly in springtime in the polar stratosphere (*Chapter 4*). Recent dramatic examples of this are the weakened springtime polar cap ozone depletion in the Antarctic in 2019 (Wargan et al., 2020) and the large depletion in the Arctic in 2020 (Lawrence et al., 2020). These interannual variations in polar cap ozone may further amplify stratospheric temperature variations and thus provide a coupling to the circulation, as described in *Box 5-4*. Given the relatively long timescales (i.e., 1–2 months) associated with stratosphere-troposphere coupling (Lim et al., 2018, 2019), ozone information could provide a source of sub-seasonal to seasonal predictability for surface climate (Son et al., 2013; Bandoro et al., 2014). However, the causality in the link between ozone extremes and surface climate to date is unclear and subject to debate, as downward coupling may come from stratospheric dynamics rather than ozone itself. In the 2018 Assessment, it was noted that interannual variations in Arctic and Antarctic ozone may be important for surface climate, but work remains to better quantify this connection. Here, we discuss the newest evidence in this field for the Antarctic (*Section 5.3.2.1.1*), the Arctic (*Section 5.3.2.1.2*), and the tropics (*Section 5.3.2.1.3*).

5.3.2.1.1 Antarctic

In previous Assessments, it was noted that there is a statistical link between Antarctic polar cap ozone in springtime and spring-to-summer surface climate, including widespread variations in precipitation and surface air temperature across the Southern Hemisphere (Son et al., 2013; Bandoro et al., 2014). However, interannual variations in springtime ozone are strongly coupled with the polar vortex through ozone transport and polar ozone depletion (see *Box 5-4, Figure 1*). Variations in the polar vortex are associated with changes in surface climate (Byrne and Shepherd, 2018; Lim et al., 2018; Thompson et al., 2005), making it difficult to tease apart the effect of ozone on the circulation from that of downward coupling from the polar vortex without such ozone effects (Karpechko, Maycock et al., 2018).

Since the last Assessment, the link between vortex variability, ozone, and surface climate on interannual timescales has been revisited using climate and sub-seasonal to seasonal (S2S) prediction models. The polar vortex weakening in spring 2019, which may have contributed to Australian New Year fires in the following summer (Lim et al., 2021), was also linked with the smallest ozone hole since the early 1980s (*Chapter 4*), but the role of ozone in these events is unclear. The observed surface signals following years with extreme ozone perturbations have been reproduced in CCMs but with mixed success. For example, one model reproduces the link between November ozone and Australian summer temperatures only when observed SSTs are prescribed, but it fails to capture the link when the ocean is coupled (Gillett et al., 2019). This hints at the role of observed SSTs, rather than ozone, in driving the ozone/SAM and ozone/surface temperature relationship in this model. Other CCMs reproduce the observed surface signals, even in ocean-coupled simulations (Damiani et al., 2020). Model biases, such as the too-long-lived SH polar vortex and/or excessive ENSO amplitudes, may hinder models' ability to simulate the interannual relationship reliably. Moreover, the observed correlation between November ozone and SH surface climate in summer is strong over the 1979–2012 period but becomes weak if a shorter period (1979–2004) is analyzed (Gillett et al., 2019), raising questions about the possible role of natural variability.

Lastly, the relative roles of ozone and dynamical downward coupling from the stratosphere are unclear, as none of these studies quantified the impact of interactive ozone on the ozone/surface climate link.

The causal impact of stratospheric ozone variations on surface climate has been quantified only for some extreme events in the SH stratosphere (Hendon et al., 2020). The major SSW of September 2002 was a unique event, with one of the largest disruptions of the stratospheric vortex on record, resulting in a strongly negative SAM (Thompson et al., 2005), and hot, dry conditions over Australia in October (Figure 5-11). In 2002, Antarctic ozone abundances in September were exceptionally high, thus offering a unique opportunity for a case study on the ozone/surface climate connection. Seasonal model forecasts using climatological ozone underpredict the SAM anomaly in October and, as a consequence, the regional signals over Australia (CTRL in Figure 5-11). Conversely, prescribing the observed ozone

anomalies of 2002 in the ACCESS forecasting model leads to enhanced regional signals, which come closer to observations (difference between EXPR and CTRL in Figure 5-11). The signature originates from enhanced persistence of the stratospheric signal of the SSW event due to ozone-circulation coupling, which drives an enhanced negative SAM. This provides evidence for ozone effects on SH surface climate but only for a specific event (2002) and in one model. A similar sub-seasonal model prediction study is consistent with these results for the entire 2004–2020 period (Oh et al., 2022). Recently, it was suggested that high ozone abundances occurring during SSWs may initially lead to a positive tropospheric SAM in spring (a “fast response”) and subsequently drive a negative SAM in early summer (a “slow response”; Jucker et al., 2022). While this hypothesis explains the observed behavior following the 2019 SSW event, it is inconsistent with observations for the 2002 SSW and remains to be tested for other cases and with more realistic configurations and other models.

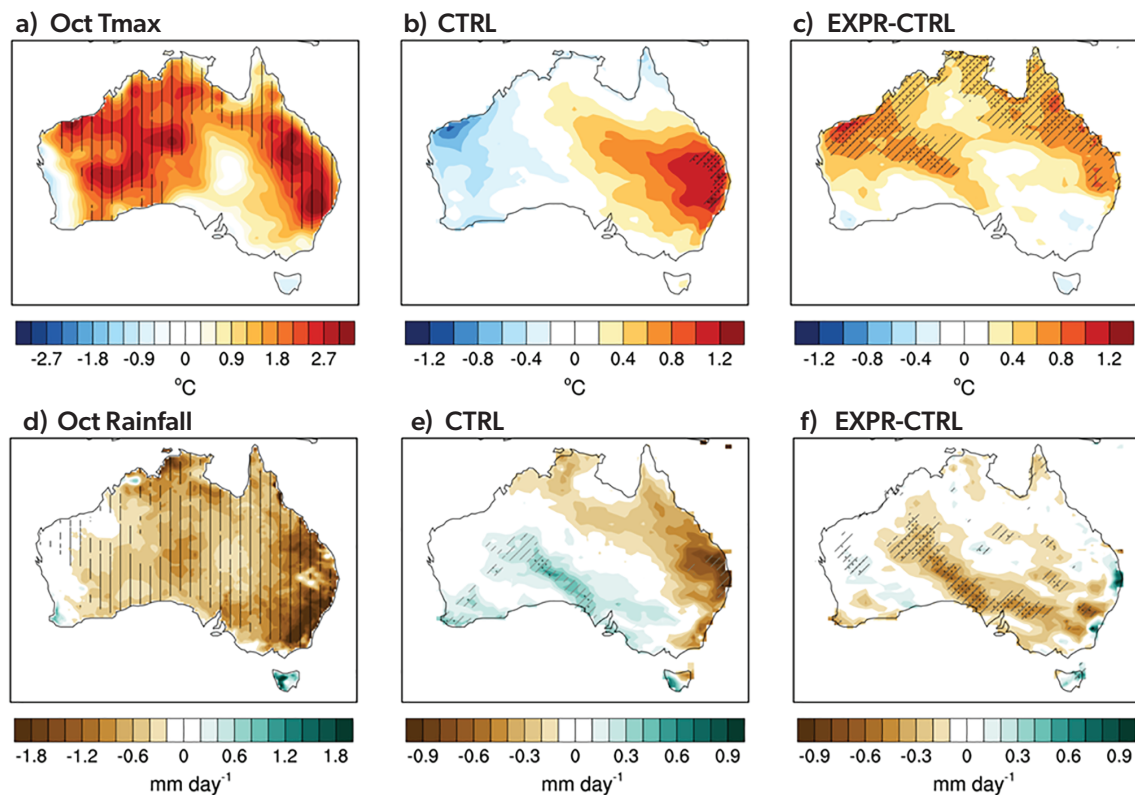


Figure 5-11. Effect of stratospheric ozone anomalies on surface climate in October 2002. Panels (a) and (d) show the observed anomaly in (a) maximum temperature (units: K) and (d) precipitation (units: mm/day) for October 2002. Panels (b) and (e) show the simulated temperature (b) and precipitation (d) anomalies, averaged across and 11 members ensemble of model simulations using the ACCESS forecasting model when fixed climatological ozone concentrations are used (CTRL). Panels (c) and (f) show the ensemble-mean difference in temperature (c) and precipitation (f) between model simulations where the observed 2002 ozone anomalies were used (EXPR) and the CTRL simulations (shown in panels b and d) using a fixed climatological ozone (CTRL). Hatching in (a) and (d) indicates where the October 2002 anomaly falls in the upper 20% and lower 20% tails, respectively, of the observed distribution for the period 1990–2012 (excluding 2002). Stippling and hatching in (b) and (e) indicate where the predicted values fall within the 5% and 10% tails, respectively, of the distribution based on the hindcast control simulations spanning the period 1990–2012 (excluding 2002). Stippling and hatching in (c) and (f) indicate where the null hypothesis of no difference between EXPR and CTRL is rejected at the 5% (10%) level based on resampling of the 11 ensemble members from the CTRL and EXPR for 2002. [Adapted from Hendon et al., 2020.]

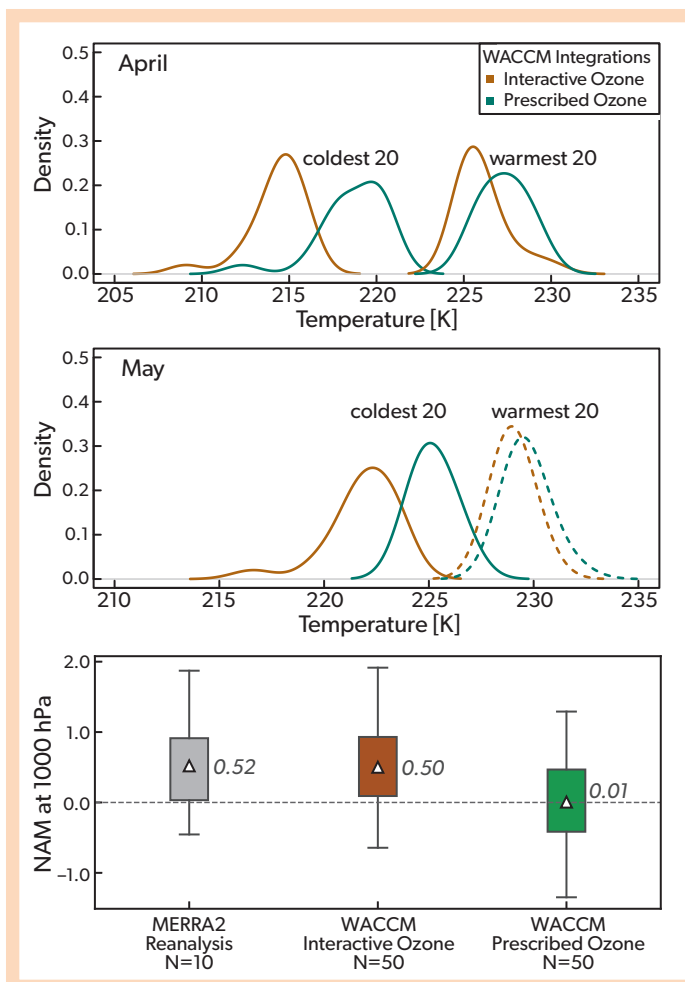


Figure 5-12. Impact of interannual Arctic ozone variations on stratospheric temperatures and tropospheric circulation. Probability distribution functions for (top) April and (middle) May monthly mean Arctic lower stratospheric (50 hPa) polar cap temperature for the coldest and warmest 20 years in perpetual year-2000 Whole Atmosphere Community Climate Model (WACCM) integrations with interactive chemistry (brown) and with prescribed climatological zonal mean ozone (green). Solid curves indicate a significant difference between the two integrations at the 95% level, while dashed curves indicate no significant difference. (bottom) Box plots of the Northern Annular Mode (NAM) index at 1000 hPa following winters with extreme ozone loss. The box plot shows the distribution of the mean NAM Index (20 - 90°N) at 1000 hPa in the month following the ozone minimum for the MERRA2 reanalysis (gray), WACCM integrations with interactive middle atmosphere chemistry (brown) and the WACCM integrations in which ozone chemistry is decoupled from the radiation scheme, i.e. the radiation scheme uses a prescribed climatological year-2000 zonal mean ozone field (green). In the bottom panel, in the WACCM integrations with prescribed ozone, chemistry is still calculated in the background so that ozone depletion events can be identified following the methodology in Friedel et al. (2022). Triangles and numbers indicate the mean NAM index in the month after the ozone minima, averaged over the 25% most extreme winters. The upper and lower edges of the boxes show the upper and lower quartile, the whiskers represent the maximum and minimum values of the respective distribution. [Top and middle panels adapted from Rieder et al., 2019, and bottom panel adapted from Friedel et al., 2022.]

Taken together, we assess that interannual variations in the severity of the Antarctic ozone hole likely affect SH surface climate by inducing variations in the tropospheric SAM (e.g., a weaker ozone hole and attendant weaker polar vortex result in a swing to the negative polarity of the SAM in the summertime, reflected by an equatorward shift of the mid-latitude westerlies). However, the robustness and causality of the ozone-SAM-surface link on interannual timescales, and thus the added value for predictability, is still unclear, especially on regional scales (Australia), where other modes of variability (e.g., the Indian Ocean Dipole and ENSO) can have a more direct impact. Climate models show only limited skill in reproducing the observed relationship, and the role of natural variability and/or model bias remains unclear.

5.3.2.1.2 Arctic

The previous Assessment noted that studies examining the influence of interannual variability in springtime Arctic stratospheric ozone on NH tropospheric and surface climate yielded mixed results. Some studies find no or limited influence (Cheung et al., 2014; Karpechko et al., 2014; Smith and Polvani, 2014) and others find a significant influence of springtime low Arctic ozone that resembles the positive phase of the North Atlantic Oscillation/Northern Annular Mode (NAO/NAM), but only in the presence of high ODS concentrations and/or sufficient chemical ozone loss (Smith and Polvani, 2014; Calvo et al., 2015; Ivy et al., 2017). The positive phase of the NAM is associated with a stronger and

poleward-shifted jet stream, anomalous surface warming over Eurasia, anomalous surface cooling over Greenland and north-eastern Canada, and anomalously high precipitation over northern Europe. Since the previous Assessment, a number of studies linking late-20th century Arctic springtime ozone variability and NH surface climate have been published (Xie et al., 2018; Ma et al., 2019; Stone et al., 2019; Ma and Xie, 2020; Maleska et al., 2020; Stone et al., 2020; Xia et al., 2021). Yet isolating any direct influence of ozone anomalies from that of stratospheric circulation anomalies and stratosphere-troposphere coupling remains a challenge as ozone and circulation are inherently coupled via both transport and chemistry (see Box 5-4; Fusco and Salby, 1999; Randel et al., 2002; Tegtmeier et al., 2008; Rieder et al., 2014; de la Cámara et al., 2018; Haase and Matthes, 2019; Harari et al., 2019; Oehrlein et al., 2020; Hong and Reichler, 2021).

New modeling evidence supports a significant correlation between Arctic springtime ozone anomalies and polar cap surface air pressure, but this correlation becomes insignificant when adjusted for stratospheric circulation anomalies (Harari et al., 2019). Consistent with this result, another modeling study found that the composite difference in sea level pressure between low and high Arctic springtime ozone years during the 1985–2005 period projected almost entirely onto the NAM, underscoring the dominant role of large-scale circulation in linking ozone extremes to surface climate (Maleska et al., 2020).

The above studies (Harari et al., 2019; Maleska et al., 2020), however, do not directly isolate the contribution of potential coupling between ozone and large-scale dynamics, and recent work comparing simulations with and without interactive middle-atmosphere chemistry in the presence of late-20th century ODS concentrations has highlighted the importance of this coupling for both NH stratospheric and tropospheric climate (Rae et al., 2019; Haase and Matthes, 2019; Rieder et al., 2019; Romanowsky et al., 2019; Oehrlein et al., 2020; Friedel et al., 2022; see also **Box 5-4**). For example, cold extremes in Arctic polar lower-stratospheric temperature are significantly colder in a model simulation with interactive chemistry than in a simulation with prescribed ozone (**Figure 5-12** top and middle panel; Rieder et al., 2019). This suggests that ozone-circulation coupling is important for NH stratospheric climate. Recent modeling work in which the radiative effects of ozone are decoupled from ozone itself provides evidence that ozone-circulation coupling in the stratosphere can have a significant impact on tropospheric and surface climate via stratosphere-troposphere coupling (**Figure 5-12** bottom panel; Friedel et al., 2022; see also **Box 5-4**): under year-2000 ODS concentrations, ozone-circulation coupling leads to a significantly more positive NAM at the surface (1000 hPa) for years with low ozone in spring. Although there is clear evidence of this coupling, the magnitude and significance of its contribution may be sensitive to statistical sampling and the configuration of the CCM (Haase and Matthes, 2019; Oehrlein et al., 2020; Friedel et al., 2022). Finally, analysis of model output during the 1985–2005 period suggests that rapid adjustments in high clouds associated with localized extreme chemical ozone loss and a decrease in upper-tropospheric stability may also contribute to the link between springtime ozone and surface climate (Maleska et al., 2020; Xia et al., 2021).

The extent to which the representation of ozone variability in forecast models leads to improved skill is mixed. One study found that when a new prognostic ozone scheme is interactive with radiation, there is improved skill in the North Atlantic region for both

medium- and long-range hindcasts due to an improvement in the representation of stratosphere-troposphere coupling (Monge-Sanz et al., 2022). In contrast, another study examining forecasts of individual extreme ozone loss years (1997, 2011, and 2020) found that the forecasts do not consistently capture the observed link between low ozone extremes and near-surface temperatures in the Northern Hemisphere (Rao and Garfinkel, 2020). The 2020 extreme ozone depletion event (Lawrence et al., 2020) was an exception, however, and the subsequent Eurasian surface warming was reasonably well predicted 2–3 weeks in advance (Rao and Garfinkel, 2020; Rao and Garfinkel, 2021c; Xia et al., 2021).

In summary, based on substantial new research since the previous Assessment, our determination is that although the influence of interannual variability in Arctic springtime ozone on NH surface climate is primarily driven by the large-scale circulation, there is evidence for a non-negligible contribution from ozone-circulation coupling during the late 20th century when high ODS concentrations contribute to chemical ozone loss (Calvo et al., 2015; Maleska et al., 2020; Friedel et al., 2022; **Box 5-4**). Uncertainty remains in the quantification of the contribution of this coupling to NH surface climate.

5.3.2.1.3 Tropics

Since the last Assessment, a few studies have shown that ozone-circulation coupling may affect the variability in the tropical stratosphere under steady-state preindustrial conditions. One study (Yook et al., 2020) simulated that interactive ozone chemistry increases the variability in tropical stratospheric temperatures in one global model by a factor of two (**Figure 5-13a**). The increased variability is primarily driven by tropical upwelling and its effects on ozone at interannual timescales; ozone in turn feeds back onto temperature via LW and SW heating, with the latter dominating near the TTL region. Due to the long radiative timescales in this region, ozone not only affects the variance but also imparts additional memory from one month to the next (**Figure 5-13b**). Most remarkably, this study shows that models

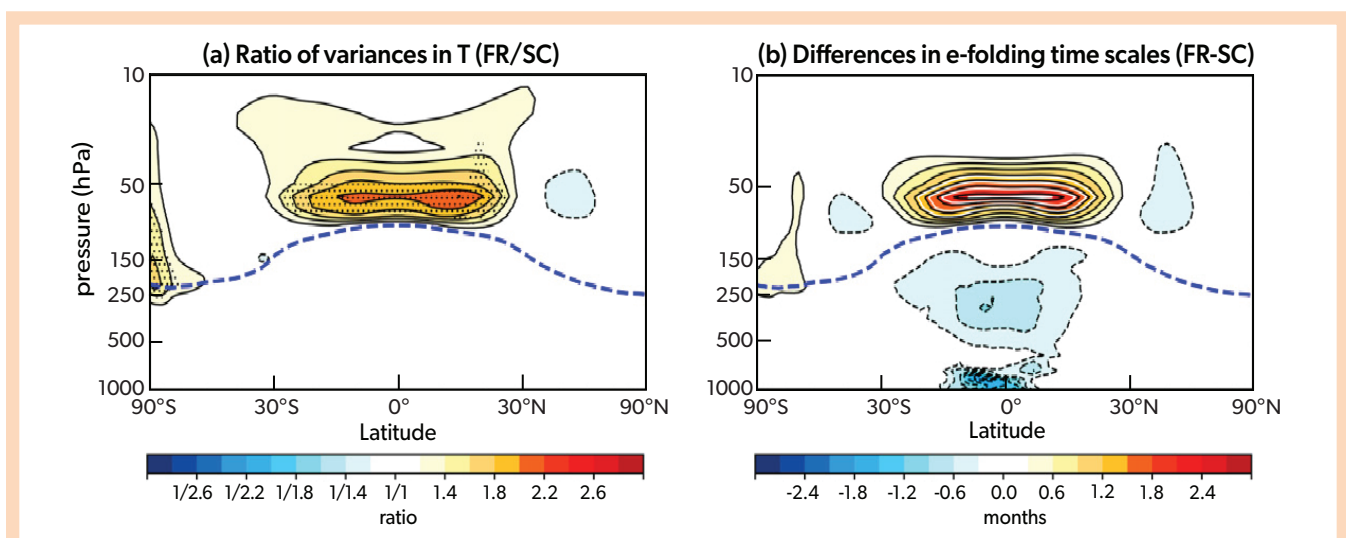


Figure 5-13. Impact of ozone variations on temperature variability. (a) Ratio of zonal mean temperature variance between a WACCM simulation with interactive ozone (FR) and one with specified ozone (SC), and (b) the difference in the e-folding timescale of temperature (in months) between the two simulations (FR-SC). [Adapted from Yook et al., 2020.]

with prescribed ozone systematically underestimate the temperature variance in this region. One caveat about this study is that an artificial QBO is nudged in this model. This may dampen the impact of ozone coupling on the tropical upwelling and thus interfere with the effects of ozone on temperature variance. In a model with an internally generated QBO, interactive ozone leads to a slight prolongation in the QBO period (from 29 to 31 months) and an intensification of the QBO amplitude (DallaSanta et al., 2021; see Section 5.2.6.2). These results are consistent with the notion of ozone-induced enhanced temperature variance in the tropical stratosphere and are also consistent with previous work using other models with an internally generated QBO and interactive ozone (Shibata and Deushi, 2005), as well as with simulations with prescribed ozone (Bushell et al., 2010), although the differences in the temperature variance are much smaller and only marginally significant.

Overall, there is new evidence since the last Assessment for effects of interannual variability in ozone, not only at high latitudes but also in the tropical regions. However, these results remain limited to a few individual model studies and are a subject of ongoing analysis.

5.3.2.2 Impact of Ozone Trends on the Tropospheric Circulation and Surface Climate

The linkages between SH ozone depletion and tropospheric circulation trends were first noted in observations in 2002 (Thompson and Solomon, 2002). The effects of stratospheric ozone losses on surface climate were simulated in fixed sea surface temperature experiments in the early 2000s (Sexton, 2001; Kindem and Christianson, 2001), and in a coupled climate model a few years later (Gillett and Thompson, 2003). The anticipated linkages between ozone recovery and the surface flow were

explored in coupled chemistry-climate models in 2008 (Son et al., 2008). Since that time, the role of stratospheric ozone depletion and recovery in tropospheric climate has been reproduced in a large number of numerical experiments (e.g., Son et al., 2010; Thompson et al., 2011; Seviour et al., 2017, and references therein). Recently produced historical reconstructions of the SAM suggest that the positive trend in the SAM during the decades prior to 2000, which is attributed to ozone depletion, is unprecedented in the last millennia and thus falls well outside the range of natural climate variability (Fogt and Marshall, 2020).

The 2010, 2014, and 2018 Assessments provided extensive reviews of the signatures of ozone depletion and recovery in the tropospheric circulation. As of the 2018 Assessment, the state of our understanding was the following:

1. Observations indicate that the SH tropospheric jets shifted poleward and the SAM shifted toward its positive polarity over the period of large SH stratospheric ozone depletion, from roughly 1980 to 2000.
2. The largest trends in the SH tropospheric climate occurred during the austral summer months.
3. Climate simulations indicate that the bulk of the observed SH trends were due to Antarctic ozone depletion.
4. Climate simulations suggest that ozone recovery will lead to a reversal of the SH trends that arose from Antarctic ozone depletion.
5. Antarctic ozone depletion and recovery-related trends in the tropospheric circulation have widespread impacts on SH surface climate.
6. There is little evidence for similarly robust linkages between stratospheric ozone depletion and surface climate in the Northern Hemisphere.

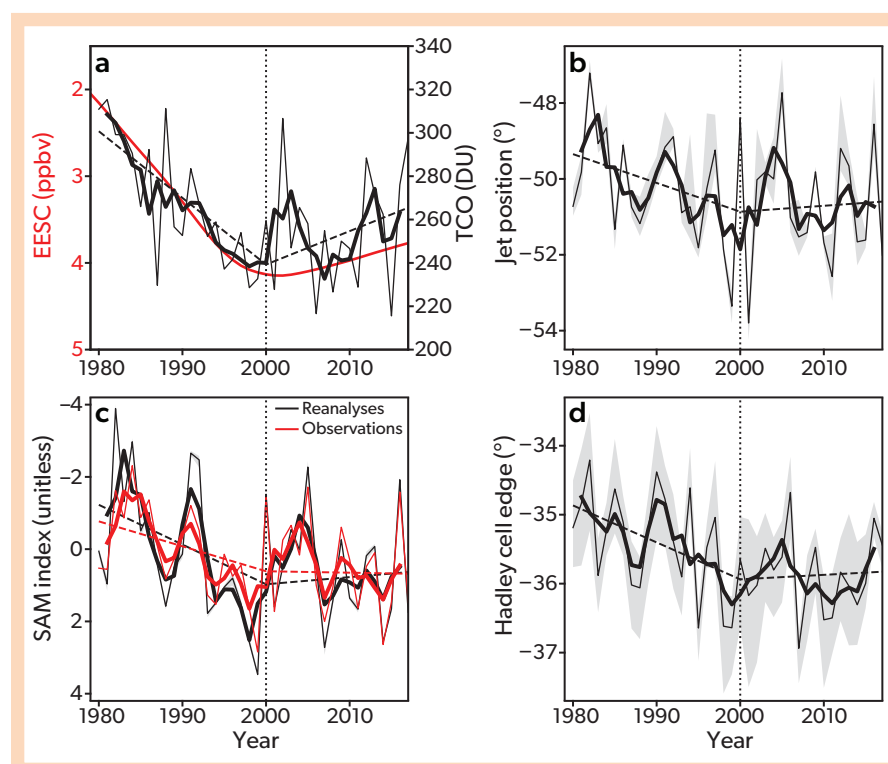


Figure 5-14. Observed total ozone and Southern Hemisphere tropospheric circulation. Time series of (a) EESC (note the inverted left y axis) for polar winter conditions and Antarctic total column ozone (TCO; right axis) averaged over September through November, with the latter measured by SBUV (in DU). (b) position of the SH mid-latitude jet in reanalysis data in DJF, (c) the SAM index (note the inverted y axis) as derived from reanalysis data and from station observations in DJF, (d) position of the edge of the Hadley cell in reanalysis data in DJF. Reanalysis data are averages across four products (ERA-I, JRA-55, MERRA2-ana and MERRA2-asm). The thin lines are unsmoothed quantities, and thick lines represent centered three-year smoothed values. Two piecewise continuous linear trend lines for the unsmoothed data (dashed lines) are drawn for the periods 1980–2000 and 2000–2017. [From Banerjee et al., 2020.]

Since the 2018 Assessment, the availability of longer data records has permitted identification of the signature of ozone recovery in tropospheric circulation trends. **Figure 5-14a** (from Banerjee et al., 2020) summarizes the long-term behavior of SH stratospheric ozone during the period of large ozone losses and the onset of recovery. Antarctic stratospheric ozone concentrations indicate signs of recovery since roughly 2000 (Solomon et al., 2016; Stone et al., 2018; *Chapter 4*). However, from **Figure 5-14a** it is also clear that identifying the trend in ozone since 2000 (dashed line) is complicated by the large interannual variability during this period (thin black line). The SAM index exhibits trends similar to those found in total column ozone (**Figure 5-14c**): 1) the large decreases in ozone concentrations prior to year 2000 are accompanied by increases in the SAM index and 2) the onset of recovery following year 2000 is accompanied by no clear trend in the SAM index. The changes in the SAM index are accompanied by consistent changes in the position of the mid-latitude jet and the edge of the Hadley cell (**Figure 5-14 b and d**).

The signature of ozone recovery in circulation trends is clearest in the changes in circulation trends between the period of large ozone depletion and the onset of recovery (Banerjee et al., 2020; Zambri et al., 2021). For example, **Figure 5-15** shows that the period prior to 2001 was marked by significant decreases in polar ozone during November (panel a), polar stratospheric temperatures during November and December (panel b), and polar geopotential height during November and December (panel c; see the caption for data sources). It was also marked by changes in the upper-tropospheric circulation in December and January, consistent with a trend toward the positive polarity of the SAM (panel d). As noted in both Banerjee et al. (2020) and Zambri et al. (2021), the period following 2001 (i.e., the onset of recovery) was not marked by significant trends in any of those fields. The differences in trends between the periods prior to and after 2001 are significant at stratospheric levels and on the fringe of significance at upper-tropospheric levels (**Figure 5-15**; Zambri et al., 2021).

Thus, observations to date indicate that:

1. consistent with the anticipated effects of ozone recovery, the observed SH springtime *stratospheric* circulation trends since ~2001 are not statistically significant, but the changes

in the circulation trends between the pre- and post-2001 periods are statistically significant (Banerjee et al., 2020; Zambri et al., 2021); and

2. the attendant changes in SH summertime *tropospheric* circulation trends are consistent with the changes found in the stratosphere (Banerjee et al., 2020; Zambri et al., 2021) but are on the fringe of significance (Zambri et al., 2021).

It is worth emphasizing that the results shown in **Figures 5-14 and 5-15** extend only through 2018 and thus do not include the strong polar vortex and large ozone losses of SH spring 2020 and spring 2021.

The inferred influence of changes in ozone trends on changes in tropospheric circulation trends is supported by experiments run on coupled chemistry-climate simulations and prescribed-ozone climate model simulations (Banerjee et al., 2020; Zambri et al., 2021; see *Section 5.4*). As noted in previous Assessments, the influence of increasing greenhouse gases on the SAM will likely oppose the effects of ozone recovery on the SAM during austral summer (e.g., Arblaster and Meehl, 2006; Thompson et al., 2011, *Figure 3*). The experiments in Banerjee et al. (2020) provide further numerical support for this hypothesis.

Various dynamical and radiative mechanisms have been proposed to explain how ozone-induced changes in the stratospheric flow are communicated to the surface. These are summarized in the 2018 Assessment. As of this writing, the relative importance of the various proposed forcing mechanisms remains unclear and is a key focus of current research.

There is novel evidence that ozone-induced trends in the SAM exhibit longitudinal variations that have potentially important implications for the surface impacts of ozone depletion (Vaugh et al., 2020). However, as concluded in *Chapter 10* of IPCC AR6 (Doblas-Reyes et al., 2021), internal climate variability and uncertainty is too strong at the regional scale to robustly attribute past regional surface climate change to specific anthropogenic forcings such as stratospheric ozone depletion. Likewise, Mindlin et al. (2021) highlight the large uncertainties in future regional climate change that arise from the uncertainties in the circulation response.

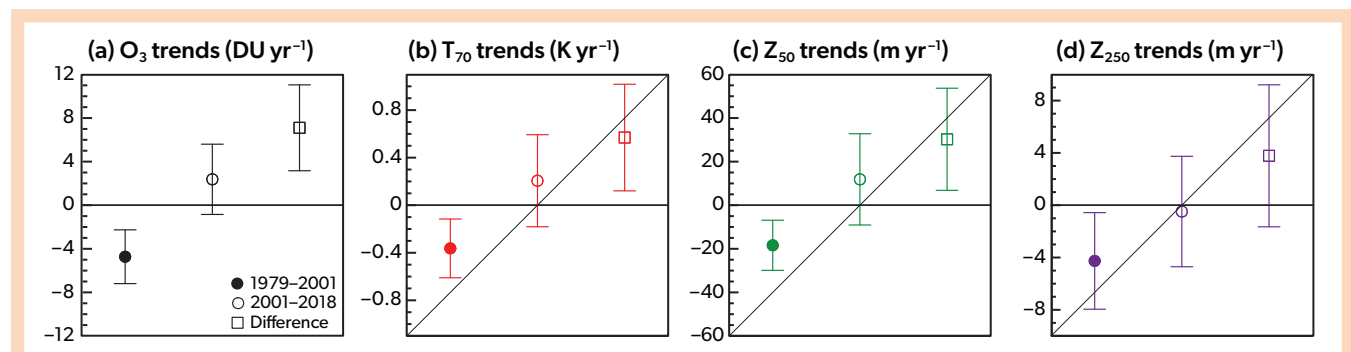


Figure 5-15. Trends in Southern Hemisphere high-latitude (65–90°S) ozone and circulation. (a) November ozone (DU yr⁻¹), (b) November–December 70 hPa temperature (K yr⁻¹), (c) November–December 50 hPa geopotential height (m yr⁻¹), and (d) December–January 250 hPa geopotential height (m yr⁻¹) for 1979–2001 (filled circles), 2001–2018 (open circles), and the difference (squares). Error bars represent the adjusted 95% confidence intervals of the trends. Ozone data are from the TOMS/OMI merged ozone dataset; temperature and geopotential height are from ERA5. [From Zambri et al., 2021.]

As was the case in the 2018 Assessment, there are no detectable NH surface impacts of long-term Arctic ozone changes over the past ~4 decades. However, for individual years with low springtime Arctic ozone, new model evidence indicates that the ozone anomalies induce changes to the stratospheric circulation, with subsequent surface impacts (as discussed in Section 5.3.2.1.2).

Comparison with the IPCC AR6. Since the 2018 Assessment, the relative roles of ozone depletion and greenhouse gases in future climate change have been quantified in CMIP6 climate change simulations (Mindlin et al., 2021; Lee et al., 2021). Simulations from the CMIP6 archive support conclusions from earlier analyses (e.g., Arblaster and Meehl, 2006; McLandress et al., 2010; Thompson et al., 2011, Figure 3); namely, that the anticipated influence of ozone recovery on the SH circulation during austral summer is opposed by the anticipated influence of increasing GHGs on the SH circulation. This opposing influence on SH summer circulation changes is consistent with their scenario dependency by the end of the century, as reported in Chapter 4 of the Working Group I contribution to IPCC AR6 (Lee et al., 2021), which stated, “there is *high confidence* that in high-emissions scenarios (SSP3-7.0 and SSP5-8.5) the SAM becomes more positive in all seasons, while in the lowest scenario (SSP1-1.9) there is a robust decrease in austral summer.” This finding is further supported by recent work (Revell et al., 2022), which in addition highlights the dependency of changes in the summer circulation jets on the evolution of stratospheric ozone in the models, in particular emphasizing the important role of consistency of stratospheric ozone with the underlying GHG scenario.

However, the IPCC AR6 report also notes that the “contribution [to the SAM] from ozone forcing evaluated with the four available models is not significant (Fig. 3.34b)” (Figure 3.34 and associated text in Eyring et al., 2021). Taken at face value, the above statement appears to contradict two decades of numerical evidence that reaches the opposite conclusion, including evidence derived from CMIP5 (Barnes and Polvani, 2013) and summarized in the past three Ozone Assessments (WMO, 2010, 2014, 2018).

There are two aspects of the evidence presented in Chapter 3 of the Working Group I contribution to IPCC AR6 (Eyring et al., 2021) that contribute to the discrepancies between their results (see Figure 3.34 of Eyring et al., 2021) and results reported here and in the last three Assessments (WMO, 2010, 2014, 2018):

1. The SAM index used in Eyring et al. (2021) is based on the algebraic difference between sea level pressure (SLP) at two discrete latitudes (40°S and 65°S) that lie very close to the nodes—not the centers of action—of the SAM in the SLP field. Variations in the SAM are better captured by indices that account for the hemispheric-scale structure of the pattern.
2. Eyring et al. (2021) summarizes simulated trends in the SAM from two periods: 1979–2019 and 2000–2019. Neither period is well positioned to isolate the signature of ozone depletion on surface climate. The former period samples not only the era of large stratospheric ozone depletion but also the era of the onset of recovery. The latter period does not sample the era of large stratospheric ozone depletion.

The summary remarks in Chapter 3 of the Working Group I contribution to IPCC AR6 (Eyring et al., 2021) align more closely with the conclusions reported here. In this case, AR6 states

“While ozone depletion contributed to the trend from the 1970s to the 1990s (*medium confidence*), its influence has been small since 2000, leading to a weaker summertime SAM trend over 2000–2019 (*medium confidence*)”. Our assessment agrees with the general conclusions in the above statement but would assign higher confidences given the evidence reviewed here and in past WMO reports (WMO, 2010, 2014, 2018).

5.3.2.2.1 Impact of Two-Way Ozone-Circulation Coupling on Antarctic/Southern Hemisphere Trends

As discussed in Section 5.3.2.1.2 and **Box 5-4**, the nature of how ozone and, consequently, coupling between ozone and circulation are represented in climate models has been an ongoing area of research. In many climate models, ozone concentrations are prescribed as a monthly and zonal mean forcing, such as the recommended IGAC/SPARC ozone fields used in the CMIP5 model runs (Eyring et al., 2013; Cionni et al., 2011). Prescribing monthly and zonal mean ozone rather than interactively computing it neglects important aspects of ozone variability and trends, including zonal asymmetries in ozone and high temporal frequency events, specifically the evolution of the seasonal ozone hole in the Southern Hemisphere (Crook et al., 2008; Gillett et al., 2009; Waugh et al., 2009; Neely et al., 2014; Haase et al., 2020), as well as ozone-circulation couplings (Rae et al., 2019; Haase et al., 2020; Ivanciu et al., 2021; Lin and Ming, 2021; see also Section 5.3.2.1.2). As such, the recommended ozone forcing for CMIP6 now includes zonal asymmetries (Checa-Garcia et al., 2018), although many models continue to use a zonal mean ozone forcing (Keeble et al., 2021).

In the previous Assessment, calculations comparing the CCMI and CMIP5 multi-model ensembles suggested that the representation of ozone (interactive in the CCMI ensemble but largely prescribed in the CMIP5 ensemble) did not affect the simulation of SH tropospheric circulation trends in December–January–February (DJF, i.e., austral summer; Son et al., 2018). In contrast, a recent analysis of CMIP6 historical DJF SAM trends noted a greater influence of ozone depletion relative to greenhouse gases in simulations with interactive ozone chemistry than those without (Morgenstern, 2021). Large systematic model differences, varying ensemble sizes, and differences in which ozone forcing is used and how it is prescribed within such multi-model ensembles contribute to the ambiguity of these results (Keeble et al., 2021). Previous single-model studies have shown that the representation of ozone can have a significant effect on SH circulation variability and trends, particularly in the stratosphere, and some studies also show an effect in the troposphere (Crook et al., 2008; Gillett et al., 2009; Waugh et al., 2009; Neely et al., 2014).

Since the last Assessment, several single-model studies have reexamined the effect of ozone-circulation coupling on summertime SH circulation trends. The studies compared ensembles of CCM integrations with either fully interactive ozone or prescribed ozone and found that both zonally asymmetric ozone and ozone-circulation coupling in the interactive integrations contribute to significantly colder and stronger SH polar cap stratospheric temperature and zonal wind trends, respectively (Haase et al., 2020; Ivanciu et al., 2021; Lin and Ming, 2021). It was suggested that zonal wind-induced wave dissipation and/or wave dissipation via ozone radiative damping may be playing an important role when ozone chemistry is interactive and may be amplified

in the presence of high concentrations of ODSs (Lin and Ming, 2021). The effect of interactive ozone on tropospheric trends, however, was ambiguous, with one study showing no effect over the 1969–1998 period (Haase et al., 2020) and the other using a different climate model showing significantly larger trends in tropospheric zonal wind over the 1958–2013 period (Ivanciu et al., 2021).

In summary, our assessment is that two-way ozone-circulation coupling has a robust influence on SH stratospheric circulation trends and amplifies the circulation response to ODS-forced ozone changes. Thus, model studies using prescribed ozone fields might underestimate those effects. Whether the amplified stratospheric circulation response also influences the tropospheric circulation trends has not yet been robustly shown.

5.3.3 Impacts of Ozone Changes on the Oceans and the Cryosphere

5.3.3.1 Ocean Impacts

Winds over the Southern Ocean play a fundamental role in driving the ocean circulation. Over the period ~1980–2000,

summer trends in the SAM and in westerly winds have been mainly attributed to ozone depletion; since 2000, summer trends in the SAM have not been significant (Section 5.3.2.2). Westerly wind stress over the Southern Ocean drives equatorward Ekman transport, resulting in mixed-layer divergence and upwelling at high latitudes (on the poleward side of the westerly wind jet) and convergence and downwelling at mid-latitudes (on the equatorward side of the westerly wind jet; Hall and Visbeck, 2002; Sen Gupta and England, 2006). A positive SAM trend implies a poleward shift and/or strengthening of the surface westerly wind stress and thus a poleward shift and/or strengthening in the regions of mixed-layer divergence and convergence. Observations of the upper 2000 m of the Southern Ocean have shown a broadscale warming and freshening (Karpechko, Maycock et al., 2018; Rintoul, 2018). The last Assessment reported a substantial role for ozone depletion, through its influence on surface wind stress, in recent trends of the Southern Ocean circulation during austral summer. The warming of the upper ocean at 30–60°S is, however, mainly driven by an increasing abundance of greenhouse gases, with ozone depletion playing a secondary role (Karpechko, Maycock et al., 2018).

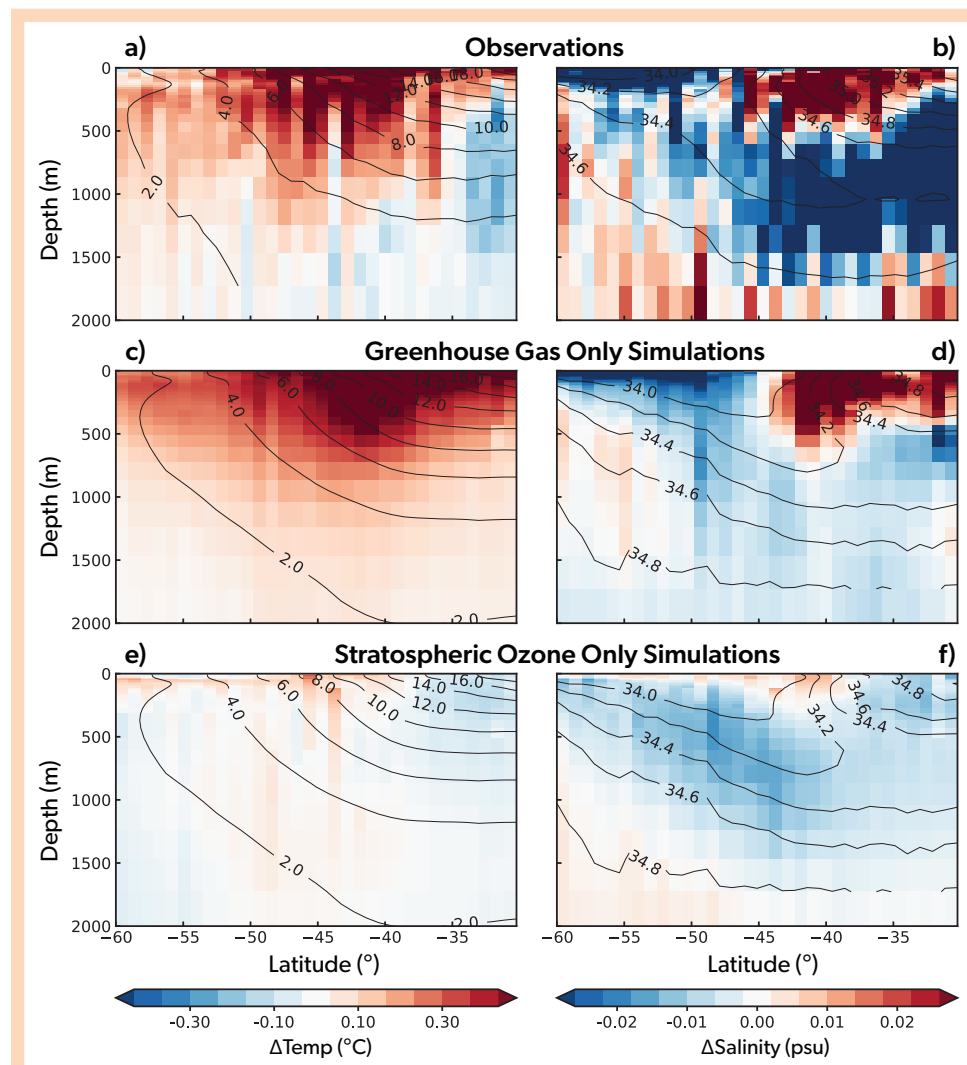


Figure 5-16. Observed and simulated changes in Southern Ocean temperature and salinity. Zonal mean (a, c, e) temperature, and (b, d, f) salinity, from (a, b) observations, (c, d) ensemble means of the CanESM2 greenhouse-gas-only simulations, and (e, f) stratospheric-ozone-only simulations. Anomalies represent the difference between the 2006–2015 mean and the mean over a 1950–1980 base period. Black contours show the climatological temperature and salinity. The CanESM2 fields (c, d, e, f) are subsampled to match observational coverage and scaled to best match the observations using scaling factors of (c) 0.70, (d) 0.74, (e) 1.77, and (f) 0.70. [Adapted from Swart et al., 2018.]

Recent studies continue to show long-term broadscale warming and freshening in the upper 2000 m of the Southern Ocean south of 35°S since the 1950s (Figure 5-16; Rintoul, 2018; Swart et al., 2018), since the 1980s (Bronse laer et al., 2020), and since the 1990s (Auger et al., 2021). Recent modeling evidence suggests that poleward-intensifying winds contribute to the broadscale warming and freshening (Bronse laer et al., 2020). A period of rapid warming in the upper 2000 m of the Southern Ocean was observed over the period 2003–2012, but the pace of warming has slowed down since, with decadal variations in warming rates related to variations in the SAM and the Interdecadal Pacific Oscillation (Wang et al., 2021). Despite the broadscale warming of the upper 2000 m of the ocean south of ~35°S, SSTs have cooled at higher latitudes (south of ~50°S) since the 1980s (Armour et al., 2016; Haumann et al., 2020) and the 1990s (Auger et al., 2021; see Figure 5-17a). The high-latitude surface cooling has been accompanied by a freshening and linked to increased sea ice (Morrow and Kestenare, 2017; Fan et al., 2014).

Since the last Assessment, further evidence suggests that increasing greenhouse gases are the primary driver of Southern Ocean subsurface warming and freshening (Figure 5-16; Swart et al., 2018; Hobbs et al., 2021), with stratospheric ozone depletion playing a secondary or lesser role in driving warming (Swart et al., 2018; Li et al., 2021; Liu et al., 2022). Physically, surface fluxes of heat and freshwater are found to be the primary driver of changes, with wind-driven changes in ocean transport playing a secondary role (Swart et al., 2018; Armour et al., 2016). The proportion of Southern Ocean changes that are attributed to stratospheric ozone depletion varies across modeling studies (Sigmond et al., 2011; Solomon et al., 2015; Swart et al., 2018; Hobbs et al., 2021; Li et al., 2021; Liu et al., 2022). While previous work found 30% of both temperature and salinity changes across the Southern Ocean to be due to increasing ODSs and the resulting ozone depletion (Solomon et al., 2015), an ozone contribution to salinity changes was not formally detected in recent studies (Swart et al., 2018; Hobbs et al., 2021). This is possibly because of the different study periods considered, because greenhouse gas and ozone fingerprints are similar for salinity and thus difficult to separate (Swart et al., 2018), because the salinity response to anthropogenic forcings across the Southern Ocean is model dependent (Hobbs et al., 2021), and/or because of different ozone forcing configurations across the studies. A recent modeling study separating the combined influences of stratospheric ozone depletion and increased tropospheric ozone from the influence of stratospheric ozone depletion only reports that both contribute to the interior Southern Ocean warming over the period 1955–2000, with increased tropospheric ozone making a larger contribution to the overall Southern Ocean heat content change (Liu et al., 2022). Based on the dominance of greenhouse gas forcing over the historical period (Solomon et al., 2015; Swart et al., 2018; Hobbs et al., 2021) and despite the projected mitigating effects of ozone recovery on wind-driven ocean changes (Sigmond et al., 2011; Wang et al., 2014; Ivanciu et al., 2022), it is expected that greenhouse gases will continue to dominate and the Southern Ocean will continue to warm and freshen over coming decades (Swart et al., 2018; Ivanciu et al., 2022).

In a variety of model simulations, the high-latitude Southern Ocean exhibits a two-timescale SST response to a hypothetical step change in the SAM such as occurs in abrupt ozone-hole experiments (when ozone is abruptly changed from pre-ozone

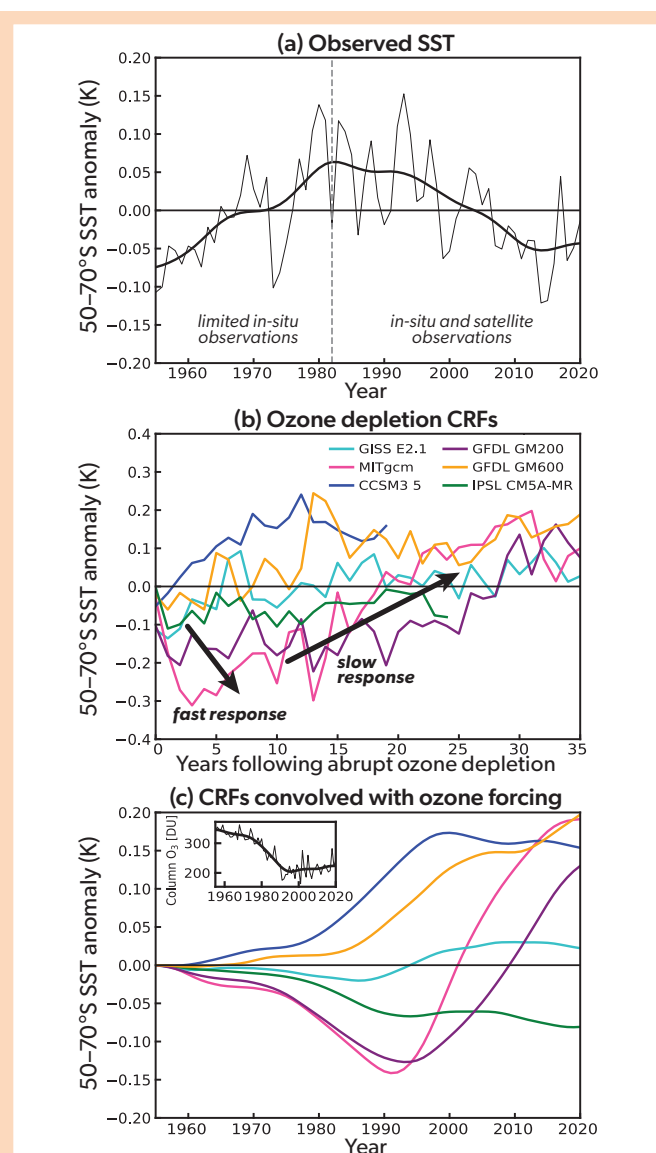


Figure 5-17. Observed and simulated evolution of high-latitude SST. (a) Observed 50–70°S average SST anomaly time series from the HadISST dataset. Anomalies are calculated relative to the 1955–2020 mean, and the bold line shows the 20-year running mean smoothed with a Hanning window. (b) Ensemble-mean time series of annual-mean SST anomaly averaged over 50–70°S from six different climate models simulating the climate response functions (CRFs) to abrupt ozone-hole conditions. The idealized ozone forcing reveals two timescales to the SST response—an initial cooling (the fast response) followed by an eventual warming (the slow response)—as indicated by large arrows; however, there is a large spread in responses across models. (c) Convolution of the anomalous SST response to abrupt ozone-hole conditions in (b) with time-evolving ozone forcing, as shown in the insert (October-mean 60–90°S column ozone from the WACCM chemistry-climate model). The convolved SST time series in (c) differ from the observed SST time series in (a), suggesting ozone depletion is unlikely to have been the primary driver of the observed high-latitude SST cooling since ~1980. [Adapted from Seviour et al., 2019.]

depletion levels to ozone-hole levels; **Figure 5-17b**; Ferreira et al., 2015; Seviour et al., 2019). The two-timescale SST response was described in detail in the last Assessment (Karpechko, Maycock et al., 2018). The fast SST response to strengthened and/or poleward-shifted westerly winds occurs over months to years and is characterized by increased northward Ekman transport, causing SST cooling (negative SST anomalies in **Figure 5-17b**); the slow response occurring over years to decades is characterized by upwelling of relatively warm water from below the mixed layer, causing an SST warming (positive SST anomalies in **Figure 5-17b**; Marshall et al., 2014). Despite additional abrupt ozone-hole simulations since the last Assessment, the timescale of transition from initial cooling to subsequent warming remains poorly constrained (Seviour et al., 2019), leading to continued uncertainty in the SST response to time-evolving ozone depletion (**Figure 5-17c**). Furthermore, since the last Assessment high-resolution modeling has found that mesoscale eddies oppose anomalous wind-driven upwelling, preventing long-term warming (Doddridge et al., 2019). Thus, the spread in model behavior in the fast and slow responses to the SAM are likely related to the parameterization and/or resolution of eddies in the different models (Seviour et al., 2019; Doddridge et al., 2019). Even when biases in model climatology are taken into account, the current model evidence for the expected SST response to observed ozone depletion (initial cooling followed by longer-term warming) suggests that ozone depletion is unlikely to have been the primary driver of the observed high-latitude surface cooling since the late 1970s (see **Figure 5-17a**; Seviour et al., 2019).

In summary, since the last Assessment, the Southern Ocean (35–60°S, 0–2000 m depth) overall has continued to warm and freshen (Rintoul, 2018; Swart et al., 2018). Two formal detection and attribution studies have identified increasing greenhouse gases as the primary driver of the Southern Ocean warming and freshening (Swart et al., 2018; Hobbs et al., 2021), with the role of ozone depletion in driving ocean warming identified as secondary (Swart et al., 2018). Further modeling evidence suggests that ozone depletion has not been the primary driver of the observed high-latitude surface cooling (Seviour et al., 2019). However, this conclusion is based on coarse-resolution models; high-resolution modeling suggests that mesoscale eddies could influence the long-term temperature response to wind changes (Doddridge et al., 2019). Overall, our confidence in the understanding and attribution of the observed high-latitude surface cooling is low. Simulations with eddy-resolving ocean models to examine the response of the Southern Ocean to increased westerly winds would be necessary to reduce this uncertainty in the response in high-latitude ocean circulation to ozone depletion.

5.3.3.2 Sea Ice Impacts

A number of studies summarized in previous Assessments have investigated the influence of the ozone hole on Antarctic sea ice trends. Over the satellite period, total Antarctic sea ice coverage has shown a modest increasing trend; however, this total increase masks both regional (Hobbs et al., 2015) and temporal (Meehl et al., 2016; Eayrs et al., 2021) variations, and lacks statistical significance (Gulev et al., 2021). The 2014 and 2018 Assessments reported that a variety of climate model simulations that isolated the impact of stratospheric ozone depletion from that of increasing greenhouse gases all simulated decreasing Antarctic sea ice in response to ozone depletion, in contrast to

the observed increasing trend in sea ice.

Since the last Assessment, there is further modeling evidence that ozone depletion has not driven the observed long-term changes in Antarctic sea ice. CMIP5 models capture the observed relationship between the SAM and sea ice extent during austral summer, but the SAM explains only 15% of interannual variability in sea ice extent during austral fall—and thus that SAM trends and ozone depletion are not the primary drivers of the observed sea ice increase over the satellite era (Polvani et al., 2021). In an assessment of the two-timescale response, Antarctic sea ice extent is shown to decline monotonically in response to abrupt ozone-hole conditions in five out of six models (Seviour et al., 2019), consistent with previous modeling studies (Holland et al., 2017), but contrasting with the weak observed sea ice changes (Handcock and Raphael, 2020).

Confidence in modeling studies involving Antarctic sea ice remains low because coupled models run under full historical forcings (CMIP5 and CMIP6) simulate a decline in Antarctic sea ice that contrasts with observed changes (as assessed in Eyring et al., 2021). Over the period 1979–2018, Antarctic sea ice area trends in CMIP6 models are marginally consistent with observed trends (Roach et al., 2020). Some recent modeling evidence suggests that internal variability alone could lead to a multi-decadal increase in Antarctic sea ice similar to observed trends (Zhang et al., 2019; Singh et al., 2019), but other lines of evidence suggest that internal variability cannot account for the modeled/observed discrepancy (Hobbs et al., 2015; Chemke and Polvani, 2020). Evidence suggests that the stronger-than-observed decline in Antarctic sea ice in coupled climate models is influenced by biased surface heat flux trends (Chemke and Polvani, 2020) and biased thermodynamics (Blanchard-Wrigglesworth et al., 2021). The Southern Ocean warm bias in CMIP models (Beadling et al., 2020) has been linked to a cloud-based shortwave radiation bias in CMIP5 models (Hyder et al., 2018). Overall, confidence in attributing changes in Antarctic sea ice is limited because of climate model deficiencies in capturing the observed Antarctic sea ice trends over the satellite era (Eyring et al., 2021).

A retreat of Antarctic sea ice unprecedented in the historical satellite record was observed during austral spring and early summer of 2016 and was discussed in the last Ozone Assessment. This sudden retreat of sea ice has been linked to changes in the SAM, which became strongly negative in November (Turner et al., 2017; Schlosser et al., 2018), with easterly wind anomalies contributing to the record low sea ice (Wang et al., 2019b; Eayrs et al., 2021). The near-record negative SAM during November has been linked to stratospheric polar vortex weakening and associated higher ozone (Wang et al., 2019b), tropical convective conditions (Meehl et al., 2019), and internal variability (Stuecker et al., 2017; Purich and England, 2019).

The last Assessment concluded that ozone-hole changes cannot explain recent trends in Antarctic sea ice, and new studies support this conclusion. As in the last Assessment, confidence in the role of the ozone hole on Antarctic sea ice trends remains low, because of the limited number of ozone-only simulations available for analysis and because the majority of climate models still do not reproduce observed Antarctic sea ice trends since 1979 due to Southern Ocean thermal and sea ice model biases. This lack of ability to simulate past sea ice trends inhibits the assessment of the role of future ozone recovery in future sea ice trends.

5.3.3.3 Ocean Carbon

The Southern Ocean accounts for about 40% of the global oceanic uptake of anthropogenic CO₂ (Khaliwala et al., 2009; Frölicher et al., 2015). As described in Section 5.3.3.1, the westerly winds over the Southern Ocean influence the meridional overturning circulation and thus the outgassing and uptake of carbon from and to the ocean. The westerly wind strengthening implied by a positive SAM trend enhances both the high-latitude upwelling, increasing outgassing, and the mid-latitude downwelling, increasing uptake (Le Quéré et al., 2007; Lovenduski et al., 2007). In the last Assessment, the availability of longer observational datasets and improved analysis techniques confirmed earlier studies showing a carbon sink slowdown between the 1980s and early 2000s (Le Quéré et al., 2007), and also revealed a reinvigoration of the carbon sink between 2002 and 2012 (Landschützer et al., 2015; Munro et al., 2015).

Since the last Assessment, further observation-based evidence suggests that the Southern Ocean carbon sink varies substantially on decadal timescales (Gruber et al., 2019; Keppler and Landschützer, 2019). A weakening of the carbon uptake during the 1990s, initially attributed to the ozone hole (Le Quéré et al., 2007; Forster, Thompson et al., 2011), has been linked to the positive SAM that enhanced the high-latitude upwelling of CO₂ during this period (DeVries et al., 2017; Gruber et al., 2019). After ~2000, the carbon uptake rebounded, increasing the global ocean carbon sink strength back to that expected based on atmospheric CO₂ levels (DeVries et al., 2017; Gruber et al., 2019). A subsequent weakening of the carbon sink since ~2011 has been observed (Gruber et al., 2019; Keppler and Landschützer, 2019).

In agreement with the last Assessment, there is little new evidence suggesting that long-term changes in ozone are affecting the Southern Ocean carbon sink. Evidence suggests that decadal atmospheric circulation changes impact the net strength of the Southern Ocean carbon sink. While the positive SAM during the 1990s has been linked with a short-term slowdown of the carbon sink (DeVries et al., 2017; Gruber et al., 2019), suggesting a possible ozone influence during this decade, evidence based on upscaled observations suggests that the total Southern Ocean carbon uptake south of 35°S over 1982–2016 has not been altered considerably by the positive SAM trend (Keppler and Landschützer, 2019). The observed decadal variations in the Southern Ocean carbon sink may be due to natural variability (Gruber et al., 2019).

5.3.3.4 Ice Sheet and Shelf Impacts

The influence of the ozone hole on Antarctic ice sheets and shelves has not been covered in detail in previous Assessments. Observational evidence suggests that the Antarctic ice sheet has only recently started responding to climate change (Noble et al., 2020). Antarctic surface mass balance shows no clear trends over the satellite era but exhibits large variability (Rignot et al., 2019), with extreme precipitation events making a large contribution to annual precipitation accumulation over the continent and determining the interannual variability (Turner et al., 2019). Trends in total mass balance since 1979 have been driven by ice discharge (Rignot et al., 2019), with recent observations over 2003–2019 showing the West Antarctic ice sheet losing mass while the East Antarctic ice sheet exhibits large variability (Smith et al., 2020). Overall, the Antarctic ice sheet lost mass between 1992 and 2017 (Gulev et al., 2021).

New evidence suggests that stratospheric ozone depletion could potentially have influenced the net balance of the Antarctic ice sheet, but this is highly uncertain. First, modeling evidence suggests that stratospheric ozone depletion and/or ODSs drove increased snow accumulation over Antarctica over the late 20th century, leading to an increase in the surface mass balance (Previdi and Polvani, 2017; Lenaerts et al., 2018; Chemke et al., 2020). However, observations show large variability and no clear trends in Antarctic surface mass balance (Rignot et al., 2019). Second, and conversely, various lines of evidence suggest that a positive SAM (i.e., a poleward shift of the mid-latitude westerlies) could be associated with increased transport of warm off-shelf waters onto the Antarctic shelf at certain locations (Spence et al., 2014; Jenkins et al., 2016), providing heat for basal melting and increasing ice sheet mass loss (Shepherd et al., 2004; The IMBIE Team, 2018). One study utilizing a regional ocean-ice model forced with anthropogenic forcings and tropical Pacific variability simulated on-shelf ocean warming and increased basal melt in the Amundsen Sea, likely due to the westerly wind trend over the shelf break (Naughten et al., 2022). However, there is a lack of evidence directly linking stratospheric ozone changes to ice shelf changes, and attributing ocean-mediated changes is highly challenging due to both observational and modeling limitations around the Antarctic margins. Our assessment concludes that there is much uncertainty over the influence of stratospheric ozone changes on ice sheets and shelves.

5.4 CLIMATE IMPACTS OF THE MONTREAL PROTOCOL

5.4.1 Realized Climate Impacts of the Montreal Protocol

The length of the observational time series over the period of relative stabilization of global ozone concentrations (see Chapter 3) allows, for the first time, an assessment of the realized impacts of the Montreal Protocol on climate based on observations and an attribution of these impacts to the Montreal Protocol using targeted model integrations. As discussed in Section 5.3.2.2, recent studies of spring and summertime SH circulation trends have detected a pause or change in sign of the trends between the late 20th century and the early 21st century (Banerjee et al., 2020; Zambri et al., 2021; Mindlin et al., 2021). Specifically, a pause in the summertime trends in SH tropospheric circulation, such as the SAM, zonal-mean zonal winds, jet position, and Hadley cell edge, have been detected in reanalyses for the 2000–2017 period (Figure 5-14; Banerjee et al., 2020). In the zonal-mean zonal wind, the pause is attributed to a “tug-of-war” between two climate forcings: a stabilization and recovery of Antarctic stratospheric ozone due to the Montreal Protocol and global warming due to greenhouse gases. This attribution is made by comparing reanalyses (Figure 5-18a–c) to model integrations where the ODS and stratospheric ozone signal is extracted in a multi-model ensemble of chemistry-climate models (Figure 5-18d–f) for two time periods, an ozone depletion period of 1980–2000 and an ozone recovery period of 2000–2017. The role of greenhouse gases is diagnosed using other single-forcing integrations (Figure 5-18g–i). A pause in the summer SAM index trend is also evident in the CMIP6 models for the historical time period, and the attribution of this pause to the reduction in ozone-depleting substances in recent decades is supported by

multiple linear regression models (Morgenstern, 2021; Mindlin et al., 2021). As highlighted in *Section 5.3.2.2* and in previous Assessments, the impact of ozone depletion on the summertime SAM and SH surface climate trends has been significant, and a pause in these trends may have implications for near- and long-term future SH climate change (Mindlin et al., 2021). The duration of the pause in the SH tropospheric circulation trends will depend on the tug-of-war described above, i.e., the pace and magnitude of future global warming (Barnes et al., 2014; Mindlin et al., 2021; Sections 4.3.3.1 and 4.5.1.6 in Lee et al., 2021) and the pace of ozone recovery, which has the potential to be delayed by unexpected CFC-11 emissions (Dhomse et al., 2019; Fleming et al., 2021), ODS emissions from natural sources (Fang et al., 2019), nitrous oxide emissions (Fang et al., 2019), and enhanced wild-fire smoke injection in a warming climate (Solomon et al., 2022; Bernath et al., 2022).

As noted in previous Assessments, “world-avoided” integrations have been used to evaluate the impact of the Montreal Protocol on climate. The world-avoided scenario is an idealized counterfactual scenario and typically assumes that uncontrolled ODSs would have increased at a rate of 3–3.5% per year in the absence of the Montreal Protocol based on expected growth in gross domestic product (GDP) and market analysis (e.g., Prather et al., 1996; Velders et al., 2007; Newman et al., 2009; Garcia et al., 2012). While ODS emissions were growing faster than this before the Montreal Protocol was signed (Table 2.5-1 in WMO, 1989), a sustained rate of emissions of ODSs of 3–3.5% per year should be viewed as only one of many possible world-avoided scenarios, which could also include scenarios with varying assumptions about future GDP growth. For the purposes of this Assessment, the world-avoided scenario allows for the examination of the sensitivity of climate to increasing ODS emissions and the accompanying ozone loss. Comparing world-avoided integrations to those including controls on ODS emissions, previous Assessments have reported that a steady increase in ODS emissions would have led to approximately double the amount of global warming by the end of the 21st century (Velders et al., 2007; Garcia et al., 2012). Here, world-avoided integrations are used to assess new evidence of the impact of the Montreal Protocol on present-day climate change.

The comparison of historical and RCP scenario integrations to world-avoided integrations provides an estimate of the impact of the Montreal Protocol on surface climate over the past several decades. Based on model simulations from three studies (Young et al., 2021; Goyal et al., 2019; Virgin and Smith, 2019), we assess that controls on ODS emissions under the Montreal Protocol have avoided at present-day (average over years 2015–2024) approximately 0.1–0.2°C global surface warming (with an ensemble weighted mean of 0.17°C ± 0.06°C²) and 0.2–0.6°C Arctic surface warming (ensemble weighted mean of 0.45°C ± 0.23°C). Using additional integrations with only world-avoided changes in stratospheric ozone included, the avoided warming is attributed primarily to the stabilization and slight decrease in ODS concentrations and is offset somewhat by cooling due to stratospheric ozone loss (Goyal et al., 2019; consistent with *Section 5.3.1.1* and **Box 5-3**).

In summary, our assessment is that the implementation of the

Montreal Protocol has had a significant effect on the climate over the past several decades in two notable ways: the stabilization of the Antarctic ozone hole has led to a pause in SH circulation trends, and the rapid decline in ODS emissions has mitigated GHG-driven global warming.

5.4.2 Future Climate Impacts of the Montreal Protocol

As in previous Assessments, world-avoided integrations are also used to quantify avoided future climate change. While there has been limited new literature on the topic since the previous Assessment, based on three new studies (Goyal et al., 2019; Virgin and Smith, 2019; Young et al., 2021) we assess that by the mid-21st century (average over years 2041–2060) the Montreal Protocol controls would result in the avoidance of approximately 0.5–1.0°C global surface warming (ensemble weighted mean of 0.79°C ± 0.24°C). The globally averaged RF from the years 2005–2065 is approximately double in world-avoided scenarios due to uncontrolled emissions of ODSs compared to the RCP4.5 scenario (Virgin and Smith, 2019). This work supports findings of previous studies that compared the world-avoided scenario to the A1B and B2 SRES scenarios (Velders et al., 2007) or the RCP4.5 scenario (Garcia et al., 2012). Avoided Arctic warming is primarily due to reductions in ODS emissions rather than the mitigation of stratospheric ozone loss (Goyal et al., 2019; see also *Section 5.3.1.2*); however, recent work suggests that the relationship between Arctic warming and polar cap-averaged radiative forcing in the world-avoided scenario appears to be complex due to the unique combination of high ODS concentrations and substantial stratospheric ozone loss (Virgin and Smith, 2019). Arctic polar cap-averaged positive radiative feedbacks (i.e., long-wave cloud feedbacks) and atmospheric heat flux convergence rather than polar cap-averaged radiative forcing alone play a key role in contributing to world-avoided Arctic warming (Virgin and Smith, 2019).

Recent work also confirms that in the absence of the Montreal Protocol, by the mid-21st century a warmer planet would have resulted in an enhanced hydrological cycle, with substantial increases in precipitation in the polar regions and a further decline in Arctic sea ice extent relative to the RCP8.5 scenario (Goyal et al., 2019; Wu et al., 2013).

As reported in Chapter 5 of the previous Assessment (Karpechko, Maycock et al., 2018), the phasedown of HFCs under the Kigali Amendment to the Montreal Protocol will also have an impact on global climate, as HFCs are potent GHGs. In *Chapter 2* of this Assessment, it is shown that this phasedown is already underway due to national and regional regulations, with HFC emissions over the 2017–2019 period being 20% lower than the WMO (2018) HFC baseline scenario (*Section 2.4.1*). Under the WMO (2018) baseline scenario, it was estimated that HFCs would contribute 0.3–0.5 K to global mean surface warming by 2100 (*Section 2.3.1* of Montzka, Velders et al. 2018). New estimates based on current policies project that HFCs would contribute 0.14–0.31 K by 2100, and with the additional provisions of the Kigali Amendment this is reduced to approximately 0.04 K (*Sections 2.4.2* and *2.4.3*; Velders et al., 2022). Independent modeling analysis confirms that HFCs have a significant climate

¹ The uncertainty bounds include uncertainty due to natural variability and model uncertainty, based on three independent model studies with 5, 3, and 1 ensemble member, respectively.

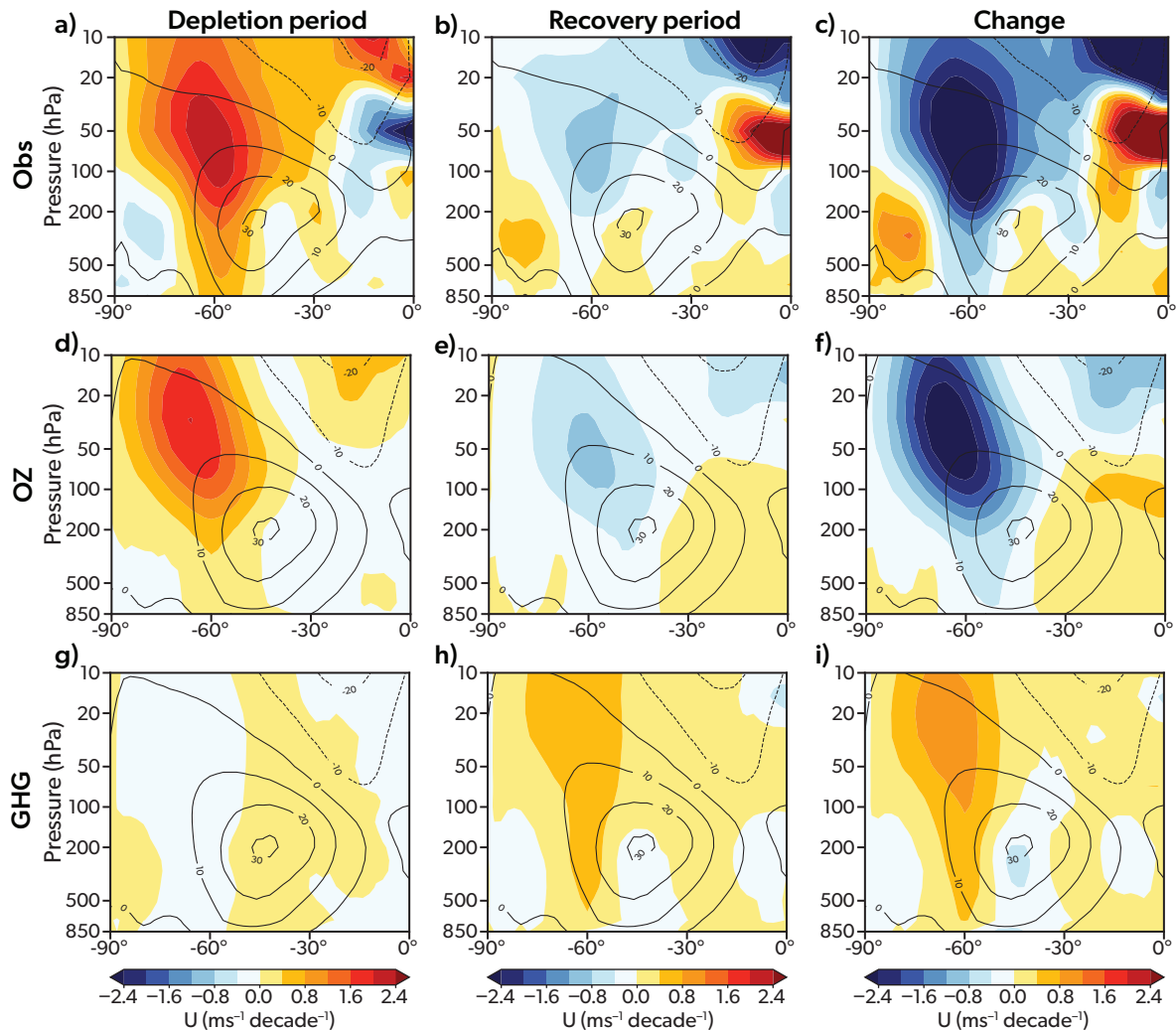


Figure 5-18. Observed and simulated Southern Hemisphere zonal average zonal wind trends. The top row shows an average of four reanalysis data products (ERA-Interim, JRA-55, MERRA2-ana, MERRA2-asm), and the middle and bottom rows show an ensemble mean of CCMVal-2 and CCM1 chemistry-climate model integrations. Latitude-altitude cross sections of zonal average zonal wind trends (color shading) for DJF are shown for the depletion period (*left column*), recovery period (*middle column*), and the difference between the two (*right column*). Fingerprints are shown for the simulations with single forcings by (d–f) ozone (OZ) and (g–i) GHGs. For illustrative purposes, the contours show the climatologies (in m s^{-1} ; for d–i, the climatologies are for the ALL-forcing integrations; for f and i, the climatology is over the entire change period). [Adapted from Banerjee et al., 2020.]

impact. Earth system model integrations following the RCP8.5 scenario with uncontrolled HFC emissions compared with a world-avoided scenario in which HFCs were not introduced indicate that HFC emissions contribute approximately 0.1 K to global warming from the 1970s to the 2050s (Goyal et al., 2019), in agreement with the previous Assessment. In addition, consistent with a previous analysis using a 2-D (latitude-pressure) interactive chemistry, radiation, and dynamics model (Hurwitz et al., 2015), a new 3-D chemistry-climate model study with prescribed SSTs shows that by the end of the century, uncontrolled HFC emissions following both the lower and upper limit of the previous scenarios of Velders et al. (2014) lead to warming of the tropical upper troposphere and lower stratosphere and a strengthening of the Brewer-Dobson circulation (BDC) but a weakening of the Hadley

cell relative to a zero HFC concentrations scenario (Dupuy et al., 2021).

Moving beyond the surface climate, a recent study found that the Montreal Protocol has significantly protected the terrestrial carbon sink by preventing a decrease in net primary production associated with UV damage of plants (Young et al., 2021). Using output from world-avoided simulations, it is estimated that atmospheric carbon dioxide concentrations may have been 18–37% higher by 2100 (Figure 5-19a) if controls on ODS emissions under the Montreal Protocol had not protected the terrestrial biosphere from UV damage, contributing to an additional 0.5–1.0 K to globally averaged surface warming by 2100 (Figure 5-19b). The large range of estimates reflects the uncertainty in the plant response to UV. Protection of the terrestrial carbon sink is a

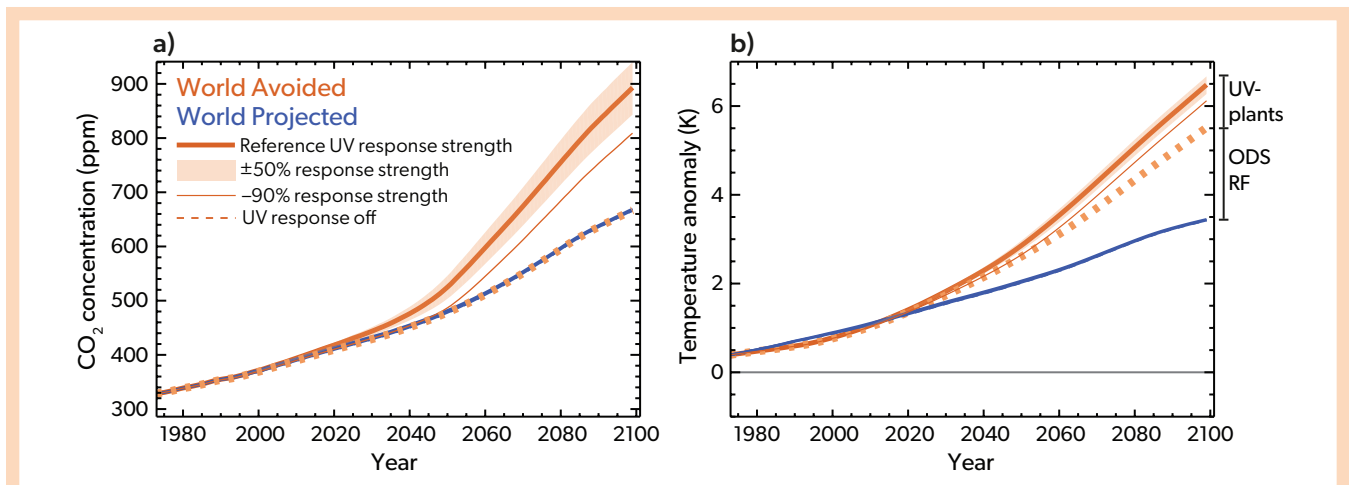


Figure 5-19. The effect of UV-driven changes in vegetation (UV-plants) on atmospheric CO₂ and surface temperature. (a) Time series of atmospheric CO₂ concentrations and (b) anomalies in global-mean surface air temperature for a regular future projection (World Projected, blue; approximately RCP6.0) and a World Avoided projection (World Avoided, orange), estimated using a carbon cycle model. The dashed orange lines are results from a World Avoided projection with the ‘UV response off’, the shading around the thick orange lines indicates the range of the responses from the simulations with 50% and 150% UV response strength (with respect to the reference UV case) and the thin orange lines show the effect of reducing the UV response strength to -90%. The labelled ranges in (b) indicate the World Avoided warming above the World Projected that results from direct radiative forcing of the additional CFCs and the additional CO₂ from the UV-driven damage to plants and their ability to act as a carbon store. [Adapted from Young et al., 2021.]

previously unexamined climate benefit of the Montreal Protocol.

With respect to projected ozone recovery and its impact on climate, earlier sections of this chapter have assessed recent literature, including *Section 5.2.4* on the BDC, *Section 5.2.6* on stratospheric winds, *Section 5.3.2.2* on SH tropospheric circulation and surface climate, and *Section 5.3.3* on the Southern Ocean and Antarctic sea ice.

Since the previous Assessment, a number of studies have examined the impact of the recent unexpected emissions of CFC-11 from 2012 to 2018 (*Section 1.2.1*) on ozone recovery, and these are assessed in *Section 3.4.4* (for global ozone) and *Section 4.5.3.2* (for polar ozone). With respect to the climate impacts of these emissions, simulations with a chemistry-climate model with prescribed sea surface temperatures show that continued CFC-11 emissions at a rate of 72.5 Gg year⁻¹ from 2017 to 2100 lead to a significant delay in global and Antarctic ozone recovery of 1 and

33 years, respectively, compared to the WMO (2018) baseline scenario (Fleming et al., 2021). In addition, a significant dynamical response in the SH stratosphere was identified, including a cooling of the polar lower stratosphere of 1.5 K and a corresponding acceleration of the polar vortex, with a delay in the vortex breakdown by four days and a decrease in the age of air by 0.1 year averaged over the 2080–2100 period (Fleming et al., 2021).

Overall, our assessment confirms that the Montreal Protocol has significantly contributed to the mitigation of anthropogenic global warming through the controls on ODS emissions. New evidence suggests an additional effect through the protection of the terrestrial carbon sink from harmful UV radiation. Potential future unexpected emissions of controlled ODSs and the associated ozone loss will have a small but significant impact on stratospheric temperature and circulation trends in the Southern Hemisphere.

REFERENCES

- Abalos, M., L. Polvani, N. Calvo, D.E. Kinnison, F. Ploeger, W.J. Randel, S. Solomon, New insights on the impact of ozone-depleting substances on the Brewer-Dobson circulation, *J. Geophys. Res. Atmos.*, **124**, 2435–2451, doi:10.1029/2018JD029301, 2019.
- Abalos, M., C. Orbe, D.E. Kinnison, D. Plummer, L.D. Oman, P. Jöckel., O. Morgenstern, R.R. Garcia, G. Zeng, K.A. Stone, and M. Dameris, Future trends in stratosphere-to-troposphere transport in CCM1 models, *Atmos. Chem. Phys.*, **20**, 6883–6901, doi:10.5194/acp-20-6883-2020, 2020.
- Abalos, M., N. Calvo, S. Benito-Barca, H. Garny, S.C. Hardiman, P. Lin, M.B. Andrews, N. Butchart, R.R. Garcia, C. Orbe, D. Saint-Martin, S. Watanabe, and K. Yoshida, The Brewer-Dobson circulation in CMIP6, *Atmos. Chem. Phys.*, **21** (17), 13,571–13,591, doi:10.5194/acp-21-13571-2021, 2021.
- Adcock, K.E., P.J. Fraser, B.D. Hall, R.L. Langenfelds, G. Lee, S.A. Montzka, D.E. Oram, T. Röckmann, F. Stroh, W.T. Sturges, B. Vogel, and J.C. Laube, Aircraft-based observations of ozone-depleting substances in the upper troposphere and lower stratosphere in and above the Asian summer monsoon, *J. Geophys. Res. Atmos.*, **126** (1), e2020JD033137, doi:10.1029/2020JD033137, 2021.
- Akritidis, D., A. Pozzer, and P. Zanis, On the impact of future climate change on tropopause folds and tropospheric ozone, *Atmos. Chem. Phys.*, **19**, 14,387–14,401, doi:10.5194/acp-19-14387-2019, 2019.
- Anstey, J.A., T.P. Banyard, N. Butchart, L. Coy, P.A. Newman, S. Osprey, and C. Wright, Prospect of increased disruption to the QBO in a changing climate, *Geophys. Res. Lett.*, **48** (15), e2021GL093058, doi:10.1029/2021GL093058, 2021.
- Anstey, J.A., S.M. Osprey, J. Alexander, M.P. Baldwin, N. Butchart, L. Gray, Y. Kawatani, P.A. Newman, and J.H. Richter, Impacts, processes and projections of the quasi-biennial oscillation. *Nat Rev Earth Environ* **3**, 588–603, doi.org/10.1038/s43017-022-00323-7, 2022.
- Aquila, V., W.H. Swartz, D.W. Waugh, P.R. Colarco, S. Pawson, L.M. Polvani, and R.S. Stolarski, Isolating the roles of different forcing agents in global stratospheric temperature changes using model integrations with incrementally added single forcings, *J. Geophys. Res. Atmos.*, **121**, 8067–8082, doi:10.1002/2015JD02384, 2016.
- Arlblaster, J.M., and G.A. Meehl, Contributions of external forcings to Southern Annular Mode trends, *J. Clim.*, **19** (12), 2896–2905, doi:10.1175/JCLI3774.1, 2006.
- Arlblaster, J.M., N.P. Gillett (Lead Authors), N. Calvo, P.M. Forster, L.M. Polvani, S.-W. Son, D.W. Waugh, and P.J. Young, Stratospheric ozone changes and climate, Chapter 4 in *Scientific Assessment of Ozone Depletion: 2014*, Global Ozone Research and Monitoring Project–Report No. 55, World Meteorological Organization, 416 pp., Geneva, Switzerland, 2014.
- Armour, K.C., J. Marshall, J.R. Scott, A. Donohoe, and E.R. Newsom, Southern Ocean warming delayed by circumpolar upwelling and equatorward transport, *Nat. Geosci.*, **9**, 549–554, doi:10.1038/ngeo2731, 2016.
- Auger, M., R. Morrow, E. Kestenare, J.B. Sallee, and R. Cowley, Southern Ocean in-situ temperature trends over 25 years emerge from interannual variability, *Nat. Commun.*, **12**, 514, doi:10.1038/s41467-020-20781-1, 2021.
- Ayarzagüena, B., L.M. Polvani, U. Langematz, H. Akiyoshi, S. Bekki, N. Butchart, M. Dameris, M. Deushi, S.C. Hardiman, P. Jöckel, A. Klekociuk, M. Marchand, M. Michou, O. Morgenstern, F.M. O'Connor, L.D. Oman, D. Plummer, L. Revell, E. Rozanov, D. Saint-Martin, J. Scinocca, A. Stenke, K. Stone, Y. Yamashita, K. Yoshida, and G. Zeng, No robust evidence of future changes in major stratospheric sudden warmings: a multi-model assessment from CCM1, *Atmos. Chem. Phys.*, **18**, 11,277–11,287, doi:10.5194/acp-18-11277-2018, 2018.
- Ayarzagüena, B., A.J. Charlton-Perez, A.H. Butler, P. Hitchcock, I. Simpson, L.M. Polvani, N. Butchart, E.P. Gerber, L. Gray, B. Hassler, P. Lin, F. Lott, E. Manzini, R. Mizuta, C. Orbe, S. Osprey, D. Saint-Martin, M. Sigmond, M. Taguchi, E.M. Volodin, and S. Watanabe, Uncertainty in the response of sudden stratospheric warmings and stratosphere-troposphere coupling to quadrupled CO₂ concentrations in CMIP6 models, *J. Geophys. Res. Atmos.*, **125** (6), e2019JD032345, doi:10.1029/2019JD032345, 2020.
- Baldwin, M.P., B. Ayarzagüena, T. Birner, N. Butchart, A.H. Butler, A.J. Charlton-Perez, D.I.V. Domeisen, C.I. Garfinkel, H. Garny, E.P. Gerber, M.I. Hegglin, U. Langematz, and N.M. Pedatella, Sudden stratospheric warmings, *Rev. Geophys.*, **59** (1), e2020RG000708, doi:10.1029/2020RG000708, 2021.
- Ball, W.T., J. Alsing, J. Staehelin, S.M. Davis, L. Froidevaux, and T. Peter, Stratospheric ozone trends for 1985–2018: sensitivity to recent large variability, *Atmos. Chem. Phys.*, **19** (19), 12,731–12,748, doi:10.5194/acp-19-12731-2019, 2019.
- Bandoro, J., S. Solomon, A. Donohoe, D.W.J. Thompson, and B.D. Santer, Influences of the Antarctic ozone hole on Southern Hemispheric summer climate change, *J. Clim.*, **27** (16), 6245–6264, doi:10.1175/JCLI-D-13-00698.1, 2014.
- Banerjee, A., A.C. Maycock, and J.A. Pyle, Chemical and climatic drivers of radiative forcing due to changes in stratospheric and tropospheric ozone over the 21st century, *Atmos. Chem. Phys.*, **18**, 2899–2911, doi:10.5194/acp-18-2899-2018, 2018.
- Banerjee, A., G. Chiodo, M. Previdi, M. Ponater, A.J. Conley, and L.M. Polvani, Stratospheric water vapor: An important climate feedback, *Clim. Dyn.*, **53**, 1697–1710, doi:10.1007/s00382-019-04721-4, 2019.
- Banerjee, A., J.C. Fyfe, L.M. Polvani, D. Waugh, and K.-L. Chang, A pause in Southern Hemisphere circulation trends due to the Montreal Protocol, *Nature*, **579**, 544–548, doi:10.1038/s41586-020-2120-4, 2020.
- Barnes, E. A. and Polvani, L. M.: Response of the Midlatitude Jets, and of Their Variability, to Increased GreenhouseGases in the CMIP5 Models. *J. Clim.*, **26**, 7117–7135. <https://doi.org/10.1175/JCLI-D-12-00536.1>, 2013.
- Barnes, E.A., N.W. Barnes, and L.M. Polvani, Delayed Southern Hemisphere climate change induced by stratospheric ozone recovery, as projected by the CMIP5 models, *J. Clim.*, **27**, 852–867, doi:10.1175/JCLI-D-13-00246.1, 2014.
- Barnett, J.J., J.T. Houghton and J.A. Pyle, The temperature dependence of the ozone concentration near the tropopause, *Q. J. Roy. Meteorol. Soc.*, **101**, 245–257, doi:10.1002/qj.49710142808, 1975.
- Beadling, R.L., J.L. Russell, R.J. Stouffer, M. Mazloff, L.D. Talley, P.J. Goodman, J.B. Sallée, H.T. Hewitt, P. Hyder and A. Pandde, Representation of Southern Ocean properties across coupled model intercomparison project generations: CMIP3 to CMIP6, *J. Clim.*, **33**, 6555–6581, doi:10.1175/JCLI-D-19-0970.1, 2020.
- Bellouin, N., W. Davies, K.P. Shine, J. Quaas, J. Mülmenstädt, P.M. Forster, C. Smith, L. Lee, L. Regayre, G. Brasseur, N. Sudarchikova, I. Bouarar, O. Boucher, and G. Myhre, Radiative forcing of climate change from the Copernicus reanalysis of atmospheric composition, *Earth Syst. Sci. Data*, **12** (3), 1649–1677, doi:10.5194/essd-12-1649-2020, 2020.
- Bernath, P., C. Boone, and J. Crouse, Wildfire smoke destroys stratospheric ozone, *Science*, **375** (6586), 1292–1295, doi:10.1126/science.abm5611, 2022.
- Blanchard-Wrigglesworth, E., L.A. Roach, A. Donohoe, and Q. Ding, Impact of winds and Southern Ocean SSTs on Antarctic sea ice trends and variability, *J. Clim.*, **34**, 949–965, doi:10.1175/jcli-d-20-0386.1, 2021.
- Breeden, M. L., Butler, A. H., Albers, J. R., Sprenger, M., and Langford, A. O., The spring transition of the North Pacific jet and its relation to deep stratosphere-to-troposphere mass transport over western North America, *Atmos. Chem. Phys.*, **21**, 2781–2794, <https://doi.org/10.5194/acp-21-2781-2021>, 2021.
- Bronseleer, B., J.L. Russell, M. Winton, N.L. Williams, R.M. Key, J.P. Dunne, R.A. Feely, K.S. Johnson, and J.L. Sarmiento, Importance of wind and meltwater for observed chemical and physical changes in the Southern Ocean, *Nat. Geosci.*, **13**, 35–42, doi:10.1038/s41561-019-0502-8, 2020.
- Bushell, A.C., D.R. Jackson, N. Butchart, S.C. Hardiman, T.J. Hinton, S.M. Osprey, and L.J. Gray, Sensitivity of GCM tropical middle atmosphere variability and climate to ozone and parameterized gravity wave changes, *J. Geophys. Res. Atmos.*, **115** (D15), doi:10.1029/2009JD013340, 2010.
- Bushell, A.C., J.A. Anstey, N. Butchart, Y. Kawatani, S.M. Osprey, J.H. Richter, F. Serva, P. Braesicke, C. Cagnazzo, C.-C. Chen, H.-Y. Chun, R.R. Garcia, L.J. Gray, K.

- Hamilton, T. Kerzenmacher, Y.-H. Kim, F. Lott, C. McLandress, H. Naoe, J. Scinocca, A.K. Smith, T.N. Stockdale, S. Versick, S. Watanabe, K. Yoshida, and S. Yukimoto, Evaluation of the Quasi-Biennial Oscillation in global climate models for the SPARC QBO-initiative, *Q. J. R. Meteorol. Soc.*, **148** (744), 1459–1489, doi:10.1002/qj.3765, 2020.
- Butchart, N., J.A. Anstey, K. Hamilton, S. Osprey, C. McLandress, A.C. Bushell, Y. Kawatani, Y.-H. Kim, F. Lott, J. Scinocca, T.N. Stockdale, M. Andrews, O. Bellprat, P. Braesicke, C. Cagnazzo, C.-C. Chen, H.-Y. Chun, M. Dobrynin, R.R. Garcia, J. Garcia-Serrano, L.J. Gray, L. Holt, T. Kerzenmacher, H. Naoe, H. Pohlmann, J.H. Richter, A.A. Scaife, V. Schenzinger, F. Serva, S. Versick, S. Watanabe, K. Yoshida, and S. Yukimoto, Overview of experiment design and comparison of models participating in phase 1 of the SPARC Quasi-Biennial Oscillation initiative (QBOi), *Geosci. Model Dev.*, **11**, 1009–1032, doi:10.5194/gmd-11-1009-2018, 2018.
- Butler, A.H., D.J. Seidel, S.C. Hardiman, N. Butchart, T. Birner, and A. Match, Defining sudden stratospheric warmings, *Bull. Amer. Meteor. Soc.*, **96** (11), 1913–1928, doi:10.1175/BAMS-D-13-00173.1, 2015.
- Butler, A.H., and D.I.V. Domeisen, The wave geometry of final stratospheric warming events, *Weather Clim. Dynam.*, **2** (2), 453–474, doi: 10.5194/wcd-2-453-2021, 2021.
- Byrne, N.J., and T.G. Shepherd, Seasonal persistence of circulation anomalies in the Southern Hemisphere stratosphere and its implications for the troposphere, *J. Clim.*, **31** (9), 3467–3483, doi:10.1175/JCLI-D-17-0557.1, 2018.
- Calvo, N., L.M. Polvani, and S. Solomon, On the surface impact of Arctic stratospheric ozone extremes, *Environ. Res. Lett.*, **10** (9), 094003, doi:10.1088/1748-9326/10/9/094003, 2015.
- Cane, M.A., A.C. Clement, A. Kaplan, Y. Kushnir, D. Pozdnyakov, R. Seager, S.E. Zebiak, and R. Murtugudde, Twentieth-century sea surface temperature trends, *Science*, **275** (5302), 957–960, doi:10.1126/science.275.5302.957, 1997.
- Carr, J. L., Á. Horváth, D.L. Wu, and M.D. Friberg, Stereo plume height and motion retrievals for the record-setting Hunga Tonga-Hunga Ha’apai eruption of 15 January 2022, *Geophys. Res. Lett.*, **49**, e2022GL098131. <https://doi.org/10.1029/2022GL098131>, 2022.
- Ceppi, P., and T.G. Shepherd, The role of the stratospheric polar vortex for the austral jet response to greenhouse gas forcing, *Geophys. Res. Lett.*, **46**, 6972–6979, doi:10.1029/2019GL082883, 2019.
- Chabrilat, S., C. Vigouroux, Y. Christophe, A. Engel, Q. Errera, D. Minganti, B. Monge-Sanz, A. Segers, and E. Mahieu, Comparison of mean age of air in five reanalyses using the BASCOE transport model, *Atmos. Chem. Phys.*, **18**, 14,715–14,735, doi:10.5194/acp-18-14715-2018, 2018.
- Charlton, A.J., and L.M. Polvani, A new look at stratospheric sudden warmings. Part I: Climatology and modeling benchmarks, *J. Clim.*, **20** (3), 449–469, doi:10.1175/JCLI3996.1, 2007.
- Checa-Garcia, R., M.I. Hegglin, D. Kinnison, D.A. Plummer, and K.P. Shine, Historical tropospheric and stratospheric ozone radiative forcing using the CMIP6 database, *Geophys. Res. Lett.*, **45** (7), 3264–3273, doi:10.1002/2017GL076770, 2018.
- Chemke, R., and L.M. Polvani, Using multiple large ensembles to elucidate the discrepancy between the 1979–2019 modeled and observed Antarctic sea ice trends, *Geophys. Res. Lett.*, **47** (15), doi:10.1029/2020gl088339, 2020.
- Chemke, R., M. Previdi, M.R. England, and L.M. Polvani, Distinguishing the impacts of ozone and ozone-depleting substances on the recent increase in Antarctic surface mass balance, *Cryosphere*, **14**, 4135–4144, doi:10.5194/tc-14-4135-2020, 2020.
- Cheung, J.C.H., J.D. Haigh, and D.R. Jackson, Impact of EOS MLS ozone data on medium-extended range ensemble weather forecasts, *J. Geophys. Res. Atmos.*, **119**, 9253–9266, doi:10.1002/2014JD021823, 2014.
- Chiodo, G., and L.M. Polvani, Reduced Southern Hemispheric circulation response to quadrupled CO₂ due to stratospheric ozone feedback, *Geophys. Res. Lett.*, **44**, 465–474, doi:10.1002/2016GL071011, 2017.
- Chiodo, G., L.M. Polvani, D.R. Marsh, A. Stenke, W. Ball, E. Rozanov, S. Muthers, and K. Tsigaridis, The response of the ozone layer to quadrupled CO₂ concentrations, *J. Clim.*, **31**, 3893–3907, doi:10.1175/JCLI-D-17-0492.1, 2018.
- Chiodo, G., and L.M. Polvani, The response of the ozone layer to quadrupled CO₂ concentrations: Implications for climate, *J. Clim.*, **32**, 7629–7642, doi:10.1175/JCLI-D-19-0086.1, 2019.
- Chiodo, G., and L.M. Polvani, New insights on the radiative impacts of ozone depleting substances, *Geophys. Res. Lett.*, **49** (10), doi:10.1029/2021GL096783, 2022.
- Chrysanthou, A., A.C. Maycock, M.P. Chipperfield, S. Dhomse, H. Garny, D.E. Kinnison, H. Akiyoshi, M. Deushi, R.R. Garcia, P. Jöckel, O. Kirner, G. Pitari, D.A. Plummer, L. Revell, E. Rozanov, A. Stenke, R.Y. Tanaka, D. Visioni, and Y. Yamashita, The effect of atmospheric nudging on the stratospheric residual circulation in chemistry–climate models, *Atmos. Chem. Phys.*, **19**, 11,559–11,586, doi:10.5194/acp-19-11559-2019, 2019.
- Cionni, I., V. Eyring, J.F. Lamarque, W.J. Randel, D.S. Stevenson, F. Wu, G.E. Bodeker, T.G. Shepherd, D.T. Shindell, and D.W. Waugh, Ozone database in support of CMIP5 simulations: results and corresponding radiative forcing, *Atmos. Chem. Phys.*, **11**, 11,267–11,292, doi:10.5194/acp-11-11267-2011, 2011.
- Clement, A.C., R. Seager, M.A. Cane, and S.E. Zebiak, An ocean dynamical thermostat, *J. Clim.*, **9** (9) 2190–2196, doi:10.1175/1520-0442(1996)009<2190:A-ODT>2.0.CO;2, 1996.
- Cohen, J., L. Agel, M. Barlow, C. I. Garfinkel, and I. White, Linking Arctic variability and change with extreme winter weather in the United States, *Science*, **373**, no. 6559, Art. no. 6559, doi: 10.1126/science.abi9167, 2021.
- Conley, A.J., J.-F. Lamarque, F. Vitt, W.D. Collins, and J. Kiehl, PORT, a CESM tool for the diagnosis of radiative forcing, *Geosci. Model Dev.*, **6**, 469–476, doi:10.5194/gmd-6-469-2013, 2013.
- Crook, J.A., N.P. Gillett, and S.P. Keeley, Sensitivity of Southern Hemisphere climate to zonal asymmetry in ozone, *Geophys. Res. Lett.*, **35** (7), doi:10.1029/2007GL032698, 2008.
- Dacie, S., L. Kluft, H. Schmidt, B. Stevens, S.A. Buehler, P.J. Nowack, S. Dietmüller, N.L. Abraham, and T. Birner, A 1D RCE study of factors affecting the tropical tropopause layer and surface climate, *J. Clim.*, **32**, 6769–6782, doi:10.1175/JCLI-D-18-0778.1, 2019.
- DallaSanta, K., C. Orbe, D. Rind, D.L. Nazarenko, and J. Jonas, Dynamical and trace gas responses of the quasi-biennial oscillation to increased CO₂, *J. Geophys. Res. Atmos.*, **126** (6), e2020JD034151, doi:10.1029/2020JD034151, 2021.
- Damiani, A., R.R. Cordero, P.J. Llanillo, S. Feron, J.P. Boisier, R. Garreaud, R. Rondanelli, H. Irie, and S. Watanabe, Connection between Antarctic ozone and climate: Interannual precipitation changes in the Southern Hemisphere, *Atmosphere*, **11** (6), 579, doi:10.3390/atmos11060579, 2020.
- Davis, N.A., S.M. Davis, R.W. Portmann, E. Ray, K.H. Rosenlof, and P. Yu, A comprehensive assessment of tropical stratospheric upwelling in the specified dynamics Community Earth System Model 1.2. 2–Whole Atmosphere Community Climate Model (CESM (WACCM)), *Geosci. Model Dev.*, **13**, 717–734, doi:10.5194/gmd-13-717-2020, 2020.
- Davis, N.A., P. Callaghan, I.R. Simpson, and S. Tilmes, Specified dynamics scheme impacts on wave-mean flow dynamics, convection, and tracer transport in CESM2 (WACCM6), *Atmos. Chem. Phys.*, **22**, 197–214, doi:10.5194/acp-22-197-2022, 2022.
- de la Cámara, A., M. Abalos, P. Hitchcock, N. Calvo, and R.R. Garcia, Response of Arctic ozone to sudden stratospheric warmings, *Atmos. Chem. Phys.*, **18**, 16,499–16,513, doi:10.5194/acp-18-16499-2018, 2018.
- DeVries, T., M. Holzer, and F. Primeau, Recent increase in oceanic carbon uptake driven by weaker upper-ocean overturning, *Nature*, **542**, 215–218, doi:10.1038/nature21068, 2017.
- Dhomse, S.S., D. Kinnison, M.P. Chipperfield, R.J. Salawitch, I. Cionni, M.I. Hegglin, N.L. Abraham, H. Akiyoshi, A.T. Archibald, E.M. Bednarz, S. Bekki, P. Braesicke, N. Butchart, M. Dameris, M. Deushi, S. Frith, S.C. Hardiman, B. Hassler, L.W. Horowitz, R.-M. Hu, P. Jöckel, B. Josse, O. Kirner, S. Kremser, U. Langematz, J. Lewis, M. Marchand, M. Lin, E. Mancini, V. Maréchal, M. Michou, O. Morgenstern, F.M. O’Connor, L. Oman, G. Pitari, D.A. Plummer, J.A. Pyle, L.E. Revell, E. Rozanov, R. Schofield, A. Stenke, K. Stone, K. Sudo, S. Tilmes, D. Visioni, Y. Yamashita, and G. Zeng, Estimates of ozone return dates from Chemistry–Climate Model Initiative simulations, *Atmos. Chem. Phys.*, **18**, 8409–8438, doi:10.5194/acp-18-8409-2018, 2018.
- Dhomse, S.S., W. Feng, S.A. Montzka, R. Hossaini, J. Keeble, J.A. Pyle, J. Daniel, and M.P. Chipperfield, Delay in recovery of the Antarctic ozone hole from unexpected CFC-11 emissions, *Nat. Commun.*, **10** (1), 5781, doi:10.1038/s41467-019-13717-x, 2019.
- Diallo, M., M. Riese, T. Birner, P. Konopka, R. Müller, M.I. Hegglin, M.L. Santee, M. Baldwin, B. Legras, and F. Ploeger, Response of stratospheric water vapor and ozone to the unusual timing of El Niño and the QBO disruption in 2015–2016, *Atmos. Chem. Phys.*, **18**, 13,055–13,073, doi:10.5194/acp-18-13055-2018, 2018.
- Diallo, M., M. Ern, and F. Ploeger, The advective Brewer–Dobson circulation in the

- ERA5 reanalysis: climatology, variability, and trends, *Atmos. Chem. Phys.*, **21**, 7515–7544, doi:10.5194/acp-21-7515-2021, 2021.
- Dietmüller, S., M. Ponater, and R. Sausen, Interactive ozone induces a negative feedback in CO₂-driven climate change simulations, *J. Geophys. Res. Atmos.*, **119**, 1796–1805, doi:10.1002/2013JD020575, 2014.
- Dietmüller, S., R. Eichinger, H. Garny, T. Birner, H. Boenisch, G. Pitari, E. Mancini, D. Visioni, A. Stenke, L. Revell, E. Rozanov, D.A. Plummer, J. Scinocca, P. Jöckel, L. Oman, M. Deushi, S. Kiyotaka, D.E. Kinnison, R. Garcia, O. Morgenstern, G. Zeng, K.A. Stone, and R. Schofield, Quantifying the effect of mixing on the mean age of air in CCMVal-2 and CCMI-1 models, *Atmos. Chem. Phys.*, **18**, 6699–6720, doi:10.5194/acp-18-6699-2018, 2018.
- Dimdore-Miles, O., L. Gray, and S. Osprey, Origins of multi-decadal variability in sudden stratospheric warmings, *Weather Clim. Dynam.*, **2** (1), 205–231, doi:10.5194/wcd-2-205-2021, 2021.
- Doblas-Reyes, F.J., A.A. Sörensson, M. Almazroui, A. Dosio, W.J. Gutowski, R. Haarsma, R. Hamdi, B. Hewitson, W.-T. Kwon, B.L. Lamptey, D. Maraun, T.S. Stephenson, I. Takayabu, L. Terray, A. Turner, and Z. Zuo, Linking Global to Regional Climate Change, Chapter 10 in *Climate Change 2021: The Physical Science Basis. Contribution of Working Group I to the Sixth Assessment Report of the Intergovernmental Panel on Climate Change*, edited by V. Masson-Delmotte, P. Zhai, A. Pirani, S.L. Connors, C. Péan, S. Berger, N. Caud, Y. Chen, L. Goldfarb, M.I. Gomis, M. Huang, K. Leitzell, E. Lonnoy, J.B.R. Matthews, T.K. Maycock, T. Waterfield, O. Yelekçi, R. Yu, and B. Zhou, Cambridge University Press, Cambridge, United Kingdom and New York, NY, USA, 149 pp., doi:10.1017/9781009157896.012, 2021.
- Doddridge, E.W., J. Marshall, H. Song, J.-M. Campin, M. Kelley, and L. Nazarenko, Eddy compensation dampens Southern Ocean sea surface temperature response to westerly wind trends, *Geophys. Res. Lett.*, **46**, 4365–4377, doi:10.1029/2019gl082758, 2019.
- Dupuy, E., H. Akiyoshi, and Y. Yamashita, Impact of unmitigated HFC emissions on stratospheric ozone at the end of the 21st century as simulated by chemistry-climate models, *J. Geophys. Res. Atmos.*, **126** (21), e2021JD035307, doi:10.1029/2021JD035307, 2021.
- Eayrs, C., X. Li, M.N. Raphael, and D.M. Holland, Rapid decline in Antarctic sea ice in recent years hints at future change, *Nat. Geosci.*, **14**, 460–464, doi:10.1038/s41561-021-00768-3, 2021.
- Eichinger, R., S. Dietmüller, H. Garny, P. Šacha, T. Birner, H. Bönisch, G. Pitari, D. Visioni, A. Stenke, E. Rozanov, L. Revell, D.A. Plummer, P. Jöckel, L. Oman, M. Deushi, D.E. Kinnison, R.R. Garcia, O. Morgenstern, G. Zeng, K.A. Stone, and R. Schofield, The influence of mixing on the stratospheric age of air changes in the 21st century, *Atmos. Chem. Phys.*, **19**, 921–940, doi:10.5194/acp-19-921-2019, 2019.
- Engel, A., T. Möbius, H. Bönisch, U. Schmidt, R. Heinz, I. Levin, E. Atlas, S. Aoki, T. Nakazawa, S. Sugawara, F. Moore, D. Hurst, J. Elkins, S. Schauffner, A. Andrews, and K. Berine, Age of stratospheric air unchanged within uncertainties over the past 30 years, *Nat. Geosci.*, **2**, 28–31, doi:10.1038/GEO388, 2009.
- Eyring, V., J.M. Arblaster, I. Cionni, J. Sedlacek, J. Perlwitz, P.J. Young, S. Bekki, D. Bergmann, P. Cameron-Smith, W. Collins, G. Faluvegi, K.-D. Gottschaldt, L. Horowitz, D. Kinnison, J.-F. Lamarque, D.R. Marsh, D. Saint-Martin, D. Shindell, K. Sudo, S. Szopa, and S. Watanabe, Long-term ozone changes and associated climate impacts in CMIP5 simulations, *J. Geophys. Res. Atmos.*, **118** (10), 5029–5060, doi:10.1002/jgrd.50316, 2013.
- Eyring, V., N.P. Gillett, K.M. Achuta Rao, R. Barimalala, M. Barreiro Parrillo, N. Bellouin, C. Cassou, P.J. Durack, Y. Kosaka, S. McGregor, S. Min, O. Morgenstern, and Y. Sun, Human Influence on the Climate System, Chapter 3 in *Climate Change 2021: The Physical Science Basis. Contribution of Working Group I to the Sixth Assessment Report of the Intergovernmental Panel on Climate Change*, edited by V. Masson-Delmotte, P. Zhai, A. Pirani, S. L. Connors, C. Péan, S. Berger, N. Caud, Y. Chen, L. Goldfarb, M. I. Gomis, M. Huang, K. Leitzell, E. Lonnoy, J. B. R. Matthews, T. K. Maycock, T. Waterfield, O. Yelekçi, R. Yu, and B. Zhou, Cambridge University Press, Cambridge, United Kingdom and New York, NY, USA, 129 pp., doi:10.1017/9781009157896.005, 2021.
- Fan, T., C. Deser, and D.P. Schneider, Recent Antarctic sea ice trends in the context of Southern Ocean surface climate variations since 1950, *Geophys. Res. Lett.*, **41**, 2419–2426, doi:10.1002/2014gl059239, 2014.
- Fang, X., J.A. Pyle, M.P. Chipperfield, J.S. Daniel, S. Park, and R.G. Prinn, Challenges for the recovery of the ozone layer, *Nat. Geosci.*, **12**, 592–596, doi:10.1038/s41561-019-0422-7, 2019.
- Feng, J., and Y. Huang, Impacts of tropical cyclones on the thermodynamic conditions in the tropical tropopause layer observed by A-Train satellites, *Atmos. Chem. Phys.*, **21**, 15,493–15,518, doi:10.5194/acp-21-15493-2021, 2021.
- Ferreira, D., J. Marshall, C.M. Bitz, S. Solomon, and A. Plumb, Antarctic Ocean and sea ice response to ozone depletion: A two-time-scale problem, *J. Clim.*, **28**, 1206–1226, doi:10.1175/jcli-d-14-00313.1, 2015.
- Fleming, E.L., Q. Liang, L.D. Oman, P.A. Newman, F. Li, and M.M. Hurwitz, Stratospheric impacts of continuing CFC-11 emissions simulated in a chemistry-climate model, *J. Geophys. Res. Atmos.*, **126** (9), doi:10.1029/2020JD033656, 2021.
- Fogt, R.L., and G.J. Marshall, The Southern Annular Mode: Variability, trends, and climate impacts across the Southern Hemisphere, *WIREs Clim. Change*, **11** (4), doi:10.1002/wcc.652, 2020.
- Forster, P., T. Storelvmo, K. Armour, W. Collins, J.-L. Dufresne, D. Frame, D.J. Lunt, T. Mauritsen, M.D. Palmer, M. Watanabe, M. Wild, and H. Zhang, The Earth's Energy Budget, Climate Feedbacks, and Climate Sensitivity, Chapter 7 in *Climate Change 2021: The Physical Science Basis. Contribution of Working Group I to the Sixth Assessment Report of the Intergovernmental Panel on Climate Change*, edited by V. Masson-Delmotte, P. Zhai, A. Pirani, S.L. Connors, C. Péan, S. Berger, N. Caud, Y. Chen, L. Goldfarb, M.I. Gomis, M. Huang, K. Leitzell, E. Lonnoy, J.B.R. Matthews, T.K. Maycock, T. Waterfield, O. Yelekçi, R. Yu, and B. Zhou, Cambridge University Press, Cambridge, United Kingdom and New York, NY, USA, 131 pp., doi:10.1017/9781009157896.009, 2021.
- Forster, P.M., and D.W.J. Thompson (Coordinating Lead Authors), M.P. Baldwin, M.P. Chipperfield, M. Dameris, J.D. Haigh, D.J. Karoly, P.J. Kushner, W.J. Randel, K.H. Rosenlof, D.J. Seidel, S. Solomon, G. Beig, P. Braesicke, N. Butchart, N.P. Gillett, K.M. Grise, D.R. Marsh, C. McLandress, T.N. Rao, S.-W. Son, G.L. Stenchikov, and S. Yoden, Stratospheric Changes and Climate, Chapter 4 in *Scientific Assessment of Ozone Depletion: 2010*, Global Ozone Research and Monitoring Project–Report No. 52, World Meteorological Organization, Geneva, Switzerland, 2011.
- Forster, P.M., T. Richardson, A.C. Maycock, C.J. Smith, B.H. Samset, G. Myhre, T. Andrews, R. Pincus, and M. Schulz, Recommendations for diagnosing effective radiative forcing from climate models for CMIP6, *J. Geophys. Res. Atmos.*, **121**, 12,460–12,475, doi:10.1002/2016JD025320, 2016.
- Forster, P.M.D.F., and K.P. Shine, Radiative forcing and temperature trends from stratospheric ozone changes, *J. Geophys. Res. Atmos.*, **102**, 10,841–10,855, doi:10.1029/96JD03510, 1997.
- Forster, P.M.D.F., and K.P. Shine, Stratospheric water vapor changes as a possible contributor to observed stratospheric cooling, *Geophys. Res. Lett.*, **26**, 3309–3312, doi:10.1029/1999GL010487, 1999.
- Forster, P.M.D.F., and M. Joshi, The role of halocarbons in the climate change of the troposphere and stratosphere, *Clim. Change*, **71**, 249–266, doi:10.1007/s10584-005-5955-7, 2005.
- Friedel, M., G. Chiodo, A. Stenke, D. Domeisen, S. Fueglistaler, J. Anet, and T. Peter, Springtime arctic ozone depletion forces northern hemisphere climate anomalies, *Nat. Geosci.*, **15**, 541–547, doi:10.1038/s41561-022-00974-7, 2022.
- Fritsch, F., H. Garny, A. Engel, H. Bönisch, and R. Eichinger, Sensitivity of age of air trends to the derivation method for non-linear increasing inert SF₆, *Atmos. Chem. Phys.*, **20**, 8709–8725, doi:10.5194/acp-20-8709-2020, 2020.
- Frölicher, T.L., J.L. Sarmiento, D.J. Paynter, J.P. Dunne, J.P. Krasting, and M. Winton, Dominance of the Southern Ocean in anthropogenic carbon and heat uptake in CMIP5 models, *J. Clim.*, **28** (2), 862–886, doi:10.1175/jcli-d-14-00117.1, 2015.
- Fu, Q., S. Solomon, H.A. Pahlavan, and P. Lin, Observed changes in Brewer–Dobson circulation for 1980–2018, *Environ. Res. Lett.*, **14** (11), 114026, doi:10.1088/1748-9326/ab44de7, 2019.
- Fusco, A.C., and M.L. Salby, Interannual variations of total ozone and their relationship to variations of planetary wave activity, *J. Clim.*, **12** (6), 1619–1629, doi:10.1175/1520-0442(1999)012<1619:IVOTOA>2.0.CO;2, 1999.
- García, R.R., W.J. Randel, and D.E. Kinnison, On the determination of age of air trends from atmospheric trace species, *J. Atmos. Sci.*, **68**, 139–154, doi:10.1175/2010JAS3527, 2011.
- García, R.R., D.E. Kinnison, and D.R. Marsh, “World avoided” simulations with the whole atmosphere community climate model, *J. Geophys. Res. Atmos.*, **117** (D23), D23303, doi:10.1029/2012JD018430, 2012.
- García, R.R., J. Yue, and J.M. Russell III, Middle atmosphere temperature trends in the twentieth and twenty-first centuries simulated with the Whole Atmosphere Community Climate Model (WACCM), *J. Geophys. Res. Space Phys.*, **124** (10), 7984–7993, doi:10.1029/2019JA026909, 2019.

- Garfinkel, C.I., O. Harari, S. Ziskin Ziv, J. Rao, O. Morgenstern, G. Zeng, S. Tilmes, D. Kinnison, F.M. O'Connor, N. Butchart, M. Deushi, P. Jöckel, A. Pozzer, and S. Davis, Influence of the El Niño–Southern Oscillation on entry stratospheric water vapor in coupled chemistry–ocean CCM1 and CMIIP6 models, *Atmos. Chem. Phys.*, **21**, 3725–3740, doi:10.5194/acp-21-3725-2021, 2021.
- Gillett, N.P., and D.W.J. Thompson, Simulation of recent Southern Hemisphere climate change, *Science*, **302**(5643), 273–275, doi:10.1126/science.1087440, 2003.
- Gillett, N.P., J.F. Scinocca, D.A. Plummer, and M.C. Reader, Sensitivity of climate to dynamically consistent zonal asymmetries in ozone, *Geophys. Res. Lett.*, **36**(10), doi:10.1029/2009GL037246, 2009.
- Gillet, Z.E., J.M. Arblaster, A.J. Dittus, M. Deushi, P. Jöckel, D.E. Kinnison, O. Morgenstern, D.A. Plummer, L.E. Revell, E. Rozanov, R. Schofield, A. Stenke, K.A. Stone, and S. Tilmes, Evaluating the relationship between interannual variations in the Antarctic ozone hole and Southern Hemisphere surface climate in chemistry–climate models, *J. Clim.*, **32**(11), 3131–3151, doi:10.1175/JCLI-D-18-0273.1, 2019.
- Goody, R.M., and Y.L. Yung, Atmospheric Radiation: Theoretical Basis, Oxford University Press, 2nd Edition, doi:10.1093/oso/9780195051346.001.0001, 1989.
- Goyal, R., M.H. England, A. Sen Gupta, and M. Jucker, Reduction in surface climate change achieved by the 1987 Montreal Protocol, *Environ. Res. Lett.*, **14**(12), doi:10.1088/1748-9326/ab4874, 2019.
- Griffiths, P.T., J. Keeble, Y.M. Shin, N.L. Abraham, A.T. Archibald, and J.A. Pyle, On the changing role of the stratosphere on the tropospheric ozone budget: 1979–2010, *Geophys. Res. Lett.*, **47**(10), e2019GL086901, doi:10.1029/2019GL086901, 2020.
- Gruber, N., P. Landschutzer, and N.S. Lovenduski, The variable Southern Ocean carbon sink, *Annu. Rev. Mar. Sci.*, **11**(1), doi:10.1146/annurev-marine-121916-063407, 2019.
- GVF (Global Volcanism Program), Report on Hunga Tonga-Hunga Ha'apai (Tonga), In: Sennert, S.K (ed.), *Weekly Volcanic Activity Report, 12 January-18 January 2022*, Smithsonian Institution and US Geological Survey, 2022.
- Gulev, S.K., P.W. Thorne, J. Ahn, F.J. Dentener, C.M. Domingues, S. Gerland, D. Gong, D.S. Kaufman, H.C. Nnamchi, J. Quaas, J.A. Rivera, S. Sathyendranath, S.L. Smith, B. Trewin, K. von Shuckmann, and R.S. Vose, Changing State of the Climate System, Chapter 2 in *Climate Change 2021: The Physical Science Basis. Contribution of Working Group I to the Sixth Assessment Report of the Intergovernmental Panel on Climate Change*, edited by V. Masson-Delmotte, P. Zhai, A. Pirani, S.L. Connors, C. Péan, S. Berger, N. Caud, Y. Chen, L. Goldfarb, M.I. Gomis, M. Huang, K. Leitzell, E. Lonnoy, J.B.R. Matthews, T.K. Maycock, T. Waterfield, O. Yelekçi, R. Yu, and B. Zhou, Cambridge University Press, Cambridge, United Kingdom and New York, NY, USA, 135 pp., doi:10.1017/9781009157896.004, 2021.
- Haase, S., and K. Matthes, The importance of interactive chemistry for stratosphere troposphere coupling, *Atmos. Chem. Phys.*, **19**(5), 3417–3432, doi:10.5194/acp-19-3417-2019, 2019.
- Haase, S., J. Fricke, T. Kruschke, S. Wahl, and K. Matthes, Sensitivity of the Southern Hemisphere circumpolar jet response to Antarctic ozone depletion: prescribed versus interactive chemistry, *Atmos. Chem. Phys.*, **20**, 14,043–14,061, doi:10.5194/acp-20-14043-2020, 2020.
- Haigh, J.D., The Sun and the Earth's climate, *Living Rev. Sol. Phys.*, **4**(1), 2, doi:10.12942/lrsp-2007-2, 2007.
- Haigh, J.D. and J.A. Pyle, Ozone perturbation experiments in a two-dimensional circulation model, *Q. J. Roy. Meteorol. Soc.*, **108**, 551–574, doi:10.1002/qj.49710845705, 1982.
- Haimberger, L., C. Tavalato, and S. Sperka, Homogenization of the global radio-sonde temperature dataset through combined comparison with reanalysis background series and neighboring stations, *J. Clim.*, **25**, 8108–8131, doi:10.1175/JCLI-D-11-00668.1, 2012.
- Hall, A., and M. Visbeck, Synchronous variability in the Southern Hemisphere atmosphere, sea ice, and ocean resulting from the annular mode, *J. Clim.*, **15**(21), 3043–3057, doi:10.1175/1520-0442(2002)015<3043:SVITSH>2.0.CO;2, 2002.
- Han, Y., W. Tian, M.P. Chipperfield, J. Zhang, F. Wang, W. Sang, J. Luo, W. Feng, A. Chrysanthou, and H. Tian, Attribution of the hemispheric asymmetries in trends of stratospheric trace gases inferred from Microwave Limb Sounder (MLS) measurements, *J. Geophys. Res. Atmos.*, **124**, 6283–6293, doi:10.1029/2018JD029723, 2019.
- Handcock, M.S., and M.N. Raphael, Modeling the annual cycle of daily Antarctic sea ice extent, *Cryosphere*, **14**, 2159–2172, doi:10.5194/tc-14-2159-2020, 2020.
- Harari, O., C.I. Garfinkel, S. Ziskin Ziv, O. Morgenstern, G. Zeng, S. Tilmes, D. Kinnison, M. Deushi, P. Jöckel, A. Pozzer, F.M. O'Connor, and S. Davis, Influence of Arctic stratospheric ozone on surface climate in CCM1 models, *Atmos. Chem. Phys.*, **19**(14), 9253–9268, doi:10.5194/acp-19-9253-2019, 2019.
- Hardiman, S.C., M.B. Andrews, T. Andrews, A.C. Bushell, N.J. Dunstone, H. Dyson, G.S. Jones, J.R. Knight, E. Neininger, F.M. O'Connor, J.K. Ridley, M.A. Ringer, A.A. Scaife, C.A. Senior, and R.A. Wood, The impact of prescribed ozone in climate projections run with HadGEM3-GC3. 1, *J. Adv. Model. Earth Syst.*, **11**, 3443–3453, doi:10.1029/2019MS001714, 2019.
- Haumann, F.A., N. Gruber, and M. Münnich, Sea-ice induced Southern Ocean subsurface warming and surface cooling in a warming climate, *AGU Adv.*, **1**(2), doi:10.1029/2019AV000132, 2020.
- Hendon, H.H., E.-P. Lim, and S. Abhik, Impact of interannual ozone variations on the downward coupling of the 2002 Southern Hemisphere stratospheric warming, *J. Geophys. Res. Atmos.*, **125**(16), doi:10.1029/2020JD032952, 2020.
- Hobbs, W.R., N.L. Bindoff, and M.N. Raphael, New perspectives on observed and simulated Antarctic sea ice extent trends using optimal fingerprinting techniques, *J. Clim.*, **28**(4), 1543–1560, doi:10.1175/jcli-d-14-00367.1, 2015.
- Hobbs, W.R., C. Roach, T. Roy, J.-B. Sallée, and N. Bindoff, Anthropogenic temperature and salinity changes in the Southern Ocean, *J. Clim.*, **34**, 215–228, doi:10.1175/jcli-d-20-0454.1, 2021.
- Hodnebrog, Ø., G. Myhre, R.J. Kramer, K.P. Shine, T. Andrews, G. Faluvegi, M. Kasoar, A. Kirkevåg, J.-F. Lamarque, J. Mülmenstädt, D. Oliví, B.H. Samset, D. Shindell, C.J. Smith, T. Takemura, and A. Voulgarakis, The effect of rapid adjustments to halocarbons and N₂O on radiative forcing, *npj Clim. Atmos. Sci.*, **3**(1), 43, doi:10.1038/s41612-020-00150-x, 2020.
- Holland, M.M., L. Landrum, Y. Kostov, and J. Marshall, Sensitivity of Antarctic sea ice to the Southern Annular Mode in coupled climate models, *Clim. Dyn.*, **49**(5), 1813–1831, doi:10.1007/s00382-016-3424-9, 2017.
- Hong, H.-J., and T. Reichler, Local and remote response of ozone to Arctic stratospheric circulation extremes, *Atmos. Chem. Phys.*, **21**, 1159–1171, doi:10.5194/acp-21-1159-2021, 2021.
- Huang, Y., Wang, Y. and H. Huang, Stratospheric water vapor feedback disclosed by a locking experiment. *Geophys. Res. Lett.*, **47**(12), p.e2020GL087987, 2020.
- Hurst, D.F., W.G. Read, H. Vomel, H.B. Selkirk, K.H. Rosenlof, S.M. Davis, E.G. Hall, A.F. Jordan, and S.J. Oltmans, Recent divergences in stratospheric water vapor measurements by frost point hygrometers and the Aura Microwave Limb Sounder, *Atmos. Meas. Tech.*, **9**(9), 4447–4457, doi:10.5194/amt-9-4447-2016, 2016.
- Hurwitz M.M., E.L. Fleming, P.A. Newman, F. Li, E. Mlawer, K. Cady-Pereira and R. Bailey, Ozone depletion by hydrofluorocarbons, *Geophys. Res. Lett.* **42** 8686–92, 2015.
- Hyder, P., J. Edwards, R.P. Allan, H.T. Hewitt, T.J. Bracegirdle, J.M. Gregory, R.A. Wood, A.J.S. Meijers, J. Mulcahy, P. Field, K. Furtado, A. Bodas-Salcedo, K.D. Williams, D. Copsey, S.A. Josey, C. Liu, C.D. Roberts, C. Sanchez, J. Ridley, L. Thorpe, S.C. Hardiman, M. Mayer, D.I. Berry, and S.E. Belcher, Critical Southern Ocean climate model biases traced to atmospheric model cloud errors, *Nat. Commun.*, **9**, 3625, doi:10.1038/s41467-018-05634-2, 2018.
- The IMBIE team, Mass balance of the Antarctic Ice Sheet from 1992 to 2017, *Nature*, **558**, 219–222, doi:10.1038/s41586-018-0179-y, 2018.
- IPCC (Intergovernmental Panel on Climate Change), Climate Change 2021: The Physical Science Basis. Contribution of Working Group I to the Sixth Assessment Report of the Intergovernmental Panel on Climate Change, edited by V. Masson-Delmotte, P. Zhai, A. Pirani, S.L. Connors, C. Péan, S. Berger, N. Caud, Y. Chen, L. Goldfarb, M.I. Gomis, M. Huang, K. Leitzell, E. Lonnoy, J.B.R. Matthews, T.K. Maycock, T. Waterfield, O. Yelekçi, R. Yu, and B. Zhou, Cambridge University Press, Cambridge, United Kingdom and New York, NY, USA, In press, doi:10.1017/9781009157896, 2021.
- Ivanciu, I., K. Matthes, S. Wahl, J. Harlaß, and A. Biastoch, Effects of prescribed CMIIP6 ozone on simulating the Southern Hemisphere atmospheric circulation response to ozone depletion, *Atmos. Chem. Phys.*, **21**, 5777–5806, doi:10.5194/acp-21-5777-2021, 2021.
- Ivanciu, I., K. Matthes, A. Biastoch, S. Wahl, and J. Harlaß, Twenty-first century Southern Hemisphere impacts of ozone recovery and climate change from the stratosphere to the ocean, *Weather Clim. Dynam.*, **3**, 139–171, doi:10.5194/wcd-3-139-2022, 2022.
- Ivy, D.J., S. Solomon, N. Calvo, and D.W.J. Thompson, Observed connections of Arctic stratospheric ozone extremes to Northern Hemisphere surface climate, *Environ. Res. Lett.*, **12**(2), 024004, doi:10.1088/1748-9326/aa574a, 2017.

- Jenkins, A., P. Dutrieux, S. Jacobs, E.J. Steig, G.H. Gudmundsson, J. Smith, and K.J. Heywood, Decadal ocean forcing and Antarctic ice sheet response: Lessons from the Amundsen Sea, *Oceanography*, **29** (4), 106–117, doi:10.5670/oceanog.2016.103, 2016.
- Jensen, E.J., L.L. Pan, S. Honomichl, G.S. Diskin, M. Kramer, N. Spelten, G. Günther, D.F. Hurst, M. Fujiwara, H. Vömel, H.B. Selkirk, J. Suzuki, M.J. Schwartz, and J.B. Smith, Assessment of observational evidence for direct convective hydration of the lower stratosphere, *J. Geophys. Res. Atmos.*, **125** (15), e2020JD032793, doi:10.1029/2020jd032793, 2020.
- Jucker, M., T. Reichler, and D.W. Waugh, How frequent are Antarctic sudden stratospheric warmings in present and future climate?, *Geophys. Res. Lett.*, **48** (11), e2021GL093215, doi:10.1029/2021GL093215, 2021.
- Jucker, M., and R. Goyal, Ozone-forced Southern Annular Mode during Antarctic stratospheric warming events, *Geophys. Res. Lett.*, **49** (4), doi:10.1029/2021GL095270, 2022.
- Karpechko, A.Y., J. Perlwitz, and E. Manzini, A model study of tropospheric impacts of the Arctic ozone depletion 2011, *J. Geophys. Res. Atmos.*, **119** (13), 7999–8014, doi:10.1002/2013JD021350, 2014.
- Karpechko, A. Y., and Manzini, E., Arctic Stratosphere Dynamical Response to Global Warming, *Journal of Climate*, **30**(17), 7071–7086, doi.org/10.1175/JCLI-D-16-0781.1, 2017.
- Karpechko, A.Y., and A.C. Maycock (Lead Authors), M. Abalos, H. Akiyoshi, J.M. Arblaster, C.I. Garfinkel, K.H. Rosenlof, and M. Sigmond, Stratospheric Ozone Changes and Climate, Chapter 5 in *Scientific Assessment of Ozone Depletion: 2018*, Global Ozone Research and Monitoring Project–Report No. 58, 73 pp., World Meteorological Organization, Geneva, Switzerland, 2018.
- Kataoka T., H. Tatebe, H. Koyama, T. Mochizuki, K. Ogochi, H. Naoe, Y. Imada, H. Shiogama, M. Kimoto, and M. Watanabe, Seasonal to decadal predictions with MIROC6: description and basic evaluation, *J. Adv. Model. Earth Syst.*, **12** (12), doi:10.1029/2019MS002035, 2020.
- Kawatani, Y., and K. Hamilton, Weakened stratospheric quasi-biennial oscillation driven by increased tropical mean upwelling, *Nature*, **497**, 478–481, doi:10.1038/nature12140, 2013.
- Keeble, J., B. Hassler, A. Banerjee, R. Checa-Garcia, G. Chiodo, S. Davis, V. Eyring, P.T. Griffiths, O. Morgenstern, P. Nowack, G. Zeng, J. Zhang, G. Bodeker, S. Burrows, P. Cameron-Smith, D. Cugnet, C. Danek, M. Deushi, L.W. Horowitz, A. Kubin, L. Li, G. Lohmann, M. Michou, M.J. Mills, P. Nabat, D. Olivie, S. Park, Ø. Seland, J. Stoll, K.-H. Wieners, and T. Wu, Evaluating stratospheric ozone and water vapour changes in CMIP6 models from 1850 to 2100, *Atmos. Chem. Phys.*, **21**, 5015–5061, doi:10.5194/acp-21-5015-2021, 2021.
- Keppeler, L., and P. Landschutzer, Regional wind variability modulates the Southern Ocean carbon sink, *Sci. Rep.*, **9**, 7384, doi:10.1038/s41598-019-43826-y, 2019.
- Khatiwal, S., F. Primeau, and T. Hall, Reconstruction of the history of anthropogenic CO₂ concentrations in the ocean, *Nature*, **462**, 346–349, doi:10.1038/nature08526, 2009.
- Kim, J., and K.Y. Kim, Characteristics of stratospheric polar vortex fluctuations associated with sea ice variability in the Arctic winter, *Clim. Dyn.*, **54**, 3599–3611, doi:10.1007/s00382-020-05191-9, 2020.
- Kindem, I., and B. Christiansen, Tropospheric response to stratospheric ozone loss, *Geophys. Res. Lett.*, **28**, 1547–1550, doi:10.1029/2000GL012552, 2001.
- Kouznetsov, R., M. Sofiev, J. Vira, and G. Stiller, Simulating age of air and the distribution of SF₆ in the stratosphere with the SILAM model, *Atmos. Chem. Phys.*, **20**, 5837–5859, doi:10.5194/acp-20-5837-2020, 2020.
- Kovács, T., W. Feng, A. Totterdill, J.M.C. Plane, S. Dhomse, J.C. Gómez-Martín, G. Stiller, F. Haenel, C. Smith, P. Forster, R.R. Garcia, D. Marsh, and M.P. Chipperfield, Determination of the atmospheric lifetime and global warming potential of sulfur hexafluoride using a three-dimensional model, *Atmos. Chem. Phys.*, **17**, 883–898, doi:10.5194/acp-17-883-2017, 2017.
- Kretschmer, M., J. Cohen, V. Matthias, J. Runge, and D. Coumou, The different stratospheric influence on cold-extremes in Eurasia and North America, *npj Clim. Atmos. Sci.*, **1**, 44, doi:10.1038/s41612-018-0054-4, 2018.
- Kretschmer, M., G. Zappa, and T.G. Shepherd, The role of Barents–Kara sea ice loss in projected polar vortex changes, *Weather Clim. Dynam.*, **1**, 715–730, doi:10.5194/wcd-1-715-2020, 2020.
- Kuilman, M.S., Q. Zhang, M. Cai, and Q. Wen, Using the climate feedback response analysis method to quantify climate feedbacks in the middle atmosphere, *Atmos. Chem. Phys.*, **20**, 12,409–12,430, doi:10.5194/acp-20-12409-2020, 2020.
- Lacis, A.A., D.J. Wuebbles, and J.A. Logan, Radiative forcing of climate by changes in the vertical distribution of ozone, *J. Geophys. Res. Atmos.*, **95**, 9971–9981, doi:10.1029/JD095iD07p09971, 1990.
- Lambert, A., W. Read, and N. Livesey, *MLS/Aura level 2 water vapor (H₂O) mixing ratio V005*, Goddard Earth Sciences Data and Information Services Center (GES DISC), Greenbelt, Maryland, USA, 2020.
- Landschützer, P., N. Gruber, F.A. Haumann, C. Rödenbeck, D.C.E. Bakker, S. Van Heuven, M. Hoppema, N. Metzl, C. Sweeney, T. Takahashi, B. Tilbrook, and R. Wanninkhof, The reinvigoration of the Southern Ocean carbon sink, *Science*, **349**, 1221–1224, doi:10.1126/science.aab2620, 2015.
- Lawrence, Z.D., J. Perlwitz, A.H. Butler, G.L. Manney, P.A. Newman, S.H. Lee, and E.R. Nash, The remarkably strong Arctic stratospheric polar vortex of winter 2020: Links to record-breaking Arctic oscillation and ozone loss, *J. Geophys. Res. Atmos.*, **125** (22), doi:10.1029/2020JD033271, 2020.
- Le Quéré, C., C. Rödenbeck, E.T. Buitenhuis, T.J. Conway, R. Langenfelds, A. Gomez, C. Labuschagne, M. Ramonet, T. Nakazawa, N. Gillett, and M. Heimann, Saturation of the Southern Ocean CO₂ sink due to recent climate change, *Science*, **316** (5832), 1735–1738, doi:10.1126/science.1136188, 2007.
- Le Quéré, C., G.P. Peters, P. Friedlingstein, R.M. Andrew, J.G. Canadell, S.J. Davis, R.B. Jackson, and M.W. Jones, Fossil CO₂ emissions in the post-COVID-19 era, *Nat. Clim. Change*, **11**, 197–199, doi:10.1038/s41558-021-01001-0, 2021.
- Lee, J.-Y., J. Marotzke, G. Bala, L. Cao, S. Corti, J.P. Dunne, F. Engelbrecht, E. Fischer, J.C. Fyfe, C. Jones, A. Maycock, J. Mutemi, O. Ndiaye, S. Panickal, and T. Zhou, Future Global Climate: Scenario-Based Projections and Near-Term Information, Chapter 4 in *Climate Change 2021: The Physical Science Basis, Contribution of Working Group I to the Sixth Assessment Report of the Intergovernmental Panel on Climate Change*, edited by V. Masson-Delmotte, P. Zhai, A. Pirani, S.L. Connors, C. Péan, S. Berger, N. Caud, Y. Chen, L. Goldfarb, M.I. Gomis, M. Huang, K. Leitzell, E. Lonnoy, J.B.R. Matthews, T.K. Maycock, T. Waterfield, O. Yelekçi, R. Yu, and B. Zhou, Cambridge University Press, Cambridge, United Kingdom and New York, NY, USA, 119 pp., doi:10.1017/9781009157896.006, 2021.
- Lee, S.H., J.C. Furtado, and A.J. Charlton-Perez, Wintertime North American weather regimes and the Arctic stratospheric polar vortex, *Geophys. Res. Lett.*, **46**, 14,892–14,900, doi:10.1029/2019GL085592, 2019.
- Leedham Elvidge, E., H. Bönisch, C.A.M. Brenninkmeijer, A. Engel, P.J. Fraser, E. Gallacher, R. Langenfelds, J. Mühle, D.E. Oram, E.A. Ray, A.R. Ridley, T. Röckmann, W.T. Sturges, R.F. Weiss, and J.C. Laube, Evaluation of stratospheric age of air from CF₄, C₂F₆, C₃F₈, CHF₃, HFC-125, HFC-227ea and SF₆; implications for the calculations of halocarbon lifetimes, fractional release factors and ozone depletion potentials, *Atmos. Chem. Phys.*, **18**, 3369–3385, doi:10.5194/acp-18-3369-2018, 2018.
- Lenaerts, J.T.M., J. Fyke, and B. Medley, The signature of ozone depletion in recent Antarctic precipitation change: A study with the Community Earth System Model, *Geophys. Res. Lett.*, **45** (23), 12,931–12,939, doi:10.1029/2018gl078608, 2018.
- Li, F., P. Newman, S. Pawson, and J. Perlwitz, Effects of greenhouse gas increase and stratospheric ozone depletion on stratospheric mean age of air in 1960–2010, *J. Geophys. Res. Atmos.*, **123** (4), 2098–2110, doi:10.1002/2017JD027562, 2018.
- Li, F., and P. Newman, Stratospheric water vapor feedback and its climate impacts in the coupled atmosphere–ocean Goddard Earth Observing System Chemistry–Climate Model, *Clim. Dynam.*, **55** (5), 1585–1595, doi:10.1007/s00382-020-05348-6, 2020.
- Li, S., W. Liu, K. Lyu, and X. Zhang, The effects of historical ozone changes on Southern Ocean heat uptake and storage, *Clim. Dyn.*, **57**, 2269–2285, doi:10.1007/s00382-021-05803-y, 2021.
- Liang, Y.-C., L.M. Polvani, M. Previdi, K.L. Smith, M.R. England, and G. Chiodo, Stronger Arctic amplification from ozone-depleting substances than from carbon dioxide, *Environ. Res. Lett.*, **17** (2), doi:10.1088/1748-9326/ac4a31, 2022.
- Lim, E.-P., H.H. Hendon, and D.W.J. Thompson, Seasonal evolution of stratosphere-troposphere coupling in the Southern Hemisphere and implications for the predictability of surface climate, *J. Geophys. Res. Atmos.*, **123**, 12,002–12,016, doi:10.1029/2018JD029321, 2018.
- Lim, E.-P., H.H. Hendon, G. Boschat, D. Hudson, D.W.J. Thompson, A.J. Dowdy, and J.M. Arblaster, Australian hot and dry extremes induced by weakenings of the stratospheric polar vortex, *Nat. Geosci.*, **12**, 896–901, doi:10.1038/s41561-019-0456-x, 2019.

- Lim, E.-P., H.H. Hendon, A.H. Butler, D.W.J. Thompson, Z.D. Lawrence, A.A. Scaife, T.G. Shepherd, I. Polichtchouk, H. Nakamura, C. Kobayashi, R. Comer, L. Coy, A. Dowdy, R.D. Garreaud, P.A. Newman, and G. Wang, The 2019 Southern Hemisphere stratospheric polar vortex weakening and its impacts, *Bull. Am. Meteorol. Soc.*, **102** (6), E1150–E1171, doi:10.1175/BAMS-D-20-0112.1, 2021.
- Lin, P., and Y. Ming, Enhanced climate response to ozone depletion from ozone–circulation coupling, *J. Geophys. Res. Atmos.*, **126** (7), doi:10.1029/2020JD034286, 2021.
- Liu, J., J.M. Rodríguez, L.D. Oman, A.R. Douglass, M.A. Olsen, and L. Hu, Stratospheric impact on the Northern Hemisphere winter and spring ozone interannual variability in the troposphere, *Atmos. Chem. Phys.*, **20**, 6417–6433, doi:10.5194/acp-20-6417-2020, 2020.
- Liu, W., M.I. Hegglin, R. Checa-Garcia, S. Li, N.P. Gillett, K. Lyu, X. Zhang, and N.C. Swart, Stratospheric ozone depletion and tropospheric ozone increases drive Southern Ocean interior warming, *Nat. Clim. Change*, **12**, 365–372, doi:10.1038/s41588-022-01320-w, 2022.
- Livesey, N.J., W.G. Read, L. Froidevaux, A. Lambert, M.L. Santee, M.J. Schwartz, L.F. Millán, R.F. Jarnot, P.A. Wagner, D.F. Hurst, K.A. Walker, P.E. Sheese, and G.E. Nedoluha, Investigation and amelioration of long-term instrumental drifts in water vapor and nitrous oxide measurements from the Aura Microwave Limb Sounder (MLS) and their implications for studies of variability and trends, *Atmos. Chem. Phys.*, **21**, 15,409–15,430, doi:10.5194/acp-21-15409-2021, 2021.
- Livesey, N.J., W.G. Read, P.A. Wagner, L. Froidevaux, M.L. Santee, M.J. Schwartz, A. Lambert, L.F. Millán Valle, H.C. Pumphrey, G.L. Manney, R.A. Fuller, R.F. Jarnot, B.W. Knosp, R.R. Lay, Version 5.0x Level 2 and 3 data quality and description document, Tech. Rep. No. JPL D-105336 Rev. B, Jet Propulsion Laboratory, California Institute of Technology Pasadena, California/Jet Propulsion Lab, 2022.
- Loeffel, S., R. Eichinger, H. Garmy, T. Reddmann, F. Fritsch, S. Versick, G. Stiller, and F. Haenel, The impact of sulfur hexafluoride (SF₆) sinks on age of air climatologies and trends, *Atmos. Chem. Phys.*, **22**, 1175–1193, doi:10.5194/acp-22-1175-2022, 2022.
- Long, C.S., M. Fujiwara, S. Davis, D.M. Mitchell, and C.J. Wright, Climatology and interannual variability of dynamic variables in multiple reanalyses evaluated by the SPARC Reanalysis Intercomparison Project (S-RIP), *Atmos. Chem. Phys.*, **17**, 14,593–14,629, doi:10.5194/acp-17-14593-2017, 2017.
- Lovenduski, N.S., N. Gruber, S.C. Doney, and I.D. Lima, Enhanced CO₂ outgassing in the Southern Ocean from a positive phase of the Southern Annular Mode, *Glob. Biogeochem. Cycles*, **21** (2), doi:10.1029/2006gb002900, 2007.
- Ma, X., F. Xie, J. Li, X. Zheng, W. Tian, R. Ding, C. Sun, and J. Zhang, Effects of Arctic stratospheric ozone changes on spring precipitation in the northwestern United States, *Atmos. Chem. Phys.*, **19**, 861–875, doi:10.5194/acp-19-861-2019, 2019.
- Ma, X., and F. Xie, Predicting April precipitation in the Northwestern United States based on Arctic stratospheric ozone and local circulation, *Front. Earth Sci.*, **8**, 56, doi:10.3389/feart.2020.00056, 2020.
- Mahieu, E., M.P. Chipperfield, J. Notholt, T. Reddmann, J. Anderson, P.F. Bernath, T. Blumenstock, M.T. Coffey, S.S. Dhomse, W. Feng, B. Franco, L. Froidevaux, D.W.T. Griffith, J.W. Hannigan, F. Hase, R. Hossaini, N.B. Jones, I. Morino, I. Murata, H. Nakajima, M. Palm, C. Paton-Walsh, J.M. Russell III, M. Schneider, C. Servais, D. Smale, and K.A. Walker, Recent Northern Hemisphere stratospheric HCl increase due to atmospheric circulation changes, *Nature*, **515**, 104–107, doi:10.1038/nature13857, 2014.
- Maleska, S., K.L. Smith, and J. Virgin, Impacts of stratospheric ozone extremes on Arctic high cloud, *J. Clim.*, **33**, 8869–8884, doi:10.1175/JCLI-D-19-0867.1, 2020.
- Manzini, E., A. Karpechko, and L. Kornbluh, Nonlinear response of the stratosphere and the North Atlantic–European climate to global warming, *Geophys. Res. Lett.*, **45**, 4255–4263, doi:10.1029/2018GL077826, 2018.
- Marshall, J., K.C. Armour, J.R. Scott, Y. Kostov, U. Hausmann, D. Ferreira, T.G. Shepherd, and C.M. Bitz, The ocean’s role in polar climate change: asymmetric Arctic and Antarctic responses to greenhouse gas and ozone forcing, *Philos. Trans. R. Soc. A*, **372** (2019), 20130040, doi:10.1098/rsta.2013.0040, 2014.
- Matsumura, S., K. Yamazaki, and T. Horinouchi, Robust asymmetry of the future Arctic polar vortex is driven by tropical Pacific warming, *Geophys. Res. Lett.*, **48** (11), e2021GL093440, doi:10.1029/2021GL093440, 2021.
- Maycock, A.C., W.J. Randel, A.K. Steiner, A.Y. Karpechko, J. Christy, R. Saunders, D.W.J. Thompson, C.-Z. Zou, A. Chrysanthou, N. Luke Abraham, H. Akiyoshi, A.T. Archibald, N. Butchart, M. Chipperfield, M. Dameris, M. Deushi, S. Dhomse, G. Di Genova, P. Jöckel, D.E. Kinnison, O. Kirner, F. Ladstätter, M. Michou, O. Morgenstern, F. O’Connor, L. Oman, G. Pitari, D.A. Plummer, L.E. Revell, E. Rozanov, A. Stenke, D. Visoni, Y. Yamashita, and G. Zeng, Revisiting the mystery of recent stratospheric temperature trends, *Geophys. Res. Lett.*, **45**, 9919–9933, doi:10.1029/2018GL078035, 2018.
- McLondress, C., A.I. Jonsson, D.A. Plummer, M.C. Reader, J.F. Scinocca, and T.G. Shepherd, Separating the dynamical effects of climate change and ozone depletion. Part I: Southern Hemisphere stratosphere, *J. Clim.*, **23** (18), 5002–5020, doi:10.1175/2010JCLI3586.1, 2010.
- McLondress, C., T.G. Shepherd, M.C. Reader, D.A. Plummer, and K.P. Shine, The climate impact of past changes in halocarbons and CO₂ in the tropical UTLS region, *J. Clim.*, **27**, 8646–8660, doi:10.1175/JCLI-D-14-00232.1, 2014.
- Mears, C.A., F.J. Wentz, P. Thorne, and D. Bernie, Assessing uncertainty in estimates of atmospheric temperature changes from MSU and AMSU using a Monte-Carlo estimation technique, *J. Geophys. Res. Atmos.*, **116** (D8), D08112, doi:10.1029/2010JD014954, 2011.
- Meehl, G.A., J.M. Arblaster, C.M. Bitz, C.T.Y. Chung, and H. Teng, Antarctic sea-ice expansion between 2000 and 2014 driven by tropical Pacific decadal climate variability, *Nat. Geosci.*, **9**, 590–595, doi:10.1038/ngeo2751, 2016.
- Meehl, G.A., J.M. Arblaster, C.T.Y. Chung, M.M. Holland, A. DuVivier, L. Thompson, D. Yang, and C.M. Bitz, Sustained ocean changes contributed to sudden Antarctic sea ice retreat in late 2016, *Nat. Commun.*, **10** (1), 14, doi:10.1038/s41467-018-07865-9, 2019.
- Michou, M., P. Nabat, D. Saint-Martin, J. Bock, B. Decharme, M. Mallet, R. Roehrig, R. Sférian, S. Sénési, and A. Voldoire, Present-day and historical aerosol and ozone characteristics in CNRM CMIP6 simulations, *J. Adv. Model. Earth Syst.*, **12** (1), doi:10.1029/2019MS001816, 2020.
- Millán, L., M.L. Santee, A. Lambert, N.J. Livesey, F. Werner, M. Schwartz, H.C. Pumphrey, G.L. Manney, Y. Wang, H. Su, W. Longtau, W.G. Read, L. Froidevaux, Hunga Tonga-Hunga Ha’apai Hydration of the Stratosphere, *Geophys. Res. Lett.*, **49**, e2022GL099381, https://doi.org/10.1029/2022GL099381, 2022.
- Mindlin, J., T.G. Shepherd, C.S. Vera, M. Osman, G. Zappa, R.W. Lee, and K.I. Hodges, Storyline description of Southern Hemisphere midlatitude circulation and precipitation response to greenhouse gas forcing, *Clim., Dyn.*, **54**, 4399–4421, doi:10.1007/s00382-020-05234-1, 2020.
- Mindlin, J., T.G. Shepherd, C. Vera, and M. Osman, Combined effects of global warming and ozone depletion/recovery on Southern Hemisphere atmospheric circulation and regional precipitation, *Geophys. Res. Lett.*, **48**, e2021GL092568, doi:10.1029/2021GL092568, 2021.
- Ming, A., A.C. Maycock, P. Hitchcock, and P. Haynes, The radiative role of ozone and water vapour in the annual temperature cycle in the tropical tropopause layer, *Atmos. Chem. Phys.*, **17**, 5677–5701, doi:10.5194/acp-17-5677-2017, 2017.
- Mitchell, D.M., Y.T. E. Lo, W. J. M. Seviour, L. Haimberger and L.M. Polvani, The vertical profile of recent tropical temperature trends: Persistent model biases in the context of internal variability, *Environ. Res. Lett.*, **15**, 1040b4, 2020.
- Montzka, S. A., Velders, G. J. M. (lead authors), Krummel, P. B., Mühle, J., Orkin, V. L., Park, S., Shah, N., and Walter-Terrinoni, H.: Hydrofluorocarbons (HFCs), Chapter 2 in: *Scientific Assessment of Ozone Depletion*: 2018, Global Ozone Research and Monitoring, World Meteorological Organization, Geneva, Switzerland, 2018.
- Monge-Sanz, B.M., A. Bozzo, N. Byrne, M.P. Chipperfield, M. Diamantakis, J. Flemming, L.J. Gray, R.J. Hogan, L. Jones, L. Magnusson, I. Polichtchouk, T.G. Shepherd, N. Wedi, and A. Weisheimer, A stratospheric prognostic ozone for seamless Earth system models: performance, impacts and future, *Atmos. Chem. Phys.*, **22**, 4277–4302, doi:10.5194/acp-22-4277-2022, 2022.
- Morgenstern, O., H. Akiyoshi, Y. Yamashita, D.E. Kinnison, R.R. Garcia, D.A. Plummer, J. Scinocca, G. Zeng, E. Rozanov, A. Stenke, L.E. Revell, G. Pitari, E. Mancini, E., G. Di Genova, S.S. Dhomse, and M.P. Chipperfield, Ozone sensitivity to varying greenhouse gases and ozone-depleting substances in CCM1-1 simulations, *Atmos. Chem. Phys.*, **18**, 1091–1114, doi:10.5194/acp-18-1091-2018, 2018.
- Morgenstern, O., The Southern Annular Mode in 6th coupled model intercomparison project models, *J. Geophys. Res. Atmos.*, **126** (5), doi:10.1029/2020JD034161, 2021.
- Morgenstern, O., S.M. Frith, G.E. Bodeker, V. Fioletov, and R.J. van der A, Reevaluation of total-column ozone trends and of the Effective Radiative Forcing of ozone-depleting substances, *Geophys. Res. Lett.*, **48** (21), doi:10.1029/2021GL095376, 2021.
- Morrow, R., and E. Kestenare, 22-year surface salinity changes in the Seasonal Ice Zone near 140°E off Antarctica, *J. Mar. Syst.*, **175**, 46–62, doi:10.1016/j.jmarsys.2017.07.003, 2017.

- Munro, D.R., N.S. Lovenduski, T. Takahashi, B.B. Stephens, T. Newberger, and C. Sweeney, Recent evidence for a strengthening CO₂ sink in the Southern Ocean from carbonate system measurements in the Drake Passage (2002–2015), *Geophys. Res. Lett.*, **42** (18), 7623–7630, doi:10.1002/2015gl065194, 2015.
- Muthers, S., Anet, J.G., Stenke, A., Raible, C.C., Rozanov, E., Brönnimann, S., Peter, T., Arfeuille, F.X., Shapiro, A.I., Beer, J. and F. Steinhilber, The coupled atmosphere–chemistry–ocean model SOCOL-MPIOM. *Geosci. Model Dev.*, **7**(5), pp.2157–2179, doi:10.5194/gmd-7-2157-2014, 2014.
- Myhre, G., D. Shindell, F.-M. Bréon, W. Collins, J. Fuglestedt, J. Huang, D. Koch, J.-F. Lamarque, D. Lee, B. Mendoza, T. Nakajima, A. Robock, G. Stephens, T. Takemura, and H. Zhang, Anthropogenic and Natural Radiative Forcing, Chapter 8 in *Climate Change 2013: The Physical Science Basis, Contribution of Working Group I to the Fifth Assessment Report of the Intergovernmental Panel on Climate Change*, edited by T.F. Stocker, D. Qin, G.-K. Plattner, M. Tignor, S.K. Allen, J. Boschung, A. Nauels, Y. Xia, V. Bex, and P.M. Midgley, Cambridge University Press, Cambridge, United Kingdom and New York, NY, USA, [available at: https://www.ipcc.ch/site/assets/uploads/2018/02/WG1AR5_Chapter08_FINAL.pdf], 2013.
- Naoe, H., M. Deushi, K. Yoshida, and K. Shibata, Future changes in the ozone quasi-biennial oscillation with increasing GHGs and ozone recovery in CCM1 simulations, *J. Clim.*, **30** (17), 6977–6997, doi:10.1175/JCLI-D-16-0464, 2017.
- Nash, J., and R. Saunders, A review of Stratospheric Sounding Unit radiance observations for climate trends and reanalyses, *Q. J. R. Meteorol. Soc.*, **141**, 2103–2113, doi:10.1002/qj.2505, 2015.
- Naughten, K.A., P.R. Holland, P. Dutrieux, S. Kimura, D.T. Bett, and A. Jenkins, Simulated twentieth-century ocean warming in the Amundsen Sea, West Antarctica, *Geophys. Res. Lett.*, **49** (5), e2021GL094566, doi:10.1029/2021GL094566, 2022.
- Neely III, R.R., D.R. Marsh, K.L. Smith, S.M. Davis, and L.M. Polvani, Biases in Southern Hemisphere climate trends induced by coarsely specifying the temporal resolution of stratospheric ozone, *Geophys. Res. Lett.*, **41** (23), 8602–8610, doi:10.1002/2014GL061627, 2014.
- Newman, P.A., L.D. Oman, A.R. Douglass, E.L. Fleming, S.M. Frith, M.M. Hurwitz, S.R. Kawa, C.H. Jackman, N.A. Krotkov, E.R. Nash, J.E. Nielsen, S. Pawson, R.S. Stolarski, and G.J.M. Velders, What would have happened to the ozone layer if chlorofluorocarbons (CFCs) had not been regulated?, *Atmos. Chem. Phys.*, **9**, 2113–2128, doi:10.5194/acp-9-2113-2009, 2009.
- Noble, T.L., E.J. Rohling, A.R.A. Aitken, H.C. Bostock, Z. Chase, N. Gomez, L.M. Jong, M.A. King, A.N. Mackintosh, F.S. McCormack, R.M. McKay, L. Menviel, S.J. Phipps, M.E. Weber, C.J. Fogwill, B. Gayen, N.R. Golledge, D.E. Gwyther, A. McC. Hogg, Y.M. Martos, B. Pena-Molino, J. Roberts, T. van de Flierdt, and T. Williams, The sensitivity of the Antarctic ice sheet to a changing climate: past, present, and future, *Rev. Geophys.*, **58** (4), doi:10.1029/2019rg000663, 2020.
- Nowack, P.J., N.L. Abraham, A.C. Maycock, P. Braesicke, J.M. Gregory, M.M. Joshi, A. Osprey, and J.A. Pyle, A large ozone–circulation feedback and its implications for global warming assessments, *Nat. Clim. Change*, **5**, 41–45, doi:10.1038/nclimate2451, 2015.
- Nowack, P.J., P. Braesicke, N.L. Abraham, and J.A. Pyle, On the role of ozone feedback in the ENSO amplitude response under global warming, *Geophys. Res. Lett.*, **44**, 3858–3866, doi:10.1002/2016GL072418, 2017.
- Nowack, P.J., N.L. Abraham, P. Braesicke, and J.A. Pyle, The impact of stratospheric ozone feedbacks on climate sensitivity estimates, *J. Geophys. Res. Atmos.*, **123**, 4630–4641, doi:10.1002/2017JD027943, 2018.
- Nuetzel, M., A. Podglajen, H. Garny, and F. Ploeger, Quantification of water vapour transport from the Asian monsoon to the stratosphere, *Atmos. Chem. Phys.*, **19**, 8947–8966, doi:10.5194/acp-19-8947-2019, 2019.
- O'Connor, F.M., N.L. Abraham, M. Dalvi, G.A. Folberth, P.T. Griffiths, C. Hardacre, B.T. Johnson, R. Kahana, J. Keeble, B. Kim, O. Morgenstern, J.P. Mulcahy, M. Richardson, E. Robertson, J. Seo, S. Shim, J.C. Teixeira, S.T. Turnock, J. Williams, A.J. Wiltshire, S. Woodward, and G. Zeng, Assessment of preindustrial to present-day anthropogenic climate forcing in UKESM1, *Atmos. Chem. Phys.*, **21**, 1211–1243, doi:10.5194/acp-21-1211-2021, 2021.
- Oehrlein, J., G. Chiodo, and L.M. Polvani, The effect of interactive ozone chemistry on weak and strong stratospheric polar vortex events, *Atmos. Chem. Phys.*, **20** (17), 10,531–10,544, doi:10.5194/acp-20-10531-2020, 2020.
- Oh, J., S.W. Son, J. Choi, E.P. Lim, C. Garfinkel, H. Hendon, Y. Kim, and H.S. Kang, Impact of stratospheric ozone on the subseasonal prediction in the southern hemisphere spring, *Prog. Earth Planet. Sci.*, **9** (1), doi:10.1186/s40645-022-00485-4, 2022.
- Olsen, M.A., G.L. Manney, and J. Liu, The ENSO and QBO impact on ozone variability and stratosphere troposphere exchange relative to the subtropical jets, *J. Geophys. Res. Atmos.*, **124**, 7379–7392, doi:10.1029/2019JD030435, 2019.
- Oman, L., D.W. Waugh, S. Pawson, R.S. Stolarski, and P.A. Newman, On the influence of anthropogenic forcings on changes in the stratospheric mean age, *J. Geophys. Res. Atmos.*, **114** (D3), D03105, doi:10.1029/2008JD010378, 2009.
- O'Neill, M.E., L. Orf, G.M. Heymsfield, and K. Halbert, Hydraulic jump dynamics above supercell thunderstorms, *Science*, **373** (6560), 1248–1251, doi:10.1126/science.abh3857, 2021.
- Orbe, C., D.A. Plummer, D.W. Waugh, H. Yang, P. Jöckel, D.E. Kinnison, B. Josse, V. Marecal, M. Deushi, N.L. Abraham, A.T. Archibald, M.P. Chipperfield, S. Dhomse, W. Feng, and S. Bekki, Description and Evaluation of the specified-dynamics experiment in the Chemistry-Climate Model Initiative, *Atmos. Chem. Phys.*, **20**, 3809–3840, doi:10.5194/acp-20-3809-2020, 2020.
- Pincus, R., S.A. Buehler, M. Brath, C. Crevoisier, O. Jamil, K.F. Evans, J. Manners, R.L. Menzel, E.J. Mlawer, D. Paynter, R.L. Perna, and Y. Tellier, Benchmark calculations of radiative forcing by greenhouse gases, *J. Geophys. Res. Atmos.*, **125** (23), e2020JD033483, doi:10.1029/2020JD033483, 2020.
- Plaza, N.P., A. Podglajen, C. Pena-Ortiz, and F. Ploeger, Processes influencing lower stratospheric water vapor in monsoon anticyclones: insights from Lagrangian modelling, *Atmos. Chem. Phys.*, **21** (12), 9585–9607, doi:10.5194/acp-21-9585-2021, 2021.
- Ploeger, F., B. Legras, E. Charlesworth, X. Yan, M. Diallo, P. Konopka, T. Birner, M. Tao, A. Engel, and M. Riese, How robust are stratospheric age of air trends from different reanalyses?, *Atmos. Chem. Phys.*, **19**, 6085–6105, doi:10.5194/acp-19-6085-2019, 2019.
- Ploeger, F., M. Diallo, E. Charlesworth, P. Konopka, B. Legras, J. C. Laube, J.-U. Groöb, G. Günther, A. Engel, and M. Riese, The stratospheric Brewer–Dobson circulation inferred from age of air in the ERA5 reanalysis, *Atmos. Chem. Phys.*, **21**, 8393–8412, doi:10.5194/acp-21-8393-2021, 2021.
- Ploeger, F. and Garny, H., Hemispheric asymmetries in recent changes in the stratospheric circulation, *Atmos. Chem. Phys.*, **22**, 5559–5576, <https://doi.org/10.5194/acp-22-5559-2022>, 2022.
- Plumb, R.A., Stratospheric transport, *J. Meteorol. Soc. Japan*, **80**, 793–809, doi:10.2151/jmsj.80.793, 2002.
- Pohlmann, H., W.A. Müller, M. Bittner, S. Hettrich, K. Modali, K. Pankatz, and J. Marotzke, Realistic quasi-biennial oscillation variability in historical and decadal hindcast simulations using CMIP6 forcing, *Geophys. Res. Lett.*, **46**, 14,118–14,125, doi:10.1029/2019GL084878, 2019.
- Polvani, L.M., M. Abalos, R. Garcia, D. Kinnison, and W.J. Randel, Significant weakening of Brewer–Dobson circulation trends over the 21st century as a consequence of the Montreal Protocol, *Geophys. Res. Lett.*, **45**, doi:10.1002/2017GL075345, 2018.
- Polvani, L.M., and K. Bellomo, The key role of ozone-depleting substances in weakening the walker circulation in the second half of the twentieth century, *J. Clim.*, **32** (5), 1411–1418, doi:10.1175/JCLI-D-17-0906.1, 2019.
- Polvani, L.M., L. Wang, M. Abalos, N. Butchart, M.P. Chipperfield, M. Dameris, M. Deushi, S.S. Dhomse, P. Jöckel, D. Kinnison, M. Michou, O. Morgenstern, L.D. Oman, D.A. Plummer, and K.A. Stone, Large impacts, past and future, of ozone-depleting substances on Brewer–Dobson circulation trends: A multimodal assessment, *J. Geophys. Res. Atmos.*, **124**, 6669–6680, doi:10.1029/2018JD029516, 2019.
- Polvani, L.M., M. Previdi, M.R. England, G. Chiodo, and K.L. Smith, Substantial twentieth-century Arctic warming caused by ozone-depleting substances, *Nat. Clim. Change*, **10**, 130–133, doi:10.1038/s41558-019-0677-4, 2020.
- Polvani, L.M., A. Banerjee, R. Chemke, E.W. Doddridge, D. Ferreira, A. Gnanadesikan, M.A. Holland, Y. Kostov, J. Marshall, W.J.M. Seviour, S. Solomon, and D.W. Waugh, Interannual SAM modulation of Antarctic sea ice extent does not account for its long-term trends, pointing to a limited role for ozone depletion, *Geophys. Res. Lett.*, **48** (21), e2021GL094871, doi:10.1029/2021GL094871, 2021.
- Prather, M., P. Midgley, F.S. Rowland, and R. Stolarski, The ozone layer: The road not taken, *Nature*, **381**, 551–554, doi:10.1038/381551a0, 1996.
- Previdi, M., and L.M. Polvani, Impact of the Montreal Protocol on Antarctic surface mass balance and implications for global sea level rise, *J. Clim.*, **30**, 7247–7253, doi:10.1175/jcli-d-17-0027.1, 2017.
- Poruch, A., and M.H. England, Tropical teleconnections to Antarctic sea ice during

- austral spring 2016 in coupled pacemaker experiments, *Geophys. Res. Lett.*, **46**, 6848–6858, doi:10.1029/2019gl082671, 2019.
- Rae, C.D., J. Keeble, P. Hitchcock, and P.A. Pyle, Prescribing zonally asymmetric ozone climatologies in climate models: Performance compared to a chemistry-climate model, *J. Adv. Model. Earth Syst.*, **11**, 918–933, doi:10.1029/2018ms001478, 2019.
- Ramanathan, V., and R.E. Dickinson, The role of stratospheric ozone in the zonal and seasonal radiative energy balance of the earth-troposphere system, *J. Atmos. Sci.*, **36** (6), 1084–1104, doi:10.1175/1520-0469(1979)036<1084:TROSOI>2.0.CO;2, 1979.
- Ramaswamy, V., M.-L. Chanin, J. Angell, J. Barnett, D. Gaffen, M. Gelman, P. Keckhut, Y. Koshelkov, K. Labitzke, J.-J.R. Lin, A. O'Neill, J. Nash, W. Randel, R. Rood, K. Shine, M. Shiotani, and R. Swinbank, Stratospheric temperature trends: Observations and model simulations, *Rev. Geophys.*, **39**(1), 71–122, doi:10.1029/1999RG000065, 2002.
- Ramaswamy, V., W. Collins, J. Haywood, J. Lean, N. Mahowald, G. Myhre, V. Naik, K.P. Shine, B. Soden, G. Stenchikov, and T. Storelvmo, Radiative forcing of climate: the historical evolution of the radiative forcing concept, the forcing agents and their quantification, and applications, *Meteorol. Monogr.*, **59** (1), doi:10.1175/AMSMONOGRAPHS-D-19-0001.1, 2019.
- Randel, W., and M. Park, Diagnosing observed stratospheric water vapor relationships to the cold point tropical tropopause, *J. Geophys. Res. Atmos.*, **124**, 7018–7033, doi:10.1029/2019JD030648, 2019.
- Randel, W.J., F. Wu, and R. Stolarski, Changes in column ozone correlated with the stratospheric EP flux, *J. Meteorol. Soc. Japan*, **80**, 849–862, doi:10.2151/jmsj.80.849, 2002.
- Randel, W.J., A.K. Smith, F. Wu, C.-Z. Zou, and H. Qian, Stratospheric temperature trends over 1979–2015 derived from combined SSU, MLS and SABER satellite observations, *J. Clim.*, **29** (13), 4843–4859, doi:10.1175/JCLI-D-15-0629.1, 2016.
- Rao, J., and C.I. Garfinkel, Arctic ozone loss in March 2020 and its seasonal prediction in CFSv2: A comparative study with the 1997 and 2011 cases, *J. Geophys. Res. Atmos.*, **125** (21), e2020JD033524, doi:10.1029/2020JD033524, 2020.
- Rao, J., C.I. Garfinkel, and I.P. White, How does the Quasi-Biennial Oscillation affect the boreal winter tropospheric circulation in CMIP5/6 models?, *J. Clim.*, **33**, 8975–8996, doi:10.1175/JCLI-D-20-0024.1, 2020.
- Rao, J., and C.I. Garfinkel, Projected changes of stratospheric final warmings in the Northern and Southern Hemispheres by CMIP5/6 models, *Clim. Dyn.*, **56**, 3353–3371, doi:10.1007/s00382-021-05647-6, 2021a.
- Rao, J., and C.I. Garfinkel, CMIP5/6 models project little change in the statistical characteristics of sudden stratospheric warmings in the 21st century, *Environ. Res. Lett.*, **16** (3), 034024, doi:10.1088/1748-9326/abd4fe, 2021b.
- Rao, J., and C.I. Garfinkel, The strong stratospheric polar vortex in March 2020 in sub-seasonal to seasonal models: Implications for empirical prediction of the low Arctic total ozone extreme, *J. Geophys. Res. Atmos.*, **126** (9), doi:10.1029/2020JD034190, 2021c.
- Remsberg, E.E., B.T. Marshall, M. Garcia-Comas, D. Krueger, G.S. Lingenfelter, J. Martin-Torres, M.G. Mlynarczyk, J.M. Russell III, A.K. Smith, Y. Zhao, C. Brown, L.L. Gordley, M.J. Lopez-Gonzalez, M. Lopez-Puertas, C.-Y. She, M.J. Taylor, and R.E. Thompson, Assessment of the quality of the Version 1.07 temperature-versus-pressure profiles of the middle atmosphere from TIMED/SABER, *J. Geophys. Res. Atmos.*, **113** (D17), doi:10.1029/2008JD010013, 2008.
- Revell, L.E., F. Robertson, H. Douglas, O. Morgenstern, and D. Frame, Influence of ozone forcing on 21st century Southern Hemisphere surface westerlies in CMIP6 models, *Geophys. Res. Lett.*, **49**, e2022GL098252, doi:10.1029/2022GL098252, 2022.
- Richter, J.H., C.C. Chen, Q. Tang, Q., S. Xie, and P.J. Rasch, Improved simulation of the QBO in E3SMv1, *J. Adv. Model. Earth Syst.*, **11**, 3403–3418, doi:10.1029/2019MS001763, 2019.
- Richter, J.H., J.A. Anstey, N. Butchart, Y. Kawatani, G.A. Meehl, S. Osprey, and I.R. Simpson, Progress in simulating the quasi-biennial oscillation in CMIP models, *J. Geophys. Res. Atmos.*, **125** (8), e2019JD032362, doi:10.1029/2019JD032362, 2020a.
- Richter, J.H., N. Butchart, Y. Kawatani, A.C. Bushell, L. Holt, F. Serva, J. Anstey, I.R. Simpson, S. Osprey, K. Hamilton, P. Braesicke, C. Cagnazzo, C.-C. Chen, R.R. Rolando, L.J. Gray, T. Kerzenmacher, F. Lott, C. McLandress, H. Naoy, J. Scinocca, T.N. Stockdale, S. Versick, S. Watanabe, K. Yoshida, and S. Yukimoto, Response of the quasi-biennial oscillation to a warming climate in global climate models, *Q. J. R. Meteorol. Soc.*, **148** (744), 1490–1518, doi:10.1002/qj.3749, 2020b.
- Rieder, H.E., L.M. Polvani, and S. Solomon, Distinguishing the impacts of ozone-depleting substances and well-mixed greenhouse gases on Arctic stratospheric ozone and temperature trends, *Geophys. Res. Lett.*, **41** (7), 2652–2660, doi:10.1002/2014GL059367, 2014.
- Rieder, H.E., G. Chiodo, J. Fritzer, C. Wienerroither, and L.M. Polvani, Is interactive ozone chemistry important to represent polar cap stratospheric temperature variability in Earth-System Models?, *Environ. Res. Lett.*, **14** (4), 044026, doi:10.1088/1748-9326/ab07ff, 2019.
- Rieger, L., W.J. Randel, A.E. Bourassa, and S. Solomon, Stratospheric temperature and ozone anomalies associated with the 2020 Australian New Year fires, *Geophys. Res. Lett.*, **48** (24), e2021GL095898, doi:10.1029/2021GL095898, 2021.
- Rignot, E., J. Mougnot, B. Scheuchl, M. van den Broeke, M.J. van Wessem, and M. Morlighem, Four decades of Antarctic Ice Sheet mass balance from 1979–2017, *Proc. Natl. Acad. Sci.*, **116**, 1095–1103, doi:10.1073/pnas.1812883116, 2019.
- Rintoul, S.R., The global influence of localized dynamics in the Southern Ocean, *Nature*, **558**, 209–218, doi:10.1038/s41586-018-0182-3, 2018.
- Roach, L.A., J. Dörr, C.R. Holmes, F. Massonnet, E.W. Blockley, D. Notz, T. Rackow, M.N. Raphael, S.P. O'Farrell, D.A. Bailey, and C.M. Bitz, Antarctic sea ice area in CMIP6, *Geophys. Res. Lett.*, **47** (9), doi:10.1029/2019gl086729, 2020.
- Romanowsky, E., D. Handorf, R. Jaiser, I. Wohltmann, W. Dorn, J. Ukita, J. Cohen, K. Dethloff, and M. Rex, The role of stratospheric ozone for Arctic-midlatitude linkages, *Sci. Rep.*, **9** (1), 7962, doi:10.1038/s41598-019-43823-1, 2019.
- Santer, B.D., S. Po-Chedley, C. Mears, J.C. Fyfe, N. Gillett, Q. Fu, J.F. Painter, S. Solomon, A.K. Steiner, F.J. Wentz, M.D. Zelinka, and C.-Z. Zou, Using climate model simulations to constrain observations, *J. Clim.*, **34** (15), 6281–6301, doi:10.1175/JCLI-D-20-0768.1, 2021.
- Schlosser, E., F.A. Haumann, and M.N. Raphael, Atmospheric influences on the anomalous 2016 Antarctic sea ice decay, *Cryosphere*, **12**, 1103–1119, doi:10.5194/tc-12-1103-2018, 2018.
- Seager, R., M.A. Cane, N. Henderson, D.E. Lee, R. Abernathy, and H. Zhang, Strengthening of the tropical Pacific zonal SST gradient is a consistent response to rising greenhouse gases, *Nature Clim. Change*, **9**, 517–522, doi:10.1038/s41558-019-0505-x, 2019.
- Seidel, D.J., J. Li, C. Mears, I. Moradi, J. Nash, W.J. Randel, R. Saunders, D.W.J. Thompson, and C.-Z. Zou, Stratospheric temperature changes during the satellite era, *J. Geophys. Res. Atmos.*, **121** (2), 664–681, doi:10.1002/2015JD024039, 2016.
- Sen Gupta, A., and M.H. England, Coupled ocean–atmosphere–ice response to variations in the Southern Annular Mode, *J. Clim.*, **19**, 4457–4486, doi:10.1175/JCLI3843.1, 2006.
- Seviour, W.J.M., Weakening and shift of the Arctic stratospheric polar vortex: Internal variability or forced response?, *Geophys. Res. Lett.*, **44**, 3365–3373, doi:10.1002/2017GL073071, 2017.
- Seviour, W.J.M., D.W. Waugh, L.M. Polvani, G.J.P. Correa, and C.I. Garfinkel, Robustness of the simulated tropospheric response to ozone depletion, *J. Clim.*, **30**, 2577–2585, doi:10.1175/JCLI-D-16-0817.1, 2017.
- Seviour, W.J.M., F. Codron, E.W. Doddridge, D. Ferreira, A. Gnanadesikan, M. Kelley, Y. Kostov, J. Marshall, L.M. Polvani, J.L. Thomas, and D.W. Waugh, The Southern Ocean sea surface temperature response to ozone depletion: a multimodel comparison, *J. Clim.*, **32**, 5107–5121, doi:10.1175/jcli-d-19-0109.1, 2019.
- Sexton, D., The effect of stratospheric ozone depletion on the phase of the Antarctic Oscillation, *Geophys. Res. Lett.*, **28** (19), 3697–3700, doi:10.1029/2001GL013376, 2001.
- Shangguan, M., W. Wang, and S. Jin, Variability of temperature and ozone in the upper troposphere and lower stratosphere from multi-satellite observations and reanalysis data, *Atmos. Chem. Phys.*, **19**, 6659–6679, doi:10.5194/acp-19-6659-2019, 2019.
- Shepherd, A., D. Wingham, and E. Rignot, Warm ocean is eroding West Antarctic ice sheet, *Geophys. Res. Lett.*, **31** (23), doi:10.1029/2004gl021106, 2004.
- Shepherd, T.G., and C. McLandress, A robust mechanism for strengthening of the Brewer-Dobson Circulation in response to climate change: Critical-layer control of subtropical wave breaking, *J. Atmos. Sci.*, **68** (4), 784–797, doi:10.1175/2010JAS3608.1, 2011.
- Shibata, K., and M. Deushi, Radiative effect of ozone on the

- quasi-biennial oscillation in the equatorial stratosphere, *Geophys. Res. Lett.*, **32**(24), doi:10.1029/2005GL023433, 2005.
- Shibata, K., Simulations of ozone feedback effects on the equatorial quasi-biennial oscillation with a chemistry–climate model, *Climate*, **9** (8), 123, doi:10.3390/cli9080123, 2021.
- Shibata, K., and H. Naoe, Decadal amplitude modulations of the stratospheric quasi-biennial oscillation, *J. Meteorol. Soc. Japan*, **100**, 29–44, doi:10.2151/jmsj.2022-001, 2022.
- Shindell, D., G. Faluvegi, L. Nazarenko, K. Bowman, J.-F. Lamarque, A. Voulgarakis, G.A. Schmidt, O. Pechony, and R. Ruedy, Attribution of historical ozone forcing to anthropogenic emissions, *Nat. Clim. Change*, **3**, 567–570, doi:10.1038/nclimate1835, 2013.
- Sigmond, M., M.C. Reader, J.C. Fyfe, and N.P. Gillett, Drivers of past and future Southern Ocean change: Stratospheric ozone versus greenhouse gas impacts, *Geophys. Res. Lett.*, **38**(12), L12601, doi:10.1029/2011GL047120, 2011.
- Simmons, A., C. Soci, J. Nicolas, B. Bell, P. Berrisford, R. Dragani, J. Flemming, L. Haimberger, S. Healy, H. Hersbach, and A. Horányi, *Global stratospheric temperature bias and other stratospheric aspects of ERA5 and ERA5.1*, ECMWF Technical Memoranda No. 859, European Centre for Medium-Range Weather Forecasts, 40 pp., doi:10.21957/rcxqfmg0, 2020.
- Singh, H.A., L.M. Polvani, and P.J. Rasch, Antarctic sea ice expansion, driven by internal variability, in the presence of increasing atmospheric CO₂, *Geophys. Res. Lett.*, **46**(24), 14,762–14,771, doi:10.1029/2019GL083758, 2019.
- Skeie, R.B., G. Myhre, Ø. Hodnebrog, P.J. Cameron-Smith, M. Deushi, M.I. Hegglin, L.W. Horowitz, R.J. Kramer, M. Michou, M.J. Mills, D.J.L. Olivé, F.M.O. Connor, D. Paynter, B.H. Samset, A. Sellar, B. Shindell, T. Takemura, S. Tilmes, and T. Wu, Historical total ozone radiative forcing derived from CMIP6 simulations, *npj Clim. Atmos. Sci.*, **3**(1), 32, doi:10.1038/s41612-020-00131-0, 2020.
- Smith, B., B. Smith, H.A. Fricker, A.S. Gardner, B. Medley, J. Nilsson, F.S. Paolo, N. Holschuh, S. Adusumilli, K. Brunt, B. Csatho, K. Harbeck, T. Markus, T. Neumann, M.R. Siegfried, and H.J. Zwally, Pervasive ice sheet mass loss reflects competing ocean and atmosphere processes, *Science*, **368** (6496), 1239–1242, doi:10.1126/science.aaz5845, 2020.
- Smith, K.L., and L.M. Polvani, The surface impacts of Arctic stratospheric ozone anomalies, *Environ. Res. Lett.*, **9**(7), doi:10.1088/1748-9326/9/7/074015, 2014.
- Solomon, A., L.M. Polvani, K.L. Smith, and R.P. Abernathy, The impact of ozone depleting substances on the circulation, temperature, and salinity of the Southern Ocean: An attribution study with CESM1(WACCM), *Geophys. Res. Lett.*, **42**, 5547–5555, doi:10.1002/2015gl064744, 2015.
- Solomon, S., K.H. Rosenlof, R.W. Portmann, J.S. Daniel, S.M. Davis, T.J. Sanford, and G.-K. Plattner, Contributions of stratospheric water vapor to decadal changes in the rate of global warming, *Science*, **327** (5970), 1219–1223, doi:10.1126/science.1182488, 2010.
- Solomon, S., D.J. Iy, D. Kinnison, M.J. Mills, R.R. Neely, and A. Schmidt, Emergence of healing in the Antarctic ozone layer, *Science*, **353**, 269–274, doi:10.1126/science.aae0061, 2016.
- Solomon, S., K. Dube, K. Stone, P. Yu, D. Kinnison, O.B. Toon, S.E. Strahan, K.H. Rosenlof, R. Portmann, S. Davis, W. Randel, P. Bernath, C. Boone, C.G. Bardeen, A. Bourassa, D. Zawada, and D. Degenstein, On the stratospheric chemistry of midlatitude wildfire smoke, *Proc. Natl. Acad. Sci.*, **119**(10), doi:10.1073/pnas.2117325119, 2022.
- Son, S.-W., L.M. Polvani, D.W. Waugh, H. Akiyoshi, R.R. Garcia, D. Kinnison, S. Pawson, E. Rozanov, T.G. Shepherd, and K. Shibata, The impact of stratospheric ozone recovery on the Southern Hemisphere westerly jet, *Science*, **320** (5882), 1486–1489, doi:10.1126/science.1155939, 2008.
- Son, S.-W., E.P. Gerber, J. Perlwitz, L.M. Polvani, N. P. Gillett, K.-H. Seo, V. Eyring, T.G. Shepherd, D. Waugh, H. Akiyoshi, J. Austin, A. Baumgaertner, S. Bekki, P. Braesicke, C. Brühl, N. Butchart, M.P. Chipperfield, D. Cugnet, M. Dameris, S. Dhomse, S. Frith, H. Garny, R. Garcia, S.C. Hardiman, P. Jöckel, J.F. Lamarque, E. Mancini, M. Marchand, M. Michou, T. Nakamura, O. Morgenstern, G. Pitari, D.A. Plummer, J. Pyle, E. Rozanov, J.F. Scinocca, K. Shibata, D. Smale, H. Teyssède, W. Tian, and Y. Yamashita, Impact of stratospheric ozone on Southern Hemisphere circulation change: A multimodel assessment, *J. Geophys. Res. Atmos.*, **115** (D3), doi:10.1029/2010JD014271, 2010.
- Son, S.-W., A. Purich, H.H. Hendon, B.-M. Kim, and L.M. Polvani, Improved seasonal forecast using ozone hole variability?, *Geophys. Res. Lett.*, **40**, 6231–6235, doi:10.1002/2013GL057731, 2013.
- Son, S.-W., B.-R. Han, C.I. Garfinkel, S.-Y. Kim, P. Rokjin, N.L. Abraham, H. Akiyoshi, A.T. Archibald, N. Butchart, M.P. Chipperfield, M. Dameris, M. Deushi, S.S. Dhomse, S.C. Hardiman, P. Jöckel, D. Kinnison, M. Michou, O. Morgenstern, F.M. O’Connor, L.D. Oman, D.A. Plummer, A. Pozzer, L.E. Revell, E. Rozanov, A. Stenke, K. Stone, S. Tilmes, Y. Yamashita, and G. Zeng, Tropospheric jet response to Antarctic ozone depletion: An update with Chemistry–Climate Model Initiative (CCMI) models, *Environ. Res. Lett.*, **13** (5), doi:10.1088/1748-9326/aabf21, 2018.
- SPARC (Stratosphere-troposphere Processes And their Role in Climate), *SPARC Reanalysis Intercomparison Project (S-RIP) Final Report*, edited by M. Fujiwara, G.L. Manney, L.J. Gray, and J.S. Wright, SPARC Report No. 10, WCRP-6/2021, doi:10.17874/800dee57d13, 2022.
- Spence, P., S.M. Griffies, M.H. England, A. McC. Hogg, O.A. Saenko, and N.C. Jourdain, Rapid subsurface warming and circulation changes of Antarctic coastal waters by poleward shifting winds, *Geophys. Res. Lett.*, **41** (13), 4601–4610, doi:10.1002/2014gl060613, 2014.
- Spencer, R.W., J.R. Christy, and W.D. Braswell, UAH Version 6 global satellite temperature products: Methodology and results, *Asia Pac. J. Atmos. Sci.*, **53**, 121–130, doi:10.1007/s13143-017-0010-y, 2017.
- Stecher, L., F. Winterstein, M. Dameris, P. Joeckel, M. Ponater, and M. Kunze, Slow feedbacks resulting from strongly enhanced atmospheric methane mixing ratios in a chemistry–climate model with mixed-layer ocean, *Atmos. Chem. Phys.*, **21**, 731–754, doi:10.5194/acp-21-731-2021, 2021.
- Steiner, A.K., F. Ladstädter, W.J. Randel, A.C. Maycock, Q. Fu, C. Claud, H. Gleisner, L. Haimberger, S.-P. Ho, P. Keckhut, T. Leblanc, C. Mears, L.M. Polvani, B.D. Santer, T. Schmidt, V. Sofieva, R. Wing, and C.-Z. Zou, Observed temperature changes in the troposphere and stratosphere from 1979 to 2018, *J. Clim.*, **33**, 8165–8194, doi:10.1175/JCLI-D-19-0998.1, 2020.
- Stevenson, D.S., P.J. Young, V. Naik, J.-F. Lamarque, D.T. Shindell, A. Voulgarakis, R.B. Skeie, S.B. Dalsoren, G. Myhre, T.K. Berntsen, G.A. Folberth, S.T. Rumbold, W.J. Collins, I.A. MacKenzie, R.M. Doherty, G. Zeng, T.P.C. van Noije, A. Strunk, D. Bergmann, P. Cameron-Smith, D.A. Plummer, S.A. Strode, L. Horowitz, Y.H. Lee, S. Szopa, K. Sudo, T. Nagashima, B. Josse, I. Cionni, M. Righi, V. Eyring, A. Conley, K.W. Bowman, O. Wild, and A. Archibald, Tropospheric ozone changes, radiative forcing and attribution to emissions in the Atmospheric Chemistry and Climate Model Intercomparison Project (ACCMIP), *Atmos. Chem. Phys.*, **13**, 3063–3085, doi:10.5194/acp-13-3063-2013, 2013.
- Stiller, G.P., T. von Clarmann, F. Haenel, B. Funke, N. Glatthor, U. Grabowski, S. Kellmann, M. Kiefer, A. Linden, S. Lossow, and M. López-Puertas, Observed temporal evolution of global mean age of stratospheric air for the 2002 to 2010 period, *Atmos. Chem. Phys.*, **12**, 3311–3331, doi:10.5194/acp-12-3311-2012, 2012.
- Stiller, G.P., F. Fierli, F. Ploeger, C. Cagnazzo, B. Funke, F.J. Haenel, T. Reddmann, M. Riese, and T. von Clarmann, Shift of subtropical transport barriers explains observed hemispheric asymmetry of decadal trends of age of air, *Atmos. Chem. Phys.*, **17**, 11,177–11,192, doi:10.5194/acp-17-11177-2017, 2017.
- Stone, K.A., S. Solomon, and D.E. Kinnison, On the identification of ozone recovery, *Geophys. Res. Lett.*, **45** (10), 5158–5165, doi:10.1029/2018GL077955, 2018.
- Stone, K.A., S. Solomon, D.E. Kinnison, C.F. Baggett, and E.A. Barnes, Prediction of Northern Hemisphere regional surface temperatures using stratospheric ozone information, *J. Geophys. Res. Atmos.*, **124**, 5922–5933, doi:10.1029/2018JD029626, 2019.
- Stone, K.A., S. Solomon, and D.E. Kinnison, Prediction of Northern Hemisphere regional sea ice extent and snow depth using stratospheric ozone information, *J. Geophys. Res. Atmos.*, **125** (22), e2019JD031770, doi:10.1029/2019JD031770, 2020.
- Strahan, S.E., D. Smale, A.R. Douglass, T. Blumenstock, J.W. Hannigan, F. Hase, N.B. Jones, E. Mahieu, J. Notholt, L.D. Oman, I. Ortega, M. Palm, M. Prignon, J. Robinson, M. Schneider, R. Sussmann, and V.A. Velasco, Observed hemispheric asymmetry in stratospheric transport trends from 1994 to 2018, *Geophys. Res. Letters*, **47**, e2020GL088567, doi:10.1029/2020GL088567, 2020.
- Stuecker, M.F., C.M. Bitz, and K.C. Armour, Conditions leading to the unprecedented low Antarctic sea ice extent during the 2016 austral spring season, *Geophys. Res. Lett.*, **44**, 9008–9019, doi:10.1002/2017gl074691, 2017.
- Suneeth, K.V., and S.S. Das, Zonally resolved water vapour coupling with tropical tropopause temperature: Seasonal and interannual variability, and influence of the Walker circulation, *Clim. Dyn.*, **54**, 4657–4673, doi:10.1007/s00382-020-05255-w, 2020.
- Swart, N.C., S.T. Gille, J.C. Fyfe, and N.P. Gillett, Recent Southern Ocean warming

- and freshening driven by greenhouse gas emissions and ozone depletion, *Nat. Geosci.*, **11**, 836–841, doi:10.1038/s41561-018-0226-1, 2018.
- Szopa, S., V. Naik, B. Adhikary, P. Artaxo, T. Berntsen, W.D. Collins, S. Fuzzi, L. Gallardo, A. Kiendler-Scharr, Z. Klimont, H. Liao, N. Unger, and P. Zanis, Short-Lived Climate Forcers, Chapter 6 in *Climate Change 2021: The Physical Science Basis. Contribution of Working Group I to the Sixth Assessment Report of the Intergovernmental Panel on Climate Change* edited by V. Masson-Delmotte, P. Zhai, A. Pirani, S.L. Connors, C. Péan, S. Berger, N. Caud, Y. Chen, L. Goldfarb, M.I. Gomis, M. Huang, K. Leitzell, E. Lonnoy, J.B.R. Matthews, T.K. Maycock, T. Waterfield, O. Yelekçi, R. Yu, and B. Zhou, Cambridge University Press, Cambridge, United Kingdom and New York, NY, USA, 105 pp., doi:10.1017/9781009157896.008, 2021.
- Tegtmeier, S., M. Rex, I. Wohltmann, and K. Krüger, Relative importance of dynamical and chemical contributions to Arctic wintertime ozone, *Geophys. Res. Lett.*, **35** (17), L17801, doi:10.1029/2008GL034250, 2008.
- Thompson, D.W.J., and S. Solomon, Interpretation of recent Southern Hemisphere climate change, *Science*, **296** (5569), 895–899, doi:10.1126/science.1069270, 2002.
- Thompson, D.W.J., M.P. Baldwin, and S. Solomon, Stratosphere–troposphere coupling in the Southern Hemisphere, *J. Atmos. Sci.*, **62** (3), 708–715, doi:10.1175/JAS-3321.1, 2005.
- Thompson, D.W.J., S. Solomon, P.J. Kushner, M.H. England, K.M. Grise, and D.J. Karoly, Signatures of the Antarctic ozone hole in Southern Hemisphere surface climate change, *Nat. Geosci.*, **4** (11), 741–749, doi:10.1038/ngeo1296, 2011.
- Thornhill, G.D., W.J. Collins, R.J. Kramer, D. Olivé, R.B. Skeie, F.M. O'Connor, N.L. Abraham, R. Checa-García, S.E. Bauer, M. Deushi, L.K. Emmons, P.M. Forster, L.W. Horowitz, B. Johnson, J. Keeble, J.-F. Lamarque, M. Michou, M.J. Mills, J.P. Mulcahy, G. Myhre, P. Nabat, V. Naik, N. Oshima, M. Schulz, C.J. Smith, T. Takemura, S. Tilmes, T. Wu, G. Zeng, and J. Zhang, Effective radiative forcing from emissions of reactive gases and aerosols—a multi-model comparison, *Atmos. Chem. Phys.*, **21** (2), 853–874, doi:10.5194/acp-21-853-2021, 2021.
- Turner, J., T. Phillips, G.J. Marshall, J.S. Hosking, J.O. Pope, T.J. Bracegirdle, and P. Deb, Unprecedented springtime retreat of Antarctic sea ice in 2016, *Geophys. Res. Lett.*, **44**, 6868–6875, doi:10.1002/2017gl073656, 2017.
- Turner, J., T. Phillips, M. Thamban, W. Rahaman, G.J. Marshall, J.D. Wille, V. Favier, V.H.L. Winton, E. Thomas, Z. Wang, M. van den Broeke, J.S. Hosking, and T. Lachlan-Cope, The dominant role of extreme precipitation events in Antarctic snowfall variability, *Geophys. Res. Lett.*, **46**, 3502–3511, doi:10.1029/2018gl081517, 2019.
- Velders, G.J.M., S.O. Andersen, J.S. Daniel, D.W. Fahey, and M. McFarland, The Importance of the Montreal Protocol in protecting climate, *Proc. Natl. Acad. Sci.*, **104** (12), 4814–4819, doi:10.1073/pnas.0610328104, 2007.
- Velders, G.J.M., J.S. Daniel, S.A. Montzka, I. Vimont, M. Rigby, P.B. Krummel, J. Muhle, S. O'Doherty, R.G. Prinn, R.F. Weiss, and D. Young, Projections of hydrofluorocarbon (HFC) emissions and the resulting global warming based on recent trends in observed abundances and current policies, *Atmos. Chem. Phys.*, **22** (9), 6087–6101, doi:10.5194/acp-2021-1070, 2022.
- Virgin, J.G., and K.L. Smith, Is Arctic amplification dominated by regional radiative forcing and feedbacks: Perspectives from the World-Avoided scenario, *Geophys. Res. Lett.*, **46**, 7708–7717, doi:10.1029/2019GL082320, 2019.
- von der Gathen, P., R. Kivi, I. Wohltmann, R.J. Salawitch, and M. Rex, Climate change favours large seasonal loss of Arctic ozone, *Nat. Commun.*, **12**, 3886, doi:10.1038/s41467-021-24089-6, 2021.
- Wang, G., W. Cai, and A. Purich, Trends in Southern Hemisphere wind-driven circulation in CMIP5 models over the 21st century: Ozone recovery versus greenhouse forcing, *J. Geophys. Res. Ocean*, **119**, 2974–2984, doi:10.1002/2013JC009589, 2014.
- Wang, G., H.H. Hendon, J.M. Arblaster, E.-P. Lim, S. Abhik, and P. van Rensch, Compounding tropical and stratospheric forcing of the record low Antarctic ozone hole in 2016, *Nat. Commun.*, **10**, 13, doi:10.1038/s41467-018-07689-7, 2019b.
- Wang, L., S.C. Hardiman, P.E. Bett, R.E. Comer, C. Kent, and A.A. Scaife, What chance of a sudden stratospheric warming in the southern hemisphere?, *Environ. Res. Lett.*, **15** (10), 104038, doi:10.1088/1748-9326/aba8c1, 2020.
- Wang, L., K. Lyu, W. Zhuang, W. Zhang, S. Makarim, and X.-H. Yan, Recent shift in the warming of the Southern Oceans Modulated by decadal climate variability, *Geophys. Res. Lett.*, **48** (3), doi:10.1029/2020gl090889, 2021.
- Wang, X., A.E. Dessler, M.R. Schoeberl, W. Yu, and T. Wang, Impact of convectively lofted ice on the seasonal cycle of water vapor in the tropical tropopause layer, *Atmos. Chem. Phys.*, **19**, 14,621–14,636, doi:10.5194/acp-19-14621-2019, 2019a.
- Wang, X., and A.E. Dessler, The response of stratospheric water vapor to climate change driven by different forcing agents, *Atmos. Chem. Phys.*, **20**, 13,267–13,282, doi:10.5194/acp-20-13267-2020, 2020.
- Wargan, K., B. Weir, G.L. Manney, S.E. Cohn, and N.J. Livesey, The anomalous 2019 Antarctic ozone hole in the GEOS Constituent Data Assimilation System with MLS observations, *J. Geophys. Res. Atmos.*, **125** (18), e2020JD033335, doi:10.1029/2020JD033335, 2020.
- Waugh, D.W., and T.M. Hall, Age of stratospheric air: Theory, observations, and models, *Rev. Geophys.*, **40** (4), doi:10.1029/2000RG000101, 2002.
- Waugh, D.W., Age of stratospheric air, *Nat. Geosci.*, **2** (1), 14–16, doi:10.1038/ngeo397, 2009.
- Waugh, D.W., L. Oman, P.A. Newman, R.S. Stolarski, S. Pawson, J.E. Nielsen, and J. Perlwitz, Effect of zonal asymmetries in stratospheric ozone on simulated Southern Hemisphere climate trends, *Geophys. Res. Lett.*, **36** (18), doi:10.1029/2009GL040419, 2009.
- Waugh, D.W., A. Banerjee, J.C. Fyfe, and L.M. Polvani, Contrasting recent trends in Southern Hemisphere westerlies across different ocean basin, *Geophys. Res. Lett.*, **47** (18), doi:10.1029/2020GL088890, 2020.
- Wilcox, L.J., and A.J. Charlton-Perez, Final warming of the Southern Hemisphere polar vortex in high- and low-top CMIP5 models, *J. Geophys. Res. Atmos.*, **118**, 2535–2546, doi:10.1002/jgrd.50254, 2013.
- WMO (World Meteorological Organization), Scientific Assessment of Ozone Depletion: 1989, Volume I, Global Ozone Research and Monitoring Project—Report No. 20, 532 pp., Geneva, Switzerland, 1989.
- WMO (World Meteorological Organization), Scientific Assessment of Ozone Depletion: 2010, Global Ozone Research and Monitoring Project—Report No. 52, 516 pp., Geneva, Switzerland, 2010.
- WMO (World Meteorological Organization), Scientific Assessment of Ozone Depletion: 2014, Global Ozone Research and Monitoring Project—Report No. 55, 416 pp., Geneva, Switzerland, 2014.
- WMO (World Meteorological Organization), Scientific Assessment of Ozone Depletion: 2018, Global Ozone Research and Monitoring Project—Report No. 58, 588 pp., Geneva, Switzerland, 2018.
- Wu, Y., L.M. Polvani, and R. Seager, The Importance of the Montreal Protocol in Protecting Earth's Hydroclimate, *Journal of Climate*, **26**(12), 4049–4068, 2013.
- Wu, Y., I.R. Simpson, and R. Seager, Intermodel spread in the Northern Hemisphere stratospheric polar vortex response to climate change in the CMIP5 models, *Geophys. Res. Lett.*, **46**, 13,290–13,298, doi:10.1029/2019GL085545, 2019.
- Xia, Y., Y. Hu, Y. Huang, C. Zhao, F. Xie, and Y. Yang, Significant contribution of severe ozone loss to the Siberian-Arctic surface warming in spring 2020, *Geophys. Res. Lett.*, **48**, e2021GL092509, doi:10.1029/2021GL092509, 2021.
- Xie, F., X. Ma, J. Li, J. Huang, W. Tian, J. Zhang, Y. Hu, C. Sun, X. Zhou, J. Feng, and Y. Yang, An advanced impact of Arctic stratospheric ozone changes on spring precipitation in China, *Clim. Dyn.*, **51**, 4029–4041, doi:10.1007/s00382-018-4402-1, 2018.
- Yook, S., D.W.J. Thompson, S. Solomon, and S.-Y. Kim, The key role of coupled chemistry–climate interactions in tropical stratospheric temperature variability, *J. Clim.*, **33**, 7619–7629, doi:10.1175/JCLI-D-20-0071.1, 2020.
- Young, P.J., A.B. Harper, C. Huntingford, N.D. Paul, O. Morgenstern, P.A. Newman, L.D. Oman, S. Madronich, and R.R. Garcia, The Montreal Protocol protects the terrestrial carbon sink, *Nature*, **596**, 384–388, doi:10.1038/s41586-021-03737-3, 2021.
- Yu, P., S.M. Davis, O.B. Toon, R.W. Portmann, C.G. Bardeen, J.E. Barnes, H. Telg, C. Maloney, and K.H. Rosenlof, Persistent stratospheric warming due to 2019–2020 Australian wildfire smoke, *Geophys. Res. Lett.*, **48** (7), doi:10.1029/2021GL092609, 2021.
- Yu, W., R. Garcia, J. Yue, J. Russell III, and M. Mlynarczyk, Variability of water vapor in the tropical middle atmosphere observed from satellites and interpreted using SD WACCM simulations, *J. Geophys. Res. Atmos.*, **127** (13), doi:10.1029/2022JD036714, 2022.
- Yue, J., J. Russell, Q. Gan, T. Wang, P. Rong, R. Garcia, and M. Mlynarczyk, Increasing

water vapor in the stratosphere and mesosphere after 2002, *Geophys. Res. Lett.*, **46**, 13,452–13,460, doi:10.1029/2019gl084973, 2019.

Zambri, B., S. Solomon, D.W.J. Thompson, and Q. Fu, Emergence of Southern Hemisphere stratospheric circulation changes in response to ozone recovery, *Nat. Geosci.*, **14**, 638–644, doi:10.1038/s41561-021-00803-3, 2021.

Zhang, J., C. Zhang, K. Zhang, M. Xu, J. Duan, M.P. Chipperfield, W. Feng, S. Zhao, and F. Xie, The role of chemical processes in the quasi-biennial oscillation (QBO) signal in stratospheric ozone, *Atmos. Environ.*, **244**, 117906, doi:10.1016/j.atmosenv.2020.117906, 2021.

Zhang, L., T.L. Delworth, W. Cooke, and X. Yang, Natural variability of Southern Ocean convection as a driver of observed climate trends, *Nat. Clim. Change*, **9**, 59–65, doi:10.1038/s41558-018-0350-3, 2019.

Zou, C.-Z., and W. Wang, Intersatellite calibration of AMSU-A observations for weather and climate applications, *J. Geophys. Res. Atmos.*, **116** (D23), D23113, doi:10.1029/2011JD016205, 2011.

Zou, C.-Z., H. Qian, W. Wang, L. Wang, and C. Long, Recalibration and merging of SSU observations for stratospheric temperature trend studies, *J. Geophys. Res. Atmos.*, **119** (23), 13,180–13,205, doi:10.1002/2014JD021603, 2014.

Zou, C.-Z., and H. Qian, Stratospheric temperature climate data record from merged SSU and AMSU-A observations, *J. Atmos. Ocean. Technol.*, **33** (9), 1967–1984, doi:10.1175/JTECH-D-16-0018.1, 2016.